Connecting AnMBR and SOFC for Blackwater Treatment and Energy Production: Influence of the AnMBR pH on the SOFC Operational Strategy

Delft University of Technology

CIE5060-09 MSc Thesis

Qinying Zha (5237025)

Assessment Committee:

Dr. Ir. Ralph Lindeboom (Chair)

Dr. Ir. Henri Spanjers

Dr. Ir. Bas Heijman

Prof. Dr. Ir. Jules van Lier

Prof. Dr. A. Purushothaman Vellayani

August 13, 2023

Abstract

Driven by the increasing demand for waste reduction and green energy production, an integrated system which combines an anaerobic membrane bioreactor (AnMBR) and a solid oxide fuel cell (SOFC) was proposed in this research project for blackwater treatment and energy production. The potentials of using an AnMBR for wastewater treatment and biogas production, and the feasibilities of producing energy from biogas with a SOFC have been investigated by many researchers. Although, combining the two equipment might raise new challenges and opportunities. The AnMBR pH has direct impacts on the biogas composition, which would subsequently affect the SOFC operational strategy. Therefore, this research project focused on the influence of the AnMBR pH on the SOFC operational strategy, which would provide insights for connecting AnMBR and SOFC. The AnMBR pH was controlled around 8 initially, and then reduced to 7. The composition of the biogas produced under each pH condition was analyzed before the biogas was conditioned for the SOFC operation. Biochar adsorption and CO_2 addition were applied for biogas conditioning. pH 8 was favorable for biochar adsorption, whereas pH 7 was favorable for CO_2 addition. The aim of biochar adsorption was to ensure that the H_2S concentration remaining in the biogas after adsorption was less than 0.5 ppm, so that sulfur poisoning could be avoided at the anode of SOFC. A biochar column (BC) was attached to the AnMBR for the adsorption of sulfur compounds in the biogas. The BC was packed with biochar made of cow manure. The adsorption capacity of the biochar was measured to determine the amount of biochar required in the BC. After biochar adsorption, the ratio between CH_4 and CO_2 was balanced by adding CO_2 to the biogas, to reduce the risk of carbon deposition at the anode of SOFC. The exhaust gas discharged by the SOFC could also be recycled as an alternative to CO_2 addition. The performance of the SOFC system using the conditioned biogas as the fuel was assessed based on electric power output and fuel utilization efficiency. Based on the results of biogas production, conditioning, and utilization, the influence of the AnMBR pH on the SOFC operational strategy was analyzed. Furthermore, the potentials and the limitations of connecting AnMBR and SOFC were discussed.

Key words: anaerobic membrane bioreactor (AnMBR), solid oxide fuel cell (SOFC), biochar, biogas, pH, blackwater treatment, energy recovery

Table of Contents

1. Introduction

1.1 AnMBR

The anaerobic membrane bioreactor (AnMBR) technology is a combination of anaerobic digestion and membrane filtration, designed for wastewater treatment and methane production. Anaerobic digestion is a biological treatment process that removes biodegradable organic compounds from wastewater. It is an alternative to aerobic biological treatment, with distinctive advantages in terms of energy conservation and waste reduction. External energy input is not required in anaerobic process, saving approximately 1 kWh per kg of chemical oxygen demand (COD) being removed from the treatment system (Henze et al., 2008). Moreover, additional energy can be recovered from the methane produced by anaerobic bioreactors. Anaerobic treatment also yields less sludge when compared with aerobic treatment. The COD uptake for biomass growth is only 5% in anaerobic treatment processes, but 30%-60% in aerobic treatment processes. AnMBR incorporates an anaerobic bioreactor with a membrane unit to further remove suspended solids from the effluent.

The potentials and limitations of implementing AnMBR as opposed to the conventional activated sludge process are summarized as follows. AnMBR is a compact system that requires less floor space (Maaz et al., 2019). The treatment process is simpler as well. AnMBR produces high quality effluent since suspended solids are separated from the effluent which is sometimes referred to as permeate. Pathogens remaining in the anaerobic sludge, including protozoa, bacteria, and viruses, can also be retained by the membrane, while the permeate is withdrawn from the AnMBR (Hai et al., 2014). AnMBR also produces more biogas for energy, but at the same time, the energy demand of AnMBR might be higher (Smith et al., 2014). AnMBR is not suitable for nutrient removal, as mineralized compounds such ammonium, phosphate, and sulfide cannot be retained during microfiltration (MF) or ultrafiltration (UF) which are commonly applied in AnMBR systems (Aslam et al., 2022; Henze et al., 2008). Membrane fouling is another constraint for commercializing of the AnMBR technology (Maaz et al., 2019). Fouling control is a major contributor to the operational cost of AnMBR. Relaxation and backwashing could be applied to remove reversible fouling due to cake formation. In case of a long-term operation, fat, protein, and minerals might accumulate on the membrane surface and block the pores. This phenomenon is known as residual fouling. Partial recovery can be achieved through chemical cleaning, but the fouling that remains is irreversible. Eventually, the membrane will have to be replaced.

1.2 Biogas Composition w.r.t. AnMBR pH

The biogas produced by AnMBR can be used in SOFC for energy production. The biogas composition would change with the AnMBR pH, and subsequently affect the SOFC performance. Therefore, the SOFC operational strategy should be adjusted as the AnMBR pH changes. The compounds in biogas that may affect the SOFC performance are CH_4, CO_2, NH_3, H_2S, and CH_3SH. CH_4 and CO_2 are the primary components in biogas. CH_4 is the fuel for SOFC, while CO_2 is the dry reforming agent. An equimolar

ratio between CH_4 and CO_2 is recommended to reduce the risk of carbon deposition at the anode of SOFC, and to maximize the electric power output of SOFC (Saadabadi et al., 2021; Yentekakis et al., 2008). NH_3, H_2S, and CH_3SH are the by-products of anaerobic digestion, and potential energy sources for SOFC. However, H_2S and CH_3SH might damage SOFC due to sulfur poisoning (Haga et al., 2008). Thus, H_2S and CH_3SH in biogas should be minimized for the SOFC operation.

CH_4 and CO_2. According to the distribution of carbonate species in water at 25 °C (Figure 1.1), when pH is below 8.3, HCO_3^- and $H_2CO_3^*$ (the sum of dissolved CO_2 and H_2CO_3) are the dominant carbonate species dissolved in water (Appelo & Postma, 2005). The conversion between HCO_3^- and $H_2CO_3^*$ is shown in Reaction 1.1, where K is the equilibrium constant at 25 °C. It is expected that CO_2 (both gas phase and liquid phase) would increase when the sludge pH in AnMBR decreases from 8 to 7, because more H^+ would be available to combine with HCO_3^- to produce $H_2CO_3^*$. As the percentage of CO_2 in biogas increases, the percentage of CH_4 in biogas would decrease accordingly. Therefore, the molar ratio between CH_4 and CO_2 would be closer to 1, which favors the SOFC operation in terms of reduction in carbon deposition.

Reaction 1.1 Conversion between H_2CO_3 and HCO_3^-*

$$H_2CO_3^* \leftrightarrow HCO_3^- + H^+, K = 10^{-6.3}$$

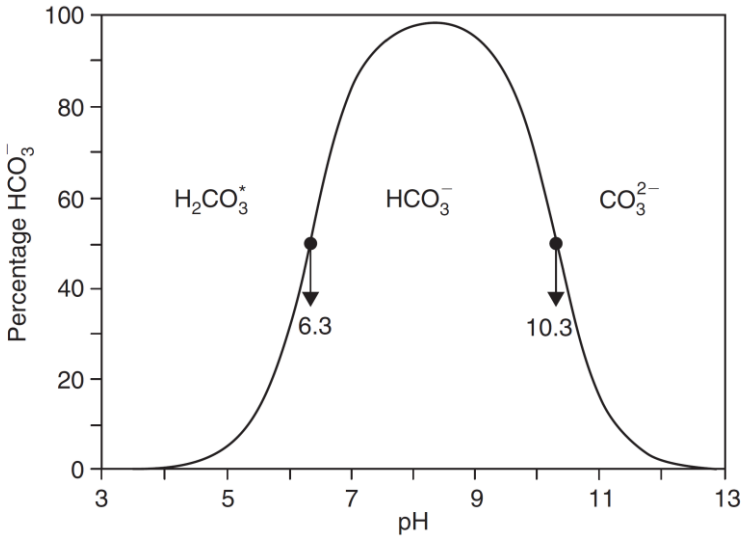

Figure 1.1 Distribution of carbonate species in water at T = 25 °C (Appelo & Postma, 2005)

NH_3. When pH decreases, the reaction shown as follows shifts to the left (Reaction 1.2) (Leyva-Ramos et al., 2004), in which case more dissolved NH_3 would be converted to NH_4^+. The relationship between dissolved NH_3 and NH_4^+ is also illustrated in Figure 1.2. Therefore, when pH is reduced from 8 to 7, less dissolved NH_3 should remain in sludge and consequently, less gaseous NH_3 should end up in biogas based on the Henry's Law. NH_3 is an energy source for SOFC. When NH_3 in biogas decreases in corresponding to the sludge pH, less NH_3 would be available for fuel oxidation during

the SOFC operation. In this way, the reduction of pH is considered as a disadvantage for SOFC.

Reaction 1.2 Conversion between and NH_4^+ and NH_3

$$NH_4^+ \leftrightarrow NH_{3\,(aq)} + H^+, K = 10^{-9.26}$$

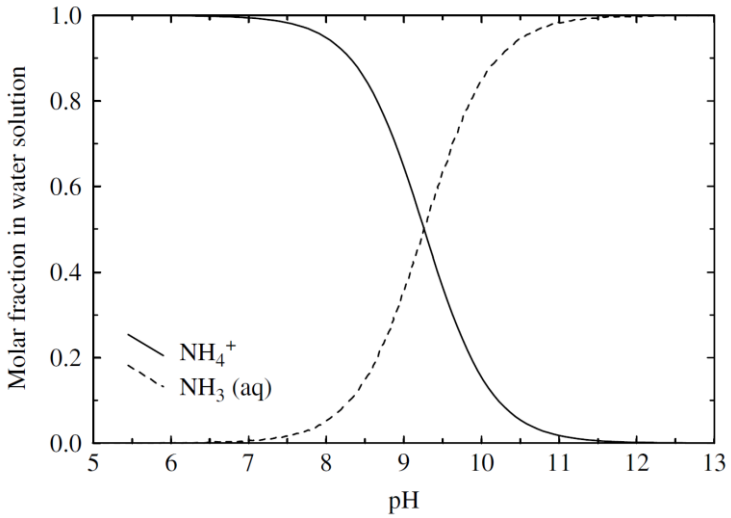

Figure 1.2 Distribution of ammonia species in water at T = 25 °C (Leyva-Ramos et al., 2004)

H_2S and CH_3SH. In contrast to NH_3, H_2S (both gas phase and liquid phase) should increase when the sludge pH is reduced from 8 to 7 according to Reaction 1.3 (Lewis, 2010; Sun et al., 2008). At pH around 7, the molar fraction of dissolved H_2S equals the molar fraction of HS^- (Figure 1.3). HS^- can be further converted into S^{2-} when pH is above 14 (Reaction 1.4). However, this pH condition is not applicable in this experiment. As the pH condition decreases from 8 to 7, more H_2S should be formed in sludge, and more H_2S should be found in biogas as well. Therefore, lowering the sludge pH would increase the H_2S concentration in biogas, which would potentially increase the risk of sulfur poisoning during the SOFC operation. Although, H_2S in biogas can be removed by the biochar column (BC). When the sludge pH is lower and the H_2S concentration in biogas is higher, more biochar might be required for H_2S removal. CH_3SH is expected to have a similar response to the change in pH as H_2S (Saleh et al., 1962).

Reaction 1.3 Conversion between H_2S and HS^-

$$H_2S_{(aq)} \leftrightarrow HS^- + H^+, K = 10^{-6.99}$$

Reaction 1.4 Conversion between HS^- and S^{2-}

$$HS^- \leftrightarrow S^{2-} + H^+, K = 10^{-17.4}$$

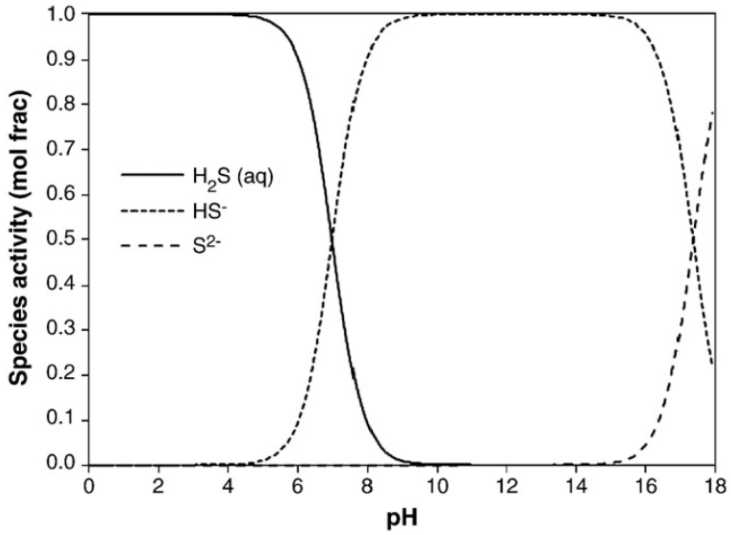

Figure 1.3 Distribution of sulfide species in water at T = 25 °C (Lewis, 2010)

1.3 Biochar Adsorption for H_2S Removal

Hydrogen sulfide (H_2S) is a contaminant in biogas that could be removed by a biochar column (BC). Biochar is produced through pyrolysis, a thermochemical process that converts organic matters to carbon-rich materials without oxygen being involved (Basu, 2018). Activated carbon is another commonly used adsorbent for H_2S removal. Activated carbon is a biochar that has been physically or chemically activated (Gęca et al., 2022). Both biochar and activated carbon are highly porous materials with large internal surface area. Their adsorption capacities depend on many factors, such as source material, pyrolysis temperature, adsorption temperature, contact time, local pH, and particle size. Activated carbon could be impregnated with an alkaline solution containing sodium hydroxide (NaOH) or potassium hydroxide (KOH) in order to enhance its H_2S removal capacity at a high adsorption temperature (550 °C) (Sitthikhankaew et al., 2011). However, impregnation lowers the ignition temperature of activated carbon (Shang et al., 2016). Therefore, high-temperature adsorption of H_2S with impregnated activated carbon presents a risk of self-ignition. On the other hand, most of biochar materials are alkaline, so that impregnation would not be necessary. Furthermore, biochar requires less energy to produce in comparison to activated carbon (Alhashimi & Aktas, 2017).

Waste organic materials such as cow manure can be reused to produce biochar for removing H_2S from the biogas produced by the AnMBR. Cow manure was prioritized in this experiment due to its waste reduction effect. Converting cow manure to biochar is also beneficial for pathogen elimination and disease transmission (Pell, 1997; Qin et al., 2019). Under the same biochar production temperature, the specific surface area (SSA) of the cow manure biochar is smaller when compared with other biochar materials derived from wastewater sludge and sawdust, indicating that the adsorption capacity of cow manure biochar is not optimum (Zhao et al., 2013). However, the adsorption capacity of the cow manure biochar could be improved by increasing the production temperature. Cow manure biochar has shown better performance for H_2S

removal in comparison to some of the other manure-based biochar. For example, under the same pyrolysis temperature (500 °C), cow manure has a higher adsorption capacity (29.81 mg H_2S/g) than pig manure (13.82 mgH_2S/g) and chicken manure (10.96 mgH_2S/g) (Su et al., 2021).

1.4 SOFC

Solid oxide fuel cells (SOFC) convert chemical energy directly to electrical energy through fuel oxidation at a high temperature (around 1000 °C) (Dwivedi, 2020). In this experiment, the biogas produced from synthetic concentrated blackwater was used as the fuel for SOFC. The main components of the SOFC are the cathode, anode, and solid electrolyte (Saadabadi et al., 2019). The solid electrolyte is a thin, porous layer that conducts oxygen ions between cathode and anode. At the cathode side, oxygen is reduced to oxygen ions (Reaction 1.5). Meanwhile, at the anode side, fuels are oxidized by the oxygen ions, and electrons are released (Reaction 1.6). Hydrogen (H_2) gas is an ideal fuel for SOFC (Saadabadi et al., 2019). In comparison, carbon monoxide (CO) molecules are larger than H_2 molecules, so that the diffusion and the oxidation of CO might be slower. Electrons released from the anode can flow to the cathode through an external circuit.

Reaction 1.5 Oxygen reduction at the cathode

$$0.5O_2 + 2e^- \rightarrow O^{2-}$$

Reaction 1.6 Fuel oxidation at the anode

$$H_2 + O^{2-} \rightarrow H_2O + 2e^-$$

$$CO + O^{2-} \rightarrow CO_2 + 2e^-$$

SOFC is a high-temperature fuel cell that is applicable for biogas conversion (Larminie & Dicks, 2003). Low-temperature fuel cells, such as alkaline (electrolyte) fuel cell (AFC) and proton exchange membrane fuel cell (PEMFC), must be fueled with hydrogen gas with high purity. SOFC, on the contrary, does not require hydrogen-rich gas as the fuel. High-temperature fuel cells, such as SOFC and molten carbonate fuel cell (MCFC), have faster kinetics than low-temperature fuel cells. MCFC can also use biogas for fuel oxidation. However, MCFC has corrosive electrolyte which might reduce its own lifespan, and additional carbon dioxide (CO_2) is required at the cathode side of MCFC.

SOFC shows significant advantages over typical energy conversion devices such as internal combustion (IC) engines and combined heat and power (CHP) systems. SOFC has a higher electrical efficiency than conventional devices. The electrical efficiency of SOFC can reach up to 50%, whereas the electrical efficiency of the conventional devices is generally between 35% and 38% (Santarelli, 2015). SOFC also has a high tolerance for the CO_2 fraction in biogas since CO_2 can be used as a methane reforming agent. An IC engine, for example, can only work with CO_2 up to 40% (Bari, 1996). Therefore, CO_2 reduction is recommended for IC engines powered by biogas. The performance of IC engines, as well as conventional CHP systems, is also restricted by ammonia (NH_3), which is a corrosive contaminant in biogas. However, ammonia can

be considered as an energy source for SOFC. Ammonia cracking can be performed internally in a SOFC when the temperature is at least 590 °C (Staniforth & Ormerod, 2003). Hydrogen (H_2) and nitrogen (N_2) are produced during this process, and electric power is produced through oxidation of H_2.

The SOFC performance is mainly influenced by fuel composition, cell materials (electrolyte, anode, and cathode), and operating temperature. The impacts of each factor have been further explained as follows with a focus on using biogas as the fuel.

Fuel composition. As the predominant compound in biogas, methane (CH_4) has a much lower electrochemical oxidation rate than H_2 and CO (Saadabadi et al., 2019). Methane reforming is a process where CH_4 is converted into H_2 and CO with the presence of a reforming agent: steam (H_2O) for steam reforming, oxygen (O_2) for partial oxidation, and carbon dioxide (CO_2) for dry reforming. Methane reforming can be either external or internal. In this project, internal dry reforming is performed, to minimize the investment cost. CO_2 is a dry reforming agent. CO_2 addition or exhaust gas recovery is recommended to avoid carbon deposition. Carbon deposition reduces the active area of the cell and promotes cell cracking due to local thermal stress. The risk of carbon deposition on the anode surface is higher when the molar ratio of CH_4 and CO_2 in biogas is greater than 1. Besides carbon deposition, sulfur poisoning is also a risk factor for biogas-fueled SOFC. As trace compounds in biogas, hydrogen sulfide (H_2S) and methyl mercaptan (CH_3SH) might poison the nickel-based anode by converting nickel (Ni) to nickel sulfide (NiS) (Haga et al., 2008; Karbanee et al., 2008; Saleh et al., 1962). As a result, the electrochemical activity of the cell reduces due to NiS precipitation.

Electrolyte material. Yttria-stabilized zirconia (YSZ) is the most widely used electrolyte material for SOFC (Dwivedi, 2020), even though there are other materials with more favorable properties. Scandia-stabilized zirconia (ScSZ), for example, has higher ionic conductivity and higher tolerance for H_2S poisoning than YSZ (Dwivedi, 2020; Saadabadi et al., 2019). However, ScSZ is not as prevalent as YSZ because of the limited availability and high cost of scandia (Dwivedi, 2020; Irvine et al.). The ionic conductivity of gadolinia-doped ceria (GDC) is even higher than the conductivity of ScSZ (Dwivedi, 2020; Zhang et al., 2020), but GDC is a mixed conductor for oxygen ions and electrons (Joshi et al., 2004; Larminie & Dicks, 2003), in which case, less electrons can be conducted externally by the current collector.

Anode material. The triple phase boundary (TPB) at the anode side is the area between the electrolyte and the anode, where oxygen ions from the electrolyte (ionic phase), react with fuel gas (gas phase), and release electrons conducted by the anode (electronic phase) (Saadabadi et al., 2019). Therefore, the anode material of SOFC requires high ionic conductivity, high porosity, and high electronic conductivity, in order to provide sufficient TPB. Ni-YSZ is the most common anode material for SOFC (Laosiripojana et al., 2009). It is a porous cermet layer (with porosity between 20% and 40%), consisting of Ni and YSZ, which are used for electronic conductivity and ionic conductivity respectively (Laosiripojana et al., 2009; Larminie & Dicks, 2003). Ni also acts as a catalyst for the methane reforming reactions, which elevates the risk of carbon deposition on the Ni-based anodes (Saadabadi et al., 2019). Ni-GDC is an alternative

to Ni-YSZ, with advantages such as promoting direct oxidation of methane for biogas-fueled SOFC, and extending TPB (Larminie & Dicks, 2003).

Cathode material. The main steps of the cathodic reaction are: (1) adsorption of oxygen molecules (O_2) on the surface of cathode or electrolyte, (2) disintegration of oxygen molecules into oxygen atoms (O), and (3) reduction of oxygen atoms to oxygen ions (O^{2-}) (Dwivedi, 2020). For cathode materials with high ionic and electronic conductivity (or mixed conductivity), the cathodic reaction takes place on the cathode surface. If the mixed conductivity of a cathode material is low, the cathodic reaction can happen at the TPB of the cathode side, which is the interactive area among oxygen, electrolyte, and cathode. Strontium-doped lanthanum manganite (LSM) is the most commonly used cathode material for SOFC (Laosiripojana et al., 2009; Larminie & Dicks, 2003). Lanthanum manganite ($LaMnO_3$) is a type of mixed conductor with the perovskite structure that has vacancies for O^{2-} (Dwivedi, 2020). The purpose of doping lanthanum manganite with strontium (Sr) is to enhance its electronic conductivity (Laosiripojana et al., 2009). In comparison to YSZ, LSM has similar thermal expansion coefficient, but lower ionic conductivity. Lanthanum strontium cobalt ferrite (LSCF) is an alternative cathode material, especially for SOFCs operated at lower temperature (500 °C – 600 °C) (Kenney & Karan, 2005). In cases where YSZ is used as the electrolyte material, a ceria-based layer between the electrolyte and the cathode is recommended in order to prevent reactions between YSZ and the cathode material (Laosiripojana et al., 2009).

Operating temperature. The operating temperature for biogas-fueled SOFC depends on the pathway of methane reforming. Methane steam reforming (MSR) is a highly endothermic reaction operated around 700 °C (Reaction 1.7) (Mogensen et al., 2014; Saadabadi et al., 2019; Saebea et al., 2020). H_2 and CO are reforming products in MSR. CO can react with the remaining H_2O to produce H_2 and CO_2. This exothermic reaction is known as the water-gas shift (WGS).

Reaction 1.7 Steam reforming

$$CH_4 + H_2O \leftrightarrow 3H_2 + CO, \Delta H_{298}^0 = 206.3\ kJ/mol$$

$$CO + H_2O \leftrightarrow H_2 + CO_2, \Delta H_{298}^0 = -41.1\ kJ/mol\ (WGS)$$

Partial oxidation (POX) is a series of exothermic reactions between CH_4 and O_2 (Reaction 1.8) (Saadabadi et al., 2019). The heat generated in POX increases with the O_2 availability. Stable POX operation can be achieved around 750 °C (Zhan et al., 2006).

Reaction 1.8 Partial oxidation

$$CH_4 + 0.5O_2 \leftrightarrow 2H_2 + CO, \Delta H_{298}^0 = -44\ kJ/mol$$

$$CH_4 + O_2 \leftrightarrow 2H_2 + CO_2, \Delta H_{298}^0 = -332\ kJ/mol$$

$$CH_4 + 2O_2 \leftrightarrow 2H_2O + CO_2, \Delta H_{298}^0 = -803.03\ kJ/mol$$

In this project, methane content in biogas is reduced through dry reforming, which is an endothermic reaction between CH_4 and CO_2 (Reaction 1.9) (Saadabadi et al., 2019). Dry forming has a higher standard enthalpy of reaction (ΔH^0) than MSR (247.3 kJ/mol versus 206.3 kJ/mol). Therefore, dry reforming requires a higher temperature (800 °C – 1000 °C) to maintain a stable operation. H_2 and CO are produced in the dry reforming reaction. H_2 also reacts with the remaining CO_2, to produce CO and H_2O. This is an endothermic reaction called the reverse water-gas shift (RWGS).

Reaction 1.9 Dry reforming

$$CH_4 + CO_2 \leftrightarrow 2H_2 + 2CO,\ \Delta H^0_{298} = 247.3\ kJ/mol$$

$$H_2 + CO_2 \leftrightarrow CO + H_2O, \Delta H^0_{298} = 41.1\ kJ/mol\ (RWGS)$$

The risk of nickel reoxidation is relatively higher for dry reforming because of its high operating temperature (Saadabadi et al., 2019). Ni is an anode catalyst that can be re-oxidized either by oxygen ions passing through the electrolyte if the amount of available fuel gas is insufficient, or by oxygen molecules that escape from the cathode side due to failure of sealing. Nickel reoxidation can cause cell or sealing fractures induced by volume expansion.

The operating temperature also affects the mechanism and probability of carbon deposition. CH_4 and CO are the main contributors to carbon deposition. When the operating temperature is above 700 °C, carbon deposition is mainly driven by the pyrolysis of CH_4 where CH_4 is converted to H_2 and C (Reaction 1.10) (Saadabadi et al., 2019; Yoon et al., 2004). Another pathway of carbon deposition is disproportionation of CO (reserve Boudouard reaction). In this case, CO is converted to CO_2 and C. Although, when temperature is above 700 °C, the formation of CO (Boudouard reaction) is thermodynamically favored instead (Hunt et al., 2013; Speight, 2019). According to the ternary diagram of C-H-O where the carbon deposition region is indicated (Saadabadi et al., 2019), when temperature increases, the location of biogas within the diagram moves further away from the carbon deposition region, meaning the risk of carbon deposition is lower when the operating temperature is higher.

Reaction 1.10 Carbon deposition

$$CH_4 \leftrightarrow 2H_2 + C, \Delta H^0_{298} = 75.6\ kJ/mol$$

$$2CO \leftrightarrow CO_2 + C, \Delta H^0_{298} = -173\ kJ/mol$$

1.5 Research Questions and Hypotheses

In this research project, the SOFC operational strategy in relation to the AnMBR pH was investigated, based on the following research questions: (Q1) How does biogas composition change when the AnMBR pH is reduced from 8 to 7? (Q2) How to operate SOFC using the conditioned biogas?

Hypothesis about Q1. According to the theoretical correlation between the biogas composition and the AnMBR pH as explained in *section 1.2 Biogas Composition w.r.t.*

AnMBR pH, it was expected that when the AnMBR pH was reduced from 8 to 7, the ratio between CH_4 and CO_2 would be more balanced (closer to 1), and the H_2S concentration would increase. The AnMBR pH would also affect the NH_3 and CH_3SH concentrations: as pH decreases, the NH_3 concentration would decrease, while the CH_3SH concentration would increase. Although, NH_3 and CH_3SH are the minor compounds that are less relevant to the research scope, so their concentrations were only monitored to verify the hypothesis. The implications of the changes in NH_3 and CH_3SH concentrations were not discussed in this paper.

Hypothesis about Q2. Biochar adsorption and CO_2 addition could be applied to condition the AnMBR biogas, so that during the SOFC operation, sulfur poisoning and carbon deposition could be avoided by biochar adsorption and CO_2 addition respectively. It was expected that biochar adsorption is favorable under pH 8, whereas CO_2 addition is favorable under pH 7. The exhaust gas discharged from the SOFC could also be recycled to adjust the ratio between CH_4 and CO_2 in the biogas. If exhaust gas recycling is employed instead of CO_2 addition, the CH_4 concentration in the conditioned biogas is expected to be lower, because in comparison to pure CO_2, exhaust gas would contain other compounds besides CO_2, and more exhaust gas would be required to balance the CH_4/CO_2 ratio.

2. Materials

2.1 AnMBR

The experimental set-up of the AnMBR unit is illustrated in Figure 2.1 and Photo 8.1. In the center of the set-up was an anaerobic digester (bioreactor) with 5.5 L of sludge. Around the bioreactor was a water bath layer, where the warm demi water (around 37 °C) was recirculated externally by a water circulator (Tamson TC16), which was set at a higher temperature (42.5 °C) to compensate the heat loss. The feed for the bioreactor was synthetic backwater, which was prepared 3 times a week (8 L on Mondays and Wednesdays, and 10 L on Fridays) according to the recipe shown in Table 2.1. The target COD concentration of the feed water was 5 g/L. The feed water was synthetic blackwater which was prepared in the lab to simulate the real blackwater with COD concentration around 5.5 g/L (Lettinga et al., 1993). The micronutrients solution as part of the ingredients was prepared separately according to the recipe shown in Table 2.2. These recipes were generated based on a literature article with modified concentrations (Ozgun et al., 2019). The feed bucket was stored in a fridge (around 9.4 °C), and the feed water was continuously mixed by the stirrer placed above the feed bucket. The acid control bottle with 2M of HCl was installed in the later stage of the experiment to maintain the sludge pH around 7, which was only necessary when the target AnMBR pH was 7. The sludge was continuously mixed within the bioreactor through an external recirculation flow, where the sludge was pumped from the bottom of the bioreactor to the top, while passing an ultrafiltration membrane unit (Pentair PVDF Helix membrane with the pore size of 30 nm). The permeate extracted from the membrane unit was collected in a bucket. Air was pumped into the bioreactor for micro-aeration. The micro-aeration pump was plugged to an automatic power switch, which would turn the power on or off every 4 hours. When the micro-aeration pump was on, the air flowrate was controlled around 0.2 L/d. An empty bottle (gas buffer) was installed between the bioreactor and the gas meter (Ritter MGC-1 PMMA with the volume measuring chamber of 3.3 mL). It would act as a buffer when the sludge level was too high or too low: when the sludge level was too high, the excessive sludge would flow into the bottle instead of the gas meter; when the sludge level was too low, the vacuum pressure above the sludge (headspace of the bioreactor) would draw the packing liquid (Ritter Silox) of the gas meter into the bottle instead of the bioreactor. A gas bag filled with pre-collected biogas could be attached to the top of the bioreactor to compensate the pressure change within the headspace when the sludge was mixed manually or when it was extracted from the bioreactor. The performance of the bioreactor was monitored by a lab computer, which was plugged to a power supply unit (Green Cell Micropower 800). It would protect the computer and ensure the consistent operation of AnMBR in case of an unexpected power shut-down. In total, 5 pumps were used in this experiment, including 4 low-capacity pumps (Watson-Marlow 120U) for feed supply, acid control, permeate extraction, and micro-aeration, and 1 high-capacity pump (Watson-Marlow 520Du) for sludge recirculation.

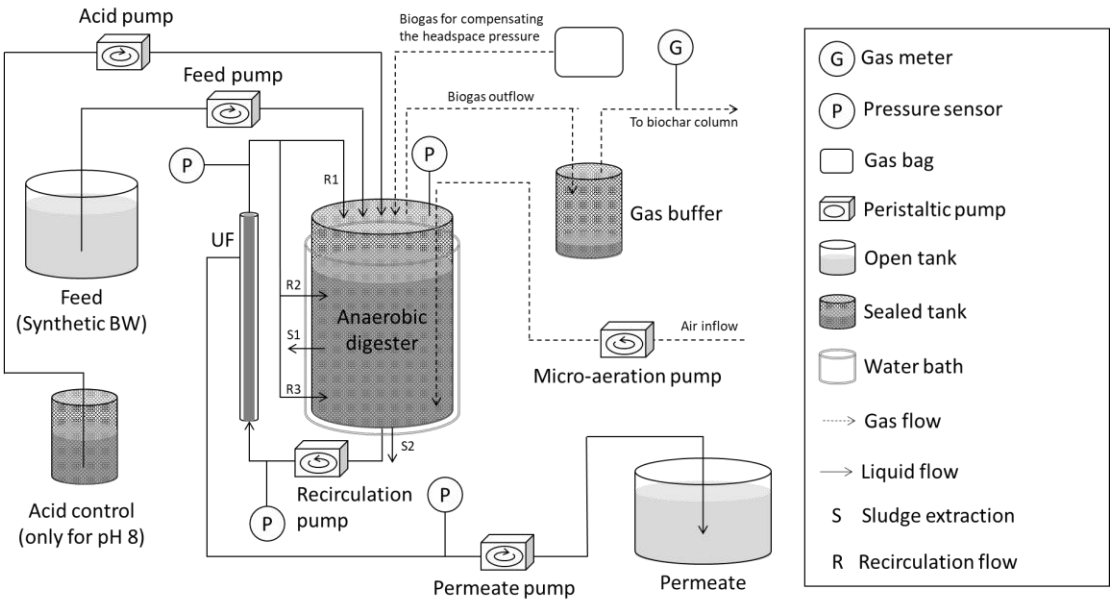

Figure 2.1 Experimental set-up of AnMBR

Table 2.1 Recipe for the synthetic backwater

Compound	Concentration	Unit
Urea	1.00	g/L
Ammonium chloride	0.80	g/L
Sodium acetate trihydrate	2.60	g/L
Ovalbumin	0.18	g/L
Magnesium sulphate heptahydrate	0.072	g/L
Potassium phosphate monobasic	0.20	g/L
Calcium chloride dihydrate	0.14	g/L
Cellulose	1.50	g/L
Milk powder	0.60	g/L
Yeast extract	0.50	g/L
Micronutrients	10.64	mL/L
Sunflower oil	2.00	Drops/L
Humic and fluvic acid	2.00	Drops/L

Table 2.2 Recipe for the micronutrients solution

Compound	Concentration	Unit
Iron (III) chloride hexahydrate	1000	mg/L
Cobalt (II) chloride hexahydrate	1000	mg/L
Manganese (II) chloride tetrahydrate	250	mg/L
Copper (II) chloride dihydrate	15	mg/L
Zinc chloride	25	mg/L
Boric acid	25	mg/L
Ammonium heptamolybdate tetrahydrate	45	mg/L
Sodium selenite	45.286	mg/L
Nickel (II) chloride hexahydrate	25	mg/L
Ethylenediaminetetraacetic acid	500	mg/L
Resazurin sodium salt	250	mg/L
Yeast extract	1000	mg/L
Hydrochloric acid 37%	0.486	mL/L

2.2 Biochar Column

The schematic design of the biogas cleaning system is demonstrated in Figure 2.2 and Photo 8.2. The biochar column (BC) was made in the lab with a rigid transparent acrylic tube and fittings for the top and bottom connections. The BC was packed with glass beads (borosilicate with diameter of 1 mm) on the bottom, cow manure biochar in the middle, and more of the same glass beads on the top. The particle size of the cow manure biochar ranged between 0.105 mm and 0.25 mm, which was obtained by filtering the biochar with two sieves. When the BC was connected to the AnMBR after the gas meter, the biogas produced by the AnMBR would enter the BC from the bottom and exit the BC from the top. After the biogas was processed by the BC, it was collected in a gas bag (Tedlar PLV gas sampling bag with maximum capacity of 25 L). An extra outlet was available for sampling the processed biogas gas, in which case a small gas bag (Tedlar PLV gas sampling bag with maximum capacity of 0.6 L) was used for biogas collection instead. The dimensions of the BC shown in Figure 2.2 are based on the BC that was used for the breakthrough tests and the continuous biogas cleaning from Day 226 to Day 244. A new BC was made according to the same dimensions for other biogas cleaning experiments. Even though the dimensions of the old BC and the new BC were similar, the inside diameter (ID) of the new BC (0.60 cm) was slightly different from the old BC (0.58 cm). The fittings for the top connection and the bottom connection were also longer for the new BC (3.8 cm between the transparent tube and the mash), so that the glass beads on the bottom of the new BC (4.0 cm in height) was barely visible, as most of them were contained in the fittings for the bottom connection.

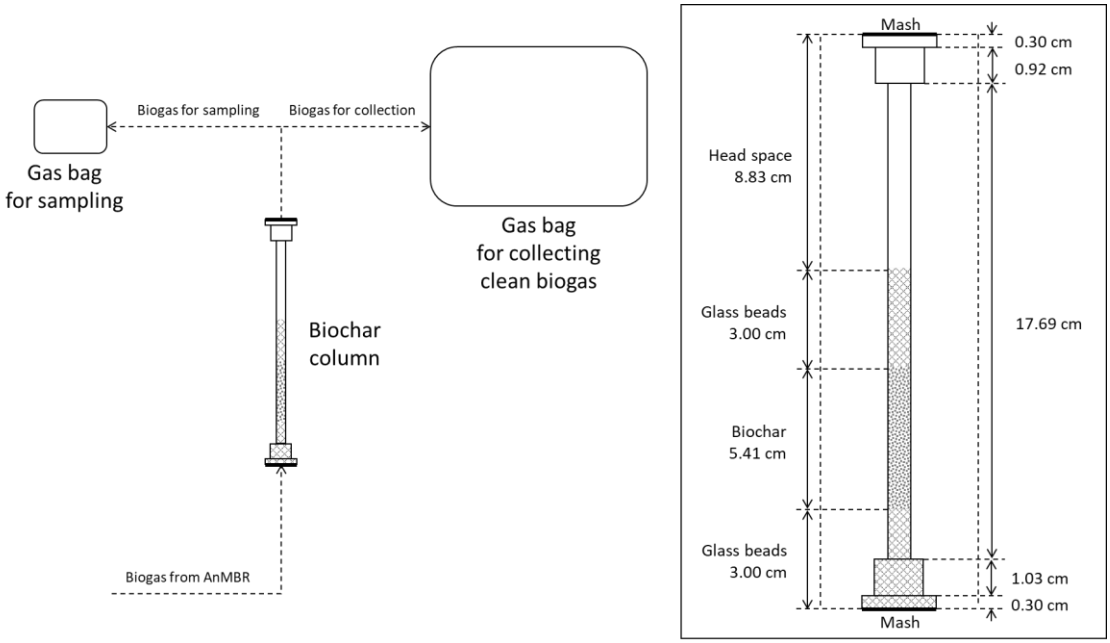

Figure 2.2 Experimental set-up of BC for H_2S removal under pH 8 (with the initial biochar height)

2.3 SOFC

The SOFC was prepared according to Figure 2.3 and Figure 2.4, where the components of the cell and the order of installation were presented. After the cell was prepared, it was flipped upside down and then placed on top of the furnace. The core of the set-up was an anode supported cell (Fiaxell 2R-Cell D25) (Photo 8.5 and Photo 8.6), comprising an anode (NiO-YSZ) for fuel oxidation, an electrolyte (YSZ) for O^{2-} conduction, and a cathode (GDC layer + LSCF) for O_2 reduction. The anode diameter was 25 mm, whereas the cathode diameter was 14 mm. The maximum current allowed according to the supplier is 5 A. Therefore, the current density of the cell could reach up to 3248 mA/cm^2. The fuel gas would enter the anode side of the cell by passing through the nickel plate (I) and the nickel foam (G). The nickel plate was the platform where the inlet of the fuel gas, the outlets of the exhaust gas, and the electrical connections of the anode were installed. The nickel foam was installed for enhancing diffusion and catalytic oxidation of the fuel gas. The diameter of the nickel foam was 20 mm. Between the nickel foam and the cell was a layer of mica sealing (H), which would isolate the exhaust gas from the anode for the purpose of recycling. On the other side of the cell, air was supplied from the entrance of the stainless steel plate (A), which was separated from the cathode of the cell by the alumino-silicate layers (B, C, and E) and the gold mash layer (D). Air would enter and exit through the alumino-silicate layers, while electrons would be conducted by the gold mash and wires. Alumino-silicate is also known as the refractory ceramic fiber, a porous material used for gas diffusion, thermal resistance, and electrical insulation (Maxim & Utell, 2014; Mehta et al., 2018). Gold (Au) has a high electrical conductivity, and it is resistant to corrosion and oxidation (Goodman, 2002). 1 of the 2 gold wires was used for current collection, which could carry maximum 7 A of current according to the supplier. The other gold wire was used as the connection for the cathode potential measurement.

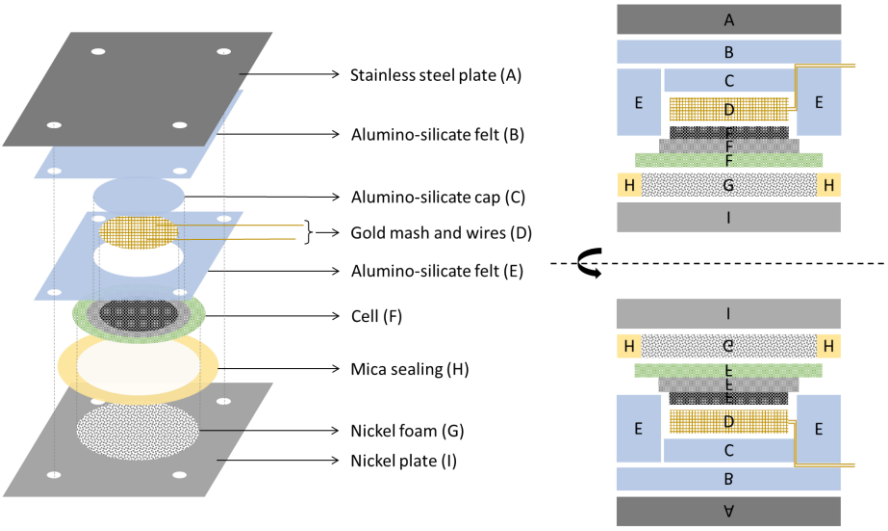

Figure 2.3 Components of the cell

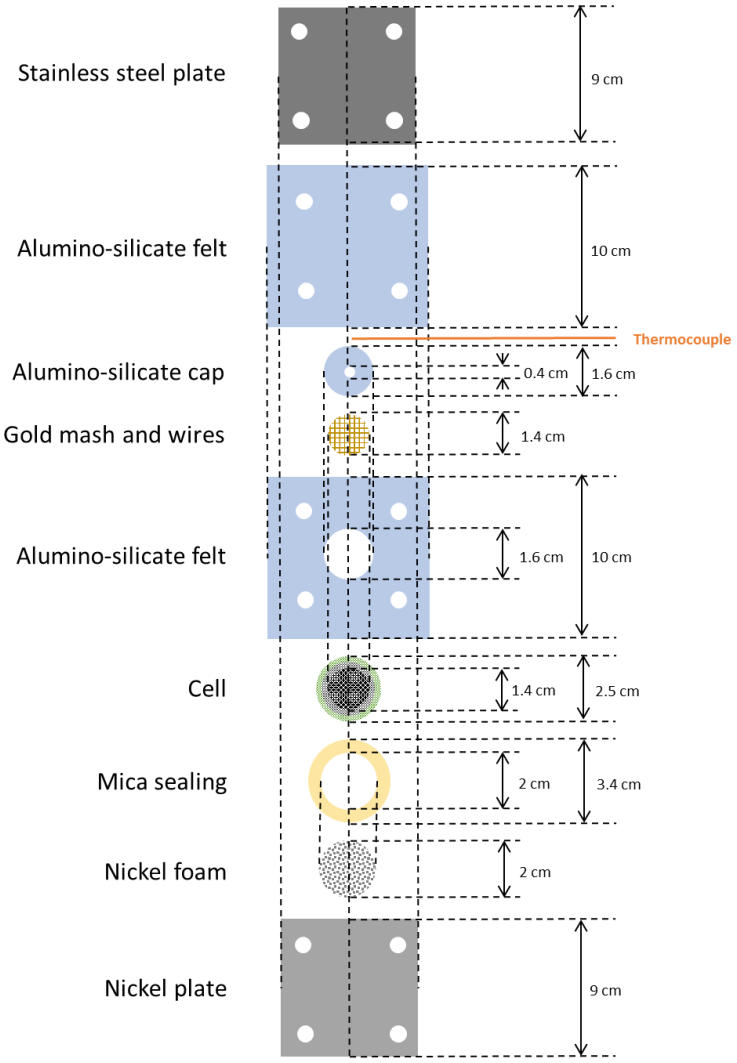

Figure 2.4 Mounting method for the 2R-Cell D25 which allows exhaust recovery

The overall experimental set-up of SOFC is shown in Figure 2.5 and Photo 8.3. This figure was adapted from the schematic design in another research article (van Linden et al., 2022). In comparison to the original schematic design, a few changes were made in this figure: (1) the liquid fuel was replaced by the gas bag containing the conditioned biogas; (2) the thermocouple wire connected with the anode was removed; (3) multimeter was removed and the sense terminal of the electronic load was used for measuring voltage instead; (4) a gas bag was added to the outlet for collecting exhaust; (5) the power generator was removed since the voltage loss can be compensated by the sense terminal of the electronic load; (6) the plastic tubes and fittings were replaced with the stainless steel ones from Swagelok. The mounted cell was heated by a furnace (Kittec SQ11 with maximum temperature setting of 1320 °C). The anode temperature and the cathode temperature during the operation were measured by a K-type thermocouple wire, which was connected to the thermometer (Lutron TM-947SD). The anode potential and the cathode potential were measured from the sense terminals of the electronic load (Rigol DL3021). The electric current from the cathode to the anode was captured by the same electronic load. The exhaust gas from the anode was cooled by an exhaust scrubber (filled half way with water), measured by a flowmeter (Ritter flowmeter with the measuring range between 0.5 L/h and 4.0 L/h), and then collected in a gas bag (Tedlar PLV gas sampling bag with maximum capacity of 25 L). Besides N_2 from the biogas itself, the exhaust gas should mainly consist of CO_2 and H_2O, which are the products of fuel oxidation. Although, CO might be in the exhaust gas as well due to incomplete utilization of the fuel. Therefore, collecting exhaust gas would not only provide the opportunity of recycling CO_2 for biogas conditioning, but also prevent CO from escaping to the environment.

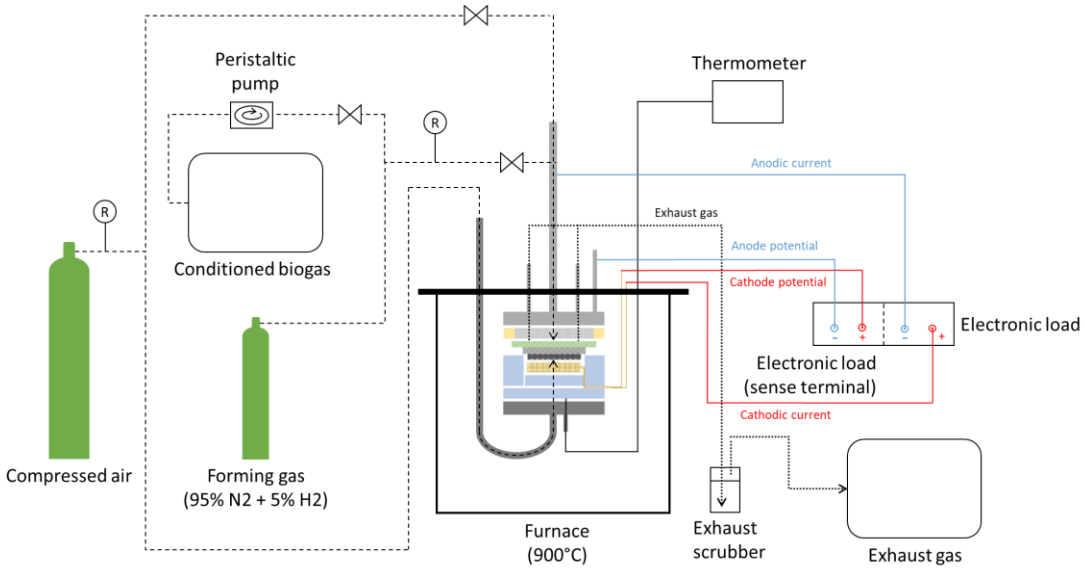

Figure 2.5 Experimental set-up of SOFC

3. Methods

3.1 Overview of the Experiment

The overall process of the AnMBR-BC-SOFC system has been illustrated Figure 3.1. The AnMBR was applied for treating synthetic blackwater, while producing biogas, permeate, and waste sludge. The biogas produced by the AnMBR was further processed by the BC for H_2S removal. CO_2 was added to the biogas so that the ratio between CH_4 and CO_2 would be 1:1. Alternatively, the exhaust gas produced by the SOFC could be recycled for CO_2 addition. Finally, the conditioned biogas was injected to the anode side of the SOFC and utilized for producing electricity. In the meantime, air was injected to the cathode side of the SOFC for oxidation.

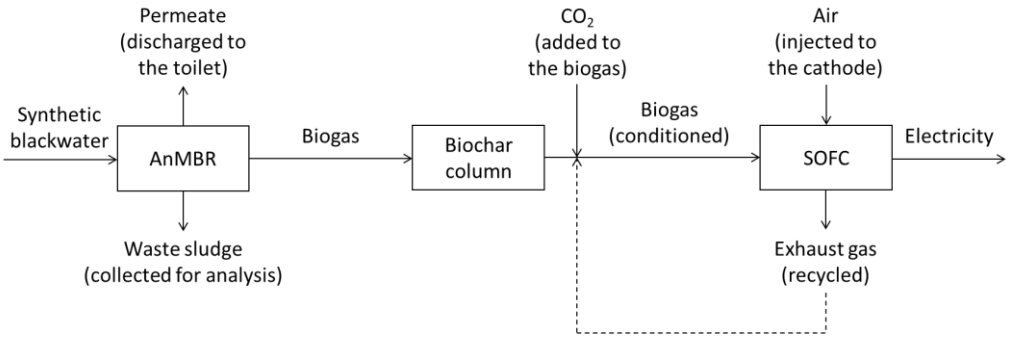

Figure 3.1 Process overview

3.2 Operational Procedure of AnMBR

Preparing and changing feed water. New feed water was prepared three times a week (8L on Mondays and Wednesdays, and 10L on Fridays). The feed water was changed according to the following steps: (1) the old feed bucket in the fridge was removed and replaced with the new feed bucket, where the feed water was continuously mixed by a mechanical stirrer; (2) the tubes and fittings for the feed flow were removed from the bioreactor, while the opening was temporarily sealed with a cap; (3) the tubes and fittings were cleaned by flushing with warm tap water; (4) after the cap was removed, the entrance of the feed flow was cleaned with a brush; (5) the tubes and fittings for the feed flow were re-connected to the bioreactor; (6) the connection (inside and outside) for the entrance was sealed with the PTFE tape; (7) the feed water was pumped to the entrance without introducing air to the bioreactor (the entrance valve was closed while the sampling valve was open); (8) the feed flowrate was calibrated manually from the sampling point until the target flowrate was reached (2.5 L/d); (9) the feed water was pumped to the bioreactor at the target flowrate (the entrance valve was open while the sampling valve was closed).

Mixing and extracting sludge. The headspace pressure would be interfered when sludge was mixed or extracted from the bioreactor. Therefore, the gas bag containing pre-collected biogas was connected to the bioreactor for compensating the headspace pressure. The bioreactor was equipped with three recirculation outlets (see R1, R2 and R3 in Figure 2.1), and two sampling points (see S1 and S2 in Figure 2.1). Sludge was

recirculated from the bottom of the bioreactor to the top (R1), while the side connections (R2 and R3) were closed. During mixing, reverse recirculation was applied when the top connection (R1) was closed, and the side connections (R2 and R3) were open. Sludge was also mixed manually with a syringe through the sampling points (S1 and S2). Sludge was extracted equally from both sampling points (S1 and S2) during the working days to maintain a constant SRT. The target sludge extraction rate was 0.275 L per working day (or 0.196 L/d).

Collecting permeate. Permeate was extracted from the membrane unit at 2.3 L/d. The permeate pump was calibrated on daily basis to achieve the target flowrate. The permeate was collected in a bucket and discharged twice a week.

Monitoring mass balance. After the daily maintenance on the bioreactor was completed, and the headspace pressure returned to the normal level (around 4 mbar), all the pumps (except for the recirculation pump) were turned off so that the feed water bucket, the permeate bucket and the acid bottle (only applicable when the sludge pH was around 7) could be weighed. As soon as the reading on the gas meter and the sludge level were recorded, all the pumps were turned back on. This moment was considered as the initial time for the mass balance calculations. The same procedure was repeated right before the daily maintenance started the next day. In this way, the mass balance of the bioreactor could be monitored every day, based on the changes in the feed water bucket, the permeate bucket, the acid bottle, the gas meter, and the sludge level.

Cleaning and replacing the membrane unit. The AnMBR was operated with an old membrane unit at the beginning of the experiment. It was replaced on Day 34 with a brand-new membrane unit, which was cleaned on Day 237, Day 286, and Day 322. The second membrane unit was replaced on Day 342 with a used membrane unit whose conditions were acceptable for re-use. The third membrane unit was cleaned before installation. The two schemes that were used for membrane cleaning have been illustrated in Figure 3.2 and Figure 3.3, and the cleaning procedures have been summarized in Table 8.1, Table 8.2, and Table 8.3 (see Appendix A). The duration of each step was the total time required for counterclockwise recirculation and clockwise recirculation.

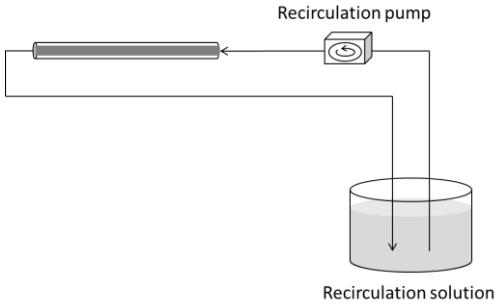

Figure 3.2 Membrane cleaning scheme A (recirculation)

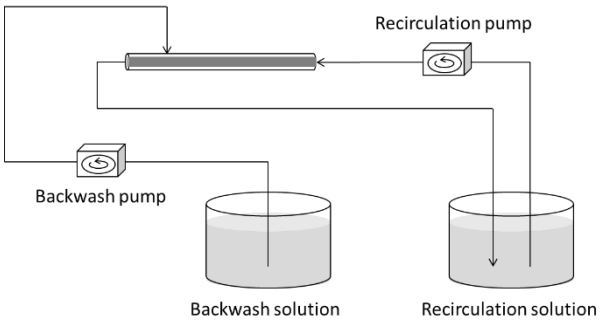

Figure 3.3 Membrane cleaning scheme B (recirculation and backwashing)

Measuring the flowrate of micro-aeration. One micro-aeration cycle was 8 hours (4 hours on and 4 hours off). The flowrate of the micro-aeration was measured with the displacement method (Figure 3.4) and calculated based on the volume of the collected air and the collection period.

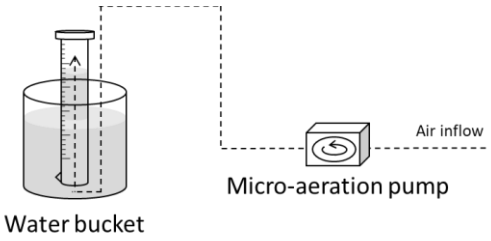

Figure 3.4 Displacement method for measuring the micro-aeration flowrate

Titration and acid addition. A titrator (Metrohm 702 SM Titrino) was used to test the alkalinity of the sludge under pH 8 and the amount of acid required for changing the sludge pH from 8 to 7. The target pH was 4.3 for the alkalinity test (single test with 0.1M HCl) and 7 for the other test (two duplicate tests with 0.1M HCl and 1M HCl respectively). In each titration test, the volume of the sludge sample was 15 mL. The HCl solution was added to the sludge sample by the titrator automatically until the target pH was reached, and the amount of HCl solution required was recorded at the end of each test. Based on the test results, the total alkalinity of the sludge was calculated (Equation 8.1), and the amount of acid required for changing the sludge pH from 8 to 7 was estimated.

3.3 Performance Indicators of AnMBR

AnMBR pH and other parameters of the sludge. The sludge level was observed before and after daily maintenance. A probe (Endress+Hauser Memosens CPS16E) was incorporated into the bioreactor on the top to measure the pH, OPR, and temperature of the sludge inside of the bioreactor. The readings of the probe were constantly logged by the PC. During daily maintenance, pH of the AnMBR sludge was also measured manually with a pH meter (WTW IDS 9430) right after the sludge was extracted from the bioreactor. The target solid retention time (SRT) for the sludge was 28 days. The actual SRT was determined based on the accumulative sludge extraction rate and the average sludge volume (5.5 L).

Organic loading rate (OLR) and chemical oxygen demand (COD) removal efficiency. Feed water COD, permeate COD, sludge total COD, and sludge soluble COD were measured 2-3 times a week in triplicates with the Hach COD test kit, including COD reagents, DRB200 reactor, and DR3900 spectrophotometer. To prepare the sludge soluble COD samples, the sludge samples collected from the reactor were centrifuged at 18500 g for 10 minutes, and then filtered with the 0.2 μm PES syringe filters. The OLR was determined by the sludge level observed, as well as the flowrate and COD concentration of the feed water. The COD removal efficiency was calculated based on COD balance of the feed water and the permeate (see Equation 8.2 in Appendix C).

Biogas composition. Biogas samples collected from the bioreactor were measured in triplicates with the gas chromatography device (GC-biogas, Agilent 7890A) for determining biogas compositions. The area under the peak for each compound was reported by GC. The percentage of each compound was calculated based on the area under the peak and the corresponding calibration curve. It was assumed that O_2 detected by GC was from the ambient environment during sampling, and should not be considered as part of the biogas. The percentage of N_2 associated with air was also deducted from the total N_2 percentage. The biogas compositions in terms of CO_2, N_2, and CH_4 were normalized so that the percentage of all the gas compounds would add up to be 100% in total.

Biogas production rate. The biogas production rate was calculated based on the amount of biogas produced and the change in sludge level from the end of the maintenance to the start of the next maintenance (Equation 8.3).

Methane production rate and efficiency. Methane production rate was determined by the biogas production rate and the biogas composition (Equation 8.4). The ideal gas law was applied to calculate the COD of produced methane (Equation 8.5). Methane production efficiency was calculated based on the COD of produced methane and the influent COD (Equation 8.6).

Solids concentrations and biomass growth. Sludge samples extracted from the bioreactor were measured once a week in triplicates for total solids (TS), volatile solids (VS), total suspended solids (TSS), and volatile suspended solids (VSS). 10 mL of sludge was applied for each measurement. Aluminum trays (for TS and VS) and aluminum trays packed with 0.7 μm glass fiber filters (for TSS and VSS) were burned in a furnace at 550 °C for 2 hours before the sludge samples were applied. Then, the samples were placed in an oven at 105 °C for at least 24 hours for TS and TSS measurements and burned at 550 °C for 2 hours for VS and VSS measurements. The biomass growth was determined by the weekly change of VSS content in the sludge.

Volatile fatty acids (VFA). The samples used for measuring permeate COD and sludge soluble COD were also tested in triplicates with gas chromatography (GC-VFA, Agilent 7890A) for VFA concentrations. VFA measurements were conducted 2-3 times a week. The VFA results were reported by GC as mass concentrations. For the total COD of VFA, the mass concentrations were further converted into COD concentrations. The total COD was used in this case to monitor the VFA level in the sludge overtime, so that acidification due to VFA accumulation could be avoided.

COD balance. COD balance was monitored based on the influent COD, effluent COD, COD of produced methane, and COD of extracted sludge. From Day 15 to Day 145, it was aimed to determine COD balance twice a week over the period of one day, during which the COD concentrations of the feed water and the permeate were assumed to be constant. From Day 146 to Day 369, COD balance was determined only once a week, but the COD concentrations of the feed water and the permeate were measured at the beginning and the end of the one-day period which was considered for COD balance.

Specific methanogenic activity (SMA). The SMA of the sludge collected under different pH conditions (pH 8 and pH 7) was measured with an automatic methane potential test system (AMPTS). The substrate was prepared with sodium acetate trihydrate ($C_2H_9NaO_5$), micronutrients solution, and demineralized water (see Table 8.4 in Appendix A). The micronutrients solution was the same one used for preparing the feed water. The ratio between the micronutrients solution and the substrate was 10.64 mL/L for the SMA tests, which was also consistent with the ratio used for preparing the feed water. The COD concentration of the substrate was designed to be 2 g/L. The amount of substrate used in each SMA test was adjusted according to the sludge VSS, so that the sludge VSS and the substrate COD ratio was 2 g/g (Table 8.5). The sludge VSS in this case was estimated. However, for the SMA calculation, the sludge VSS was determined based on measurement results. 6 test bottles were prepared for each SMA test, including 3 bottles for negative control and 3 bottles for substrate addition (Table 8.6 and Table 8.7). 250 mL of sludge was applied in each bottle and the total volume of each bottle was 400 mL. Each bottle was equipped with a mechanical stirring device, a clamp at the inlet, and a one-way valve at the outlet. Before the bottles were placed in the water bath (37°C), they were flushed with N_2 for 2 minutes. The inlet of each bottle was only used for flushing and should be clogged with the clamp at the end of flushing. The outlets of the sample bottles were connected to the inlets of the buffer bottles which were used for CO_2 absorption (Table 8.8). 80 mL of buffer solution was applied in each buffer bottle. The outlets of the buffer bottles were connected to the gas volume measuring device where CH_4 production was recorded. The test period for SMA was around 10 days. The specific methane production over time was calculated and plotted for each SMA test, where the average methane production of the negative control bottles was subtracted from the average methane production of the substrate bottles (Equation 8.7). SMA was represented by the slope of the steepest part of each curve.

Biochemical methane potential (BMP). The BMP of the sludge collected under pH 8 was measured with another AMPTS device. 3 types of samples were tested in triplicates (9 samples in total), including 3 negative control samples, 3 positive control samples, and 3 samples for substrate addition (Table 8.9). Each test bottle was filled with 300 mL of sludge. For positive control samples, cellulose with mass concentration of 5 g/L was added as the feed. To calculate the amount of cellulose required in each test bottle for positive control, the sludge VS was measured in prior to the BMP test and the cellulose was assumed to be 100% volatile. The VS ratio between the sludge and the cellulose was designed to be 2 g/g. The COD concentration of cellulose and feed water was measured with the Hach COD test kit, to determine the amount of feed water required for substrate addition, so that the COD content in the positive control bottles

was the same as the COD content in the substrate bottles. Each test bottle was filled up to 400 mL. The procedure for flushing the test bottles with N_2 and installing them in AMPTS was the same for the SMA test and the BMP test. Although, the BMP test would take longer than the SMA test so that the cellulose or the feed water added to the test bottles would be exhausted at the end of the BMP test. The methane production over time attributed to cellulose addition and feed water addition was determined by subtracting the average methane production of the negative control bottles from the average methane production of the positive control bottles and the average methane production of the substrate bottles respectively (Equation 8.8). BMP was obtained by dividing the accumulative methane production at the end of the BMP test by the COD content of cellulose (for positive control bottles) or feed water (for substrate bottles).

Transmembrane pressure (TMP), flux and permeability. TMP of the membrane unit was automatically calculated and continuously logged by the PC, according to the readings provided by the three pressure sensors for monitoring the feed pressure (pressure of the sludge entering the membrane unit from the bottom), the concentrate pressure (pressure of the sludge exiting the membrane unit from the top), and the permeate pressure (Equation 8.9). Flux was determined based on the permeate flowrate measured upon daily calibration, and the membrane area (0.0105 m^2) (Equation 8.10). Permeability, also known as the temperature compensated specific flux (TCSF), was calculated using flux and TMP (Equation 8.11) and adjusted according to the sludge temperature (37 °C).

3.4 Measuring the Adsorption Capacity of the Biochar

The breakthrough tests were conducted in a fume hood, separately from the AnMBR set-up. The aim of the breakthrough tests was to evaluate the adsorption capacity of the biochar, which would be used for removing H_2S from the biogas produced by the bioreactor. The following procedure was applied for the breakthrough tests.

Step 1. Biogas was collected from Day 162 to Day 202 for the breakthrough tests. The initial H_2S concentration of the biogas was 20 ppm according to the Dräger tubes (Hydrogen Sulfide 1/c, 10 – 200 ppm).

Step 2. The biochar characteristics were determined. The cow-manure based biochar was sieved so that the range of the particle size was between 0.25 mm and 0.63mm. Preliminary breakthrough tests were conducted to determine the target mass of biochar required for adsorption. According to the test results, at least 0.21 g of biochar was required to avoid immediate breakthrough. Therefore, approximately 0.21 g of biochar with particle size ranging from 0.25 mm to 0.63mm was used in the first breakthrough test (Test 1). Subsequently, the particle size of the biochar was reduced to 0.105 mm – 0.25 mm in the second breakthrough test (Test 2), while the target mass remained the same. The biochar density was measured in prior to each breakthrough test. The target height was calculated based on the measured biochar density, the measured biochar mass, and the inside diameter of the column (0.58 cm). The biochar characteristics have been summarized in the following table (Table 3.1).

Table 3.1 Biochar characteristics (Test 1 and Test 2)

Parameter	Biochar (Test 1)	Biochar (Test 2)
Particle Size [mm]	0.25 - 0.63	0.105 - 0.25
Density [g/cm3]	0.3308	0.3960
Target Mass [g]	0.2100	0.2100
Target Height [cm]	2.39	2.10

Step 3. The biochar column (BC) was packed with glass beads on the bottom (3 cm in height), biochar in the middle (target height), and more glass beads on the top (3 cm in height). The biochar used in each breakthrough test was prepared according to the target mass listed in Table 3.1. The biochar mass was measured again by subtracting the mass of the residual biochar remaining in the sampling dish from the total mass of the biochar. After the column was packed with glass beads on the bottom and biochar in the middle, the column was tapped gently until the biochar sank to the target level of height. Then, the column was packed with more glass beads on the top. The height of the biochar layer was measured in the end for verification.

Step 4. Mass balance was checked to ensure that the BC set-up was properly sealed. PTFE tape, laboratory film, and vacuum grease were applied for sealing, before and after the fittings were connected to the top and the bottom of the BC. The mass balance between the inflow (Figure 3.5) and the outflow (Figure 3.6) was checked with N_2 gas to ensure the BC was completely sealed after installation. The gas meter was removed after the mass balance check because according to the negative control test, where no biochar was added to the column, the H_2S concentration in the biogas collected after the gas meter was only 15 ppm. Therefore, the packing liquid (Ritter Silox) of the gas meter might have an H_2S removal effect, and the gas meter was removed from the set-up to avoid its disturbance during the breakthrough tests.

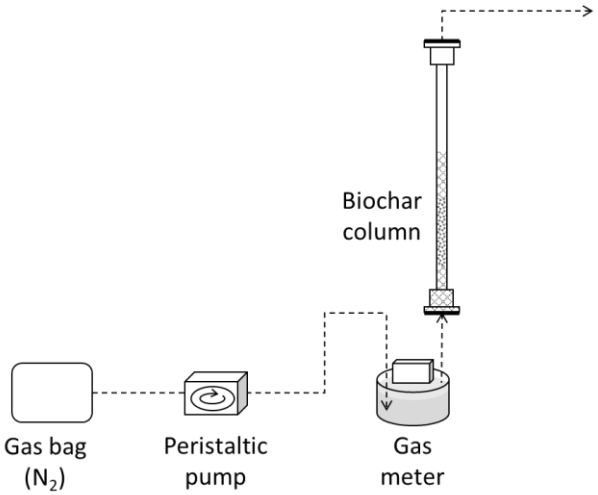

Figure 3.5 Mass balance check (inflow)

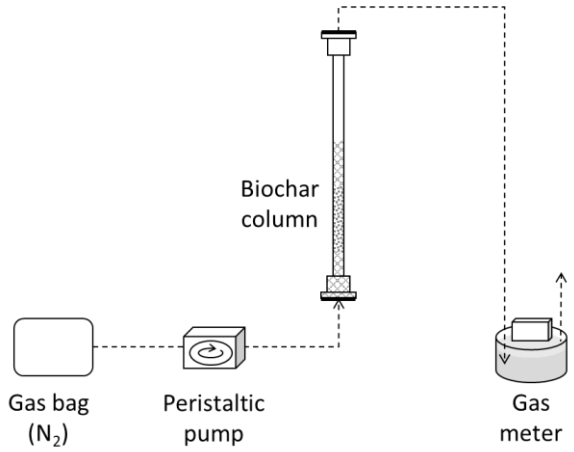

Figure 3.6 Mass balance check (outflow)

Step 5. The N_2 gas bag was replaced with the gas bag containing biogas with initial H_2S concentration of 20 ppm. The breakthrough tests started without the sampling gas bag attached to the BC, so that the system could be flushed with biogas for the first 5 minutes (Figure 3.7). Then, the sampling gas bag was attached to the outlet of the BC to collect the cleaned biogas (Figure 3.8). After 5 minutes, the sampling gas bag was detached for H_2S measurement with the Dräger tubes (Hydrogen Sulfide 0.2/b, 0.2 – 6 ppm). The measurement result would represent the H_2S concentration in the middle of the biogas collection period. During the first half hour of Test 1, the sampling gas bag was detached and attached every 5 minutes. Afterwards, the sampling gas bag was detached for 10 minutes, and attached for 5 minutes. Test 2 was completed over the course of 2 days. On the first day, the sampling gas bag was detached and attached every 5 minutes for 4.5 hours. The BC was flushed with N_2 at the end of the first day for preservation. At the beginning of the second day, the sampling gas bag was detached and attached every 5 minutes for half an hour, then detached for 10 minutes and attached for 5 minutes for the rest of the test.

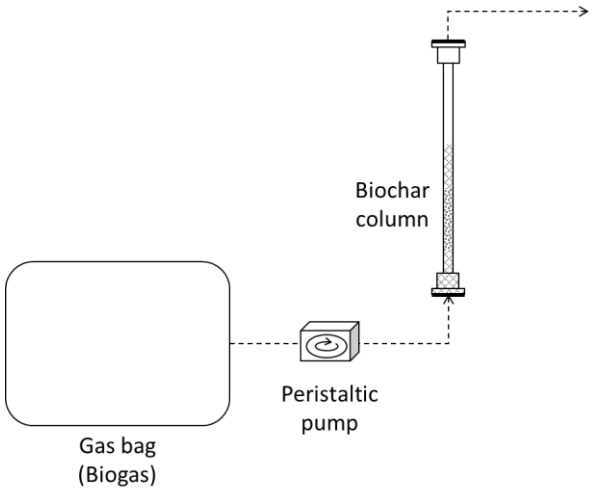

Figure 3.7 Biogas bag for sampling detached from the column

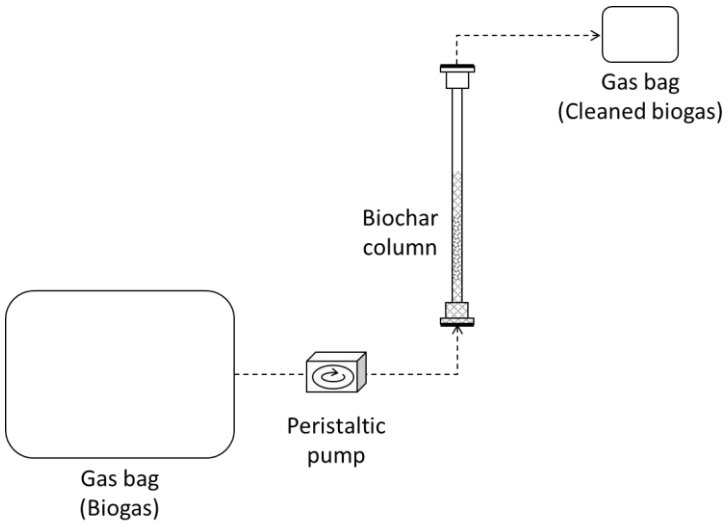

Figure 3.8 Biogas bag for sampling attached to the column

Step 6. The mass balance between the inflow and outflow was checked again with N_2 gas. The mass balance at the beginning and the end of each test was necessary, so that it would be valid to calculate the amount of H_2S processed by the BC based on the flowrate of the biogas, as long as there was no leakage in the system throughout the whole test according to the mass balance check.

The results of the breakthrough tests were analyzed in the end to evaluate the BC performance and determine the adsorption capacity of the biochar. The volume of the biochar added to the column was calculated based on the inside diameter of the BC (0.58 cm) and the measured height. The biochar density was calculated again based on the measured mass and the volume. The biogas flowrate was determined by the average flowrate (inflow) of the biogas measured at the beginning and the end of each test during the mass balance check. Gas hourly space velocity (GHSV) was assessed based on the biochar volume and biogas velocity (Equation 8.12). The amount of H_2S processed by the BC was determined with the flowrate, the processing time, and the initial H_2S concentration in the biogas (Equation 8.13 and Equation 8.14). The breakthrough concentration of H_2S was specific to the SOFC tolerance. Depending on the cell material, H_2S should be 5 ppm or lower to avoid sulfur poisoning; for internal methane reforming, H_2S should be less than 1 ppm to minimize the effect of sulfur poisoning on the methane conversion rate (Saadabadi et al., 2019). In this experiment, 0.5 ppm H_2S was set to be the limit of SOFC for safe operation. The adsorption capacity of the biochar was determined by the amount of H_2S processed by the BC right before breakthrough and the amount of biochar added to the BC initially (Equation 8.15).

3.5 Biogas Conditioning

Removing H_2S from the biogas. To measure the initial H_2S concentration, biogas produced by the AnMBR was collected without treatment in a gas bag with maximum capacity of 25 L. Subsequently, the BC was attached to the AnMBR for H_2S removal, and biogas was collected after the BC. It was assumed that the H_2S concentration overtime remained the same as the initial H_2S concentration. While the sludge pH in the AnMBR was controlled around 8, the amount of biochar required for H_2S removal

was determined based on the adsorption capacity of the biochar, the H_2S concentration, and the target volume of the biogas to be collected (25 L). When the sludge pH was reduced to 7, the H_2S concentration would increase according to the hypothesis for Q1. Due to the limitation of the column size, the target volume of biogas to be processed by the BC was reduced to 10 L, so that the amount of biochar required would not exceed the column capacity. Then, the BC performance was tested under its maximum capacity when the column was filled up with biochar besides the glass beads on the top and the bottom of the column. To increase the reliability of the test results, (1) mass balance between the inflow and outflow was checked with N_2 gas at the beginning of each test to ensure that the BC was properly sealed, and (2) the BC was flushed with biogas for 1 hour and 30 minutes (included as part of the processing time) before the biogas bag was attached to the outlet of the BC.

Adding CO_2 to the biogas. To mix the AnMBR biogas with CO_2, four gas bags were used for containing (1) N_2 collected from the N_2 gas cylinder (100% N_2), (2) the biogas produced from Day 83 (May 02, 2022) to Day 106 (May 25, 2022) under pH 8, or the biogas produced from Day 311 (Dec 16, 2022) to Day 315 (Dec 20, 2022) under pH 7, (3) CO_2 collected from the CO_2 gas cylinder (100% CO_2), and (4) the mixed gas as the final product. The set-up for CO_2 addition has been shown in Figure 3.9. First, the peristaltic pump was calibrated with N_2 gas so that the rpm setting would result in a suitable flowrate for the gas meter whose flowrate range was 0.5 – 4.0 L/h (or 8.3 – 66.7 mL/min). Second, the N_2 bag was replaced with the biogas bag, and the system was flushed with biogas at the flowrate of 65.2 mL/min (160 rpm) until 117 mL of biogas was discharged. Third, the empty gas bag for containing the mixed gas was attached to the outlet of the gas meter, and 15.99 L of biogas produced under pH 8 (or 2.67 L of biogas produced under pH 7) was transferred to the empty gas bag at the same flowrate. Fourth, the biogas bag was replaced with the CO_2 bag, and 9.22 L of CO_2 (or 2.16 L of CO_2 for mixing with the biogas produced under pH 7) was transferred at the same flowrate. Finally, 0.48 L of sample (or 0.09 L sample from the biogas conditioned under pH 7) was withdrawn from the mixed gas for measurements. The remaining biogas was used for the SOFC operation.

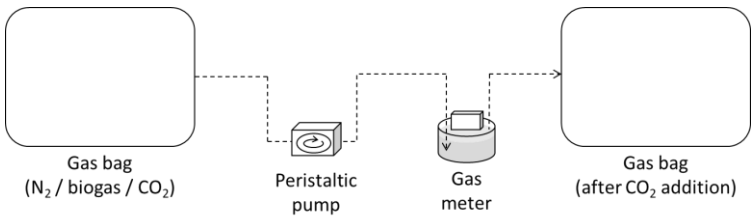

Figure 3.9 Set-up for CO_2 addition

3.6 Operational Procedure of SOFC

At the beginning of the SOFC experiment, the cell was mounted according to Figure 2.3, where the anode and the cathode were isolated by the mica sealing, so that only the exhaust from the anode side would leave the system via the exhaust outlets, allowing the possibility of exhaust recovery. To test if the mica sealing was installed properly,

air was injected to both sides of the cell. If the mica sealing was installed properly, air bubbles would appear in the exhaust scrubber, and disappear when the plug valve at the anode entrance was closed.

After the cell was mounted and installed in the SOFC set-up, the electrical cables were connected according to Figure 3.10. The voltage across SOFC was measured from the sense terminal of the electronic load, which could automatically compensate the voltage drop on the load and measure the cell voltage accurately. The current was measured from the electronic load as well under the constant resistance (CR) mode.

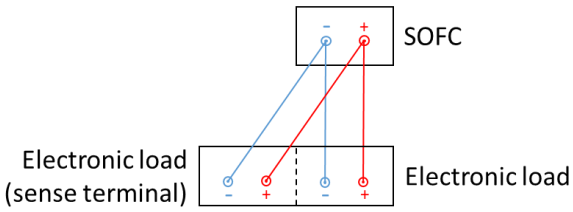

Figure 3.10 Electrical connection

Once the electrical cables were connected, the gas lines were installed according to the P&ID shown in Figure 3.11. Leakage tests were conducted to check if the gas lines were installed properly. The gas line for supplying air was tested first, in which case plug valve B was removed and re-installed at the entrance of the cathode. The gas line was pressurized with air up to 3 bars while both plug valves were closed. The pressure would not drop overnight if there was no leakage along the gas line. Then, plug valve B was removed and re-installed back to its original position for the second leakage test, where the gas line for supplying forming gas and biogas was pressurized with forming gas up to 3 bars while plug valve B and the ball valve were closed. Similarly, the pressure would sustain overnight if the gas line was installed properly.

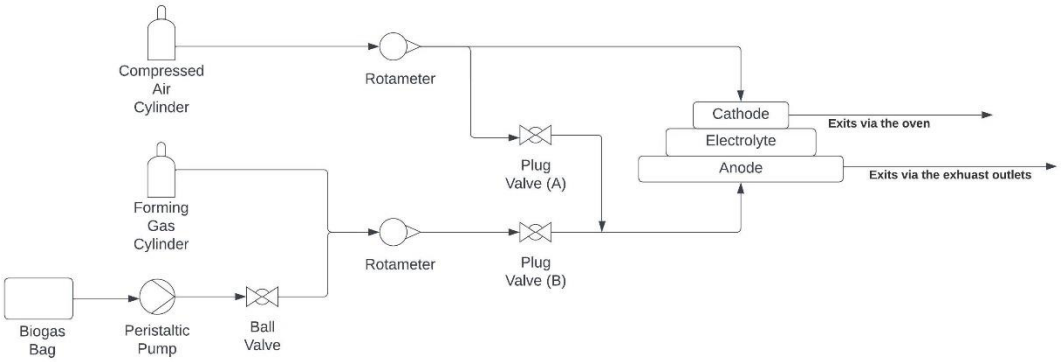

Figure 3.11 P&ID of the SOFC system

During the experiment, the SOFC set-up was operated under 3 different modes: initializing mode (Figure 3.12), forming gas mode (Figure 3.13), and biogas mode (Figure 3.14).

Initializing mode. At the beginning of each experiment, the furnace was heated up at the rate of 180 °C per hour until the temperature reached 900 °C (approximately 4 hours and 52 minutes was required). In the meantime, air was injected into both sides of the cell (200 mL/min according to the rotameter), so that the tapes and glues applied to the cell for mounting could be burnt off. Under the initializing mode, all of the valves should be closed except for plug valve A.

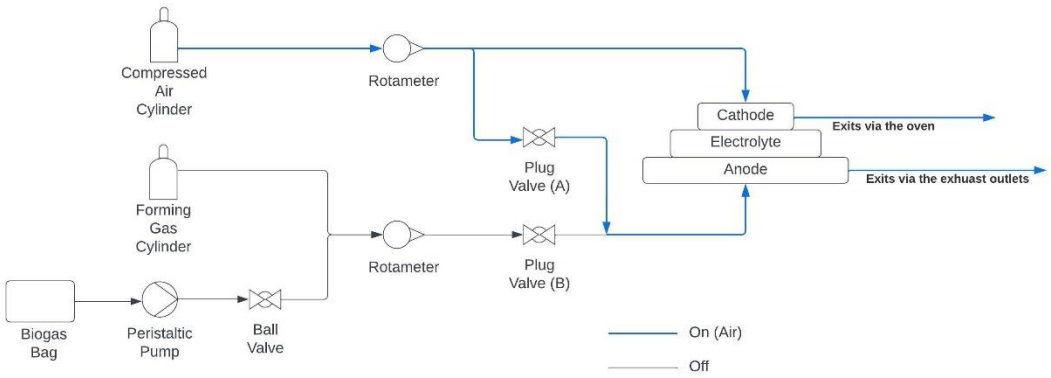

Figure 3.12 Initializing mode

Forming gas mode. Once the target temperature was reached, the initializing mode was switched to the forming gas mode by (1) closing plug valve A, (2) opening plug valve B, and (3) opening the valve connected to the forming gas cylinder slowly until the target flowrate was reached (250 mL/min according to the rotameter). This step was essential for purging air out of the anode side and reducing NiO to Ni. The duration of purging should be at least 10 minutes, to ensure that there would be no air remining in the fuel gas line.

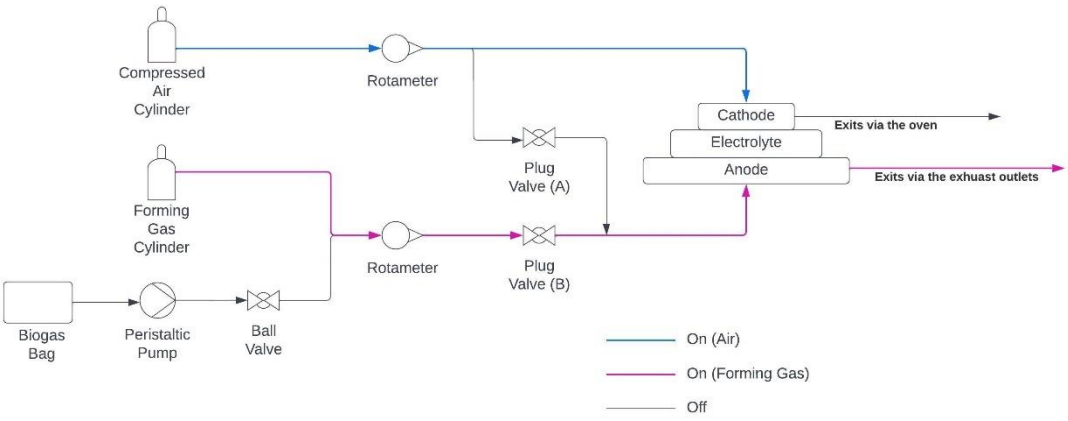

Figure 3.13 Forming gas mode

Biogas mode. After purging was completed, the forming gas mode was switched to the biogas mode by (1) closing the valve connected to the forming gas cylinder slowly until the forming gas flow stopped completely, (2) opening the ball valve, and (3) turning on the peristaltic pump with the correct rpm setting (87 rpm according to the calibration curve of the pump) so that the biogas flowrate would be 35 mL/min.

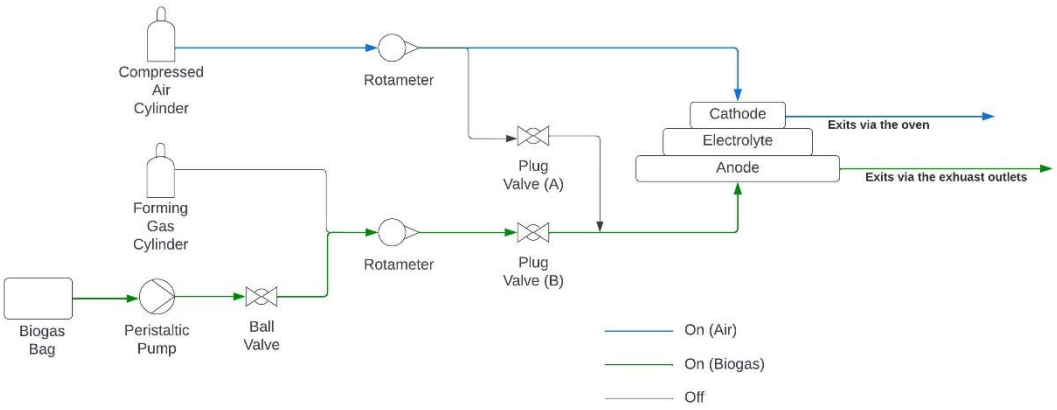

Figure 3.14 Biogas mode

Determining biogas input. The biogas used for the first SOFC experiment was originally produced by the AnMBR from Day 83 to Day 106 under pH 8 without being processed by the BC. After CO_2 addition, the ratio between CH_4 and CO_2 was expected to be 1:1, and the H_2S concentration should be less than 0.5 ppm. The biogas flowrate was designed to be 35 mL/min. Based on the CH_4 concentration measured in prior to the SOFC experiment (31.2%), and the biogas utilization efficiency assumed (60%), the flowrate of utilized CH_4 would be 6.55 mL/min.

Estimating power output. The current and voltage were estimated for the first SOFC experiment and illustrated in Figure 3.15. The current was expected to be 3.50 A, which was calculated based on the CH_4 flowrate of 6.55 mL/min (Equation 8.18). Therefore, according to the Ohm's law (Equation 8.19), the output voltage of SOFC should be 1.75 V if the electronic load could provide 0.5 Ω of resistance. The expected current and voltage were used for estimating the electric power output of SOFC, which would be 6.13 W (Equation 8.20).

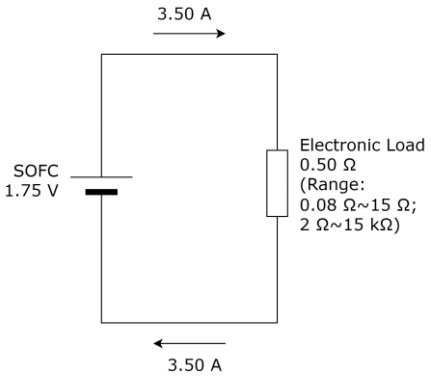

Figure 3.15 Circuit diagram

3.7 Performance Indicators of SOFC

Power output and power density. The electric power output was calculated based the voltage and current measured by the electronic load (Equation 8.20). The electric power output in relation to cathode area was expressed as power density (Equation 8.21).

Fuel utilization rate. To determine the fuel utilization rate, the amount of current measured by the electronic load was compared with the amount of current that could be produced by the SOFC theoretically using the methane in the biogas bag as the fuel (Equation 8.23).

4. Results

4.1 Performance of AnMBR

4.1.1 AnMBR pH

The measurement results of the sludge pH were continuously logged by the PC (online measurement) and were consistent with the pH results obtained by the pH meter (manual measurement) (Figure 4.1). From Day 0 to Day 268, sludge pH was 8.09 ± 2% according to the online measurement and 8.04 ± 2% according to the manual measurement. The alkalinity of the sludge collected under pH 8 was 4.276 $gCaCO_3/L$. On Day 269, 114.47 mL of HCl solution (1M) was added to the bioreactor, and based on the online measurement, pH reduced from 8.23 to 7.46. However, on Day 272, the pH measured online reached 7.82 even though HCl solution (0.1M) had been continuously added to the reactor at 98.6 mL/d since Day 269. On Day 273, 70.40 mL of HCl solution (1M) was added to the bioreactor, and the pH decreased from 7.82 to 7.37. The 0.1M HCl solution was replaced by the 1M solution for continuous acid addition on Day 274, and the concentration of the HCl solution was increased again on Day 279 to 2M. The acid addition bottle was refilled with 2M HCl for the rest of the experiment. The flowrate for acid addition was 34.5 mL/d ± 0.03%. The PC was programed to dose acid automatically at 0.83 mL/min when the pH measured online was above 7.2, and the pump for acid addition would be turned off by the PC once the pH was below 7.1.

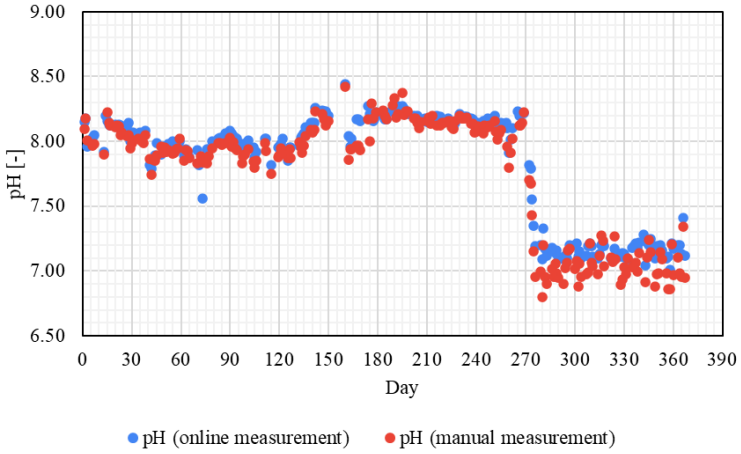

Figure 4.1 Sludge pH

4.1.2 OLR and COD Removal Efficiency

The target organic loading rate (OLR) was 2.27 $gCOD \cdot L^{-1} \cdot d^{-1}$). Starting on Day 101, the method to monitor the mass balance was implemented, so that the flowrate of the feed water for calculating the OLR was based on the mass balance instead of the calibration results for the flowrate. From Day 15 to Day 139, the feed water COD was measured with the sample collected from the sampling point close to the entrance where the feed water was added into the bioreactor and the feed water COD was used for calculating the OLR of the previous day. From Day 146 to Day 369, the feed water

COD was measured with the sample collected from the feed water bucket instead, and feed water COD was used for calculating the OLR of the same day. In comparison, the OLR from Day 146 to Day 369 (2.32 $gCOD \cdot L^{-1} \cdot d^{-1}$ ± 17%) was closer to the target OLR than the OLR from Day 15 to Day 139 (1.47 $gCOD \cdot L^{-1} \cdot d^{-1}$ ± 29%) (Figure 4.2). The permeate COD was always measured with the sample collected from the sampling point close to the permeate bucket on the same days when the feed water samples were collected for the COD measurement. The COD removal efficiency was above 90% throughout the whole experiment (Figure 4.3). The average COD removal efficiency was 96% and the relative standard deviation was 2%.

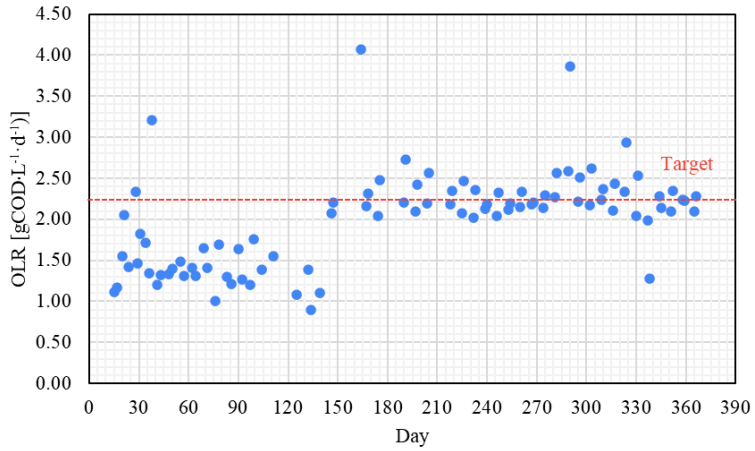

Figure 4.2 OLR

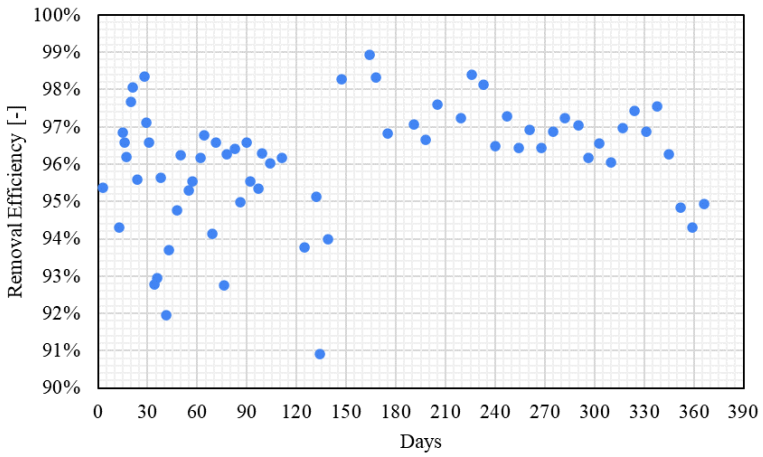

Figure 4.3 COD removal efficiency

4.1.3 Biogas Composition

CH_4, CO_2, and N_2 were considered for the composition of biogas (Figure 4.4 and Figure 4.5). According to the measurement results from Day 9 to Day 267 when the bioreactor was operated under pH 8, the biogas was composed of 79.6% CH_4, 3.6% CO_2, and 16.8% N_2. From Day 274 to Day 369 when the sludge pH was controlled around 7, 72.8% CH_4, 22.4% CO_2, and 4.8% N_2 were found in the biogas.

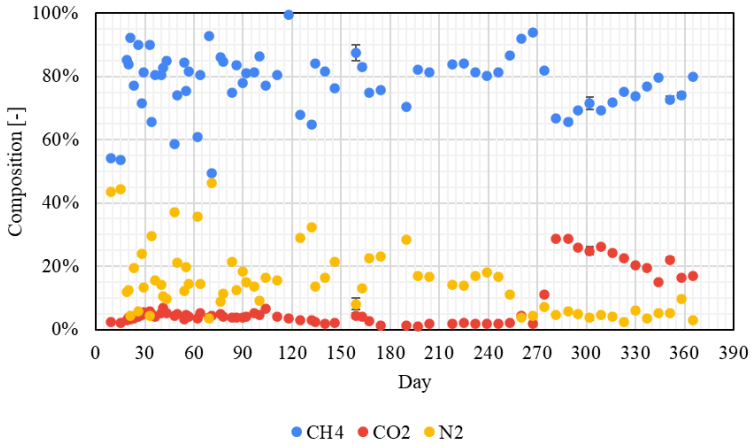

Figure 4.4 Biogas composition

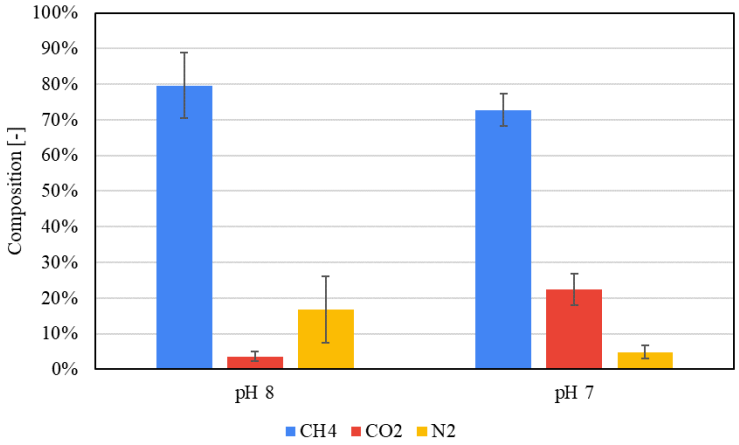

Figure 4.5 Summary for Biogas compositions under different pH conditions

4.1.4 Biogas Production Rate

The overall biogas production rate at the room temperature was 1.49 L/d ± 29% (Figure 4.6). From Day 15 to Day 268 when the sludge pH was maintained around 8, the biogas production rate was 1.31 L/d ± 24%. In comparison, from Day 279 to Day 369 when the sludge pH was controlled around 7, the biogas production rate increased to 1.94 L/d ± 18%.

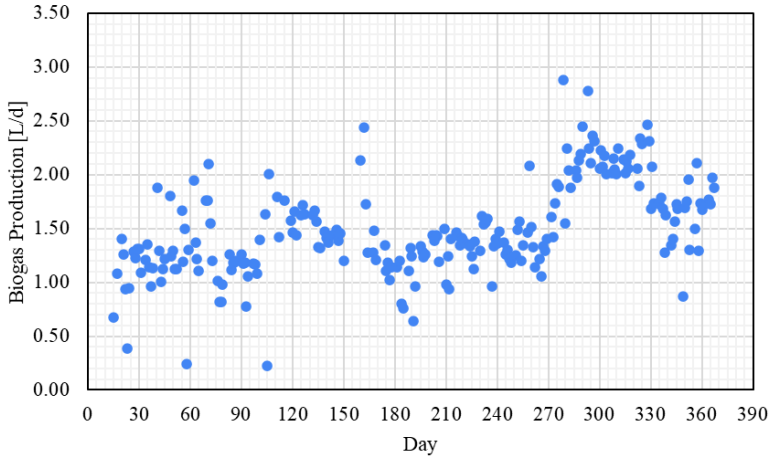

Figure 4.6 Biogas production rate

4.1.5 Methane Production Rate and Efficiency

The methane production rate was determined based on the biogas production rate measured at the room temperature and the proportion of methane in biogas. The methane production rate was 1.14 L/d ± 23% throughout the experiment, 1.07 L/d ± 24% under pH 8 and 1.36 L/d ± 11% under pH 7 (Figure 4.7). The methane production efficiency on the other hand was determined by comparing the COD of the produced methane to the COD of the influent. The methane production efficiency was 33.1% throughout the experiment, 34.3% under pH 8 and 29.5% under pH 7, with relative standard deviation (RSTD) of 30%, 33%, and 11% respectively (Figure 4.8). As mentioned previously in *section 4.1.2 OLR and COD Removal Efficiency*, the influent COD was measured with a new method starting on Day 146. As a result, while pH was maintained at 8, the methane production efficiency was 37.3% from Day 15 Day 145, and 26.0% from Day 146 to Day 268, with RSTD of 31% and 13% respectively.

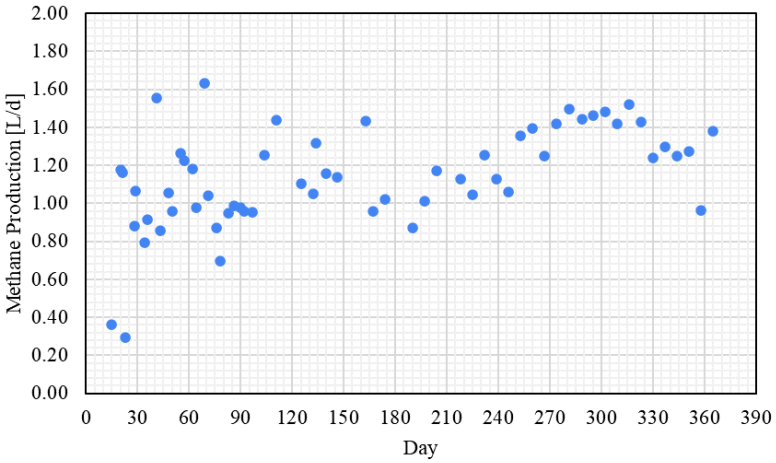

Figure 4.7 Methane production rate

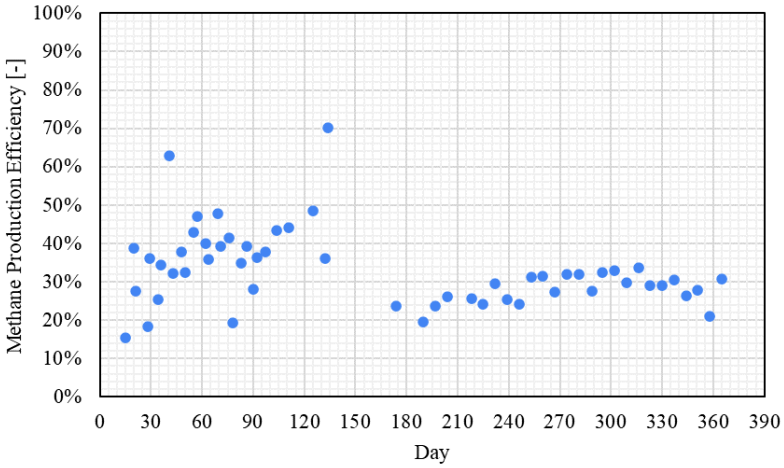

Figure 4.8 Methane production efficiency

4.1.6 Other Parameters

Sludge Conditions (ORP, temperature, sludge level, SRT). The oxidation-reduction potential (ORP) results were measured with the same probe as the one for pH. The sludge ORP throughout the experiment was -493.55 mV ± 11% (Figure 8.1). It was observed that the sludge ORP would become less negative during daily maintenance, and after the daily maintenance was completed, the sludge ORP would slowly recover and become more negative again. From Day 15 to Day 191, the waterbath temperature and the sludge temperature were 40.1 °C ± 0.5% and 36.0 °C ± 1.9% respectively (Figure 8.2). On Day 192, the temperature setting of the waterbath was increased to 43.0 °C due to the decline in sludge temperature. As a result, the waterbath temperature was 42.7 °C ± 0.7% from Day 192 to Day 369, and the corresponding sludge temperature was 37.4 °C ± 2.3%. The sludge level would decrease during daily maintenance due to sludge extraction and increase after the maintenance since the flowrate of the feedwater was higher than the flowrate of the permeate. The sludge level was 5.58 L ± 4.8% from Day 15 to Day 369 (Figure 8.3). The solid retention time (SRT) was 32.7 days ± 17% from Day 2 to Day 369 (Figure 8.4). Although, at the beginning of the experiment (before Day 27), SRT had a large fluctuation since the sludge extraction rate was not stable. Based on the sludge extraction rate from Day 27 to Day 268 when the sludge pH was around 8, SRT was 28.4 days ± 17%. From Day 279 to Day 369 when the sludge pH was controlled around 7, SRT was 35.1 days ± 10%.

Solids concentrations and biomass growth. The solids concentrations of the sludge have been plotted in Figure 8.5 and Figure 8.6, and summarized in Figure 8.7. VSS concentrations were further used for calculating the biomass net growth as shown in Figure 8.8. The overall biomass net growth was around 0 gCOD/d.

VFA. The VFA contained in sludge and permeate was mainly acetic acid. Propionic acid and isocaproic acid were sometimes found in VFA measurements as well. From Day 41 to Day 337, the concentration of the VFA accumulated in sludge was 64 mgCOD/L ± 49%, which was close to the permeate VFA (67 mgCOD/L ± 49%)

measured during the same period (Figure 8.9). From Day 344, excessive VFA accumulation was observed in both sludge and permeate samples.

COD balance. Due to the change in the method for COD measurement, the COD balance from Day 15 to Day 145 (Figure 8.10) was differentiated from the COD balance from Day 146 to Day 268 (Figure 8.11), even though the pH condition was 8 in both cases. The COD balance from Day 279 to Day 369 was determined with the new method under pH 7 (Figure 8.12). COD of the produced methane (methane COD), COD of the sludge extracted from the bioreactor (extracted sludge COD), and COD of the permeate (permeate COD) were considered for the COD balance calculations. The average gap in the COD balance for case A, B, and C was 55%, 32% and 35%. The corresponding RSTD was 36%, 54%, and 37% respectively.

SMA. The SMA experiment was conducted using a batch set-up (AMPTS). The sludge collected under pH 8 (from Day 225 to Day 252), and pH 7 (from Day 279 to Day 304) were tested for SMA at the same time. According to the slopes shown in Figure 8.13, the SMA of the sludge collected under pH 8 was 0.19 $gCOD \cdot gVSS^{-1} \cdot d^{-1}$, and the SMA of the sludge collected under pH 7 was 0.48 $gCOD \cdot gVSS^{-1} \cdot d^{-1}$.

BMP. The BMP experiment was also conducted using an AMPTS system. The sludge collected under pH 8 (from Day 190 to Day 224) was tested for BMP. The cellulose and the feed water added to the test bottles were designed to have the same COD content (0.293 gCOD). At the end of the experiment, 102.5 mL of CH4 was produced due to the cellulose addition, and 124.6 mL of CH_4 was produced due to the feed water addition (Figure 8.14). Therefore, the BMP of the cellulose and the feed water was 350.4 mL-CH4/ gCOD and 425.9 mL-CH4/ gCOD respectively.

TMP, flux and permeability. TMP, flux and permeability are the indicators for the filtration performance of the AnMBR. From Day 1 to Day 34, when the AnMBR was operated with the first membrane unit, TMP was above 200 mbar (Figure 8.15), flux was instable fluctuating between 4.0 LMH and 9.5 LMH (Figure 8.17), and permeability was below 30 LMH/bar (Figure 8.18). The second membrane unit was installed on Day 34. It was a brand-new membrane unit with an initial permeability of 1119 LMH/bar ± 4%. The initial permeability was tested with demineralized water at the room temperature (20 °C) under 3.2 bar pressure. After the initial permeability test, the membrane unit was installed in the AnMBR set-up. From Day 35 to Day 195, TMP was 30.9 mbar ± 15%, flux was 9.2 LMH ± 3%, and permeability was 178.9 LMH/bar ± 16%. From Day 196 to Day 342, the changes in TMP due to membrane fouling and membrane cleaning were observed (see Figure 8.16 where exponential curves were indicated to predict TMP in case of membrane fouling). The flux during this period remained consistent (9.1 LMH ± 5%), but fluctuated more towards the end. Based on the TMP and permeability values before and after each membrane cleaning (Table 8.10), the TMP reduction efficiency and the permeability recovery efficiency were calculated (Table 8.11). The reduced TMP and the recovered permeability were also indicated as red arrows in Figure 8.15 and Figure 8.18. As the need for membrane cleaning became more frequent, the second membrane unit was replaced with the third one on Day 342. The third membrane unit was relatively new. It had only been used for about 30 days. Although, the filtration performance did not reach expectation. From Day 343 to Day

369, when the AnMBR was operated with the third membrane unit, TMP was 124.1 mbar ± 16%, flux was 9.4 LMH ± 7%, and permeability was 45.6 LMH/bar ± 15%.

4.2 Adsorption Capacity of The Biochar

4.2.1 Summary of the Breakthrough Tests

The results of the breakthrough tests have been summarized in Table 4.1. The particle size of the biochar used in Test 2 was reduced in comparison to Test 1, while the other parameters were controlled. Reducing the particle size increased the H_2S adsorption capacity of the biochar. Therefore, the cow manure biochar with particle size ranging between 0.105 mm and 0.25 mm was selected to remove H_2S from the biogas produced by the AnMBR.

Table 4.1 Summary of the test results

Parameter	Biochar (Test 1)	Biochar (Test 2)
Particle Size [mm]	0.25 - 0.63	0.105 - 0.25
Mass [g]	0.2100 (Target) 0.2093 (Measured)	0.2100 (Target) 0.2202 (Measured)
Height [cm]	2.39 (Target) 2.00 (Measured)	2.10 (Target) 2.20 (Measured)
Volume [cm^3]	0.5284	0.5813
Density [g/cm^3]	0.3308 [1] 0.3961 [2]	0.3960 [1] 0.3788 [2]
Flowrate [mL/min]	25.80	25.25 (Day 1) 25.04 (Day 2)
GHSV [1/h]	2930	2606 (Day 1) 2585 (Day 2)
H_2S Adsorption Capacity [mg/g]	0.5068	1.2297

[1] These values were obtained from the preliminary density measurements with a separate bottle of biochar sample. Based on the density and the target volume of the biochar, the amount of biochar required in each test was able to be calculated.
[2] These values were determined based on the measured mass and the measured height of the biochar layer in the adsorption column.

4.2.2 Breakthrough Test 1

According to the mass balance check (Table 8.12), the adsorption system was properly sealed. The gap between the inflow and the outflow was 0.22% at the start of breakthrough test and -0.77% in the end. The H_2S concentration measured at the outlet of the biochar column and the amount of H_2S processed by the adsorption column have been plotted in Figure 4.9. At 2.5 hours, the biochar reached its maximum adsorption capacity without exceeding the limit of SOFC (0.5 ppm). The corresponding H_2S concentration measured at the outlet was 0.35 ppm, and the amount of H_2S processed by the adsorption column after 2.5 hours was 0.11 mg. Therefore, 0.11 mg of H_2S could be adsorbed by the 0.2093 g of biochar loaded to the column without the risk of breakthrough, meaning the adsorption capacity of biochar in this case was 0.5068 mg/g.

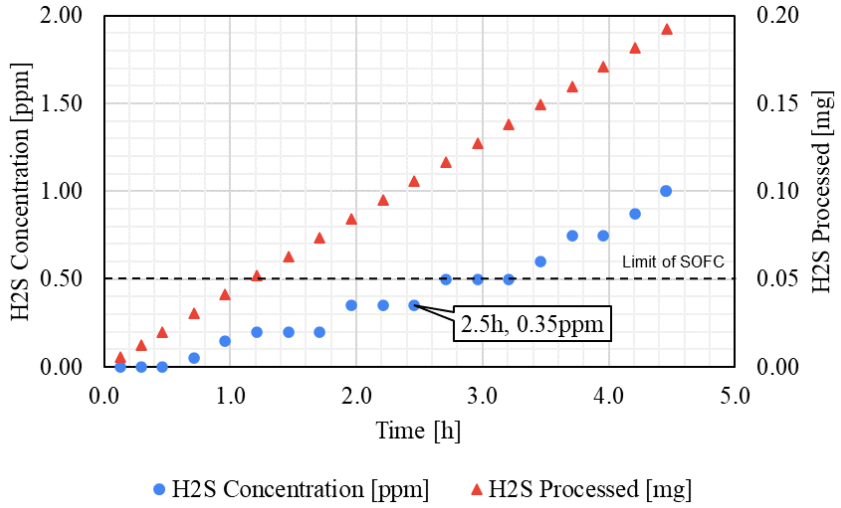

Figure 4.9 Breakthrough Test 1 with 0.25 - 0.63 mm biochar

4.2.3 Breakthrough Test 2

The time required for breakthrough was longer when the particle size was reduced. Therefore, the second breakthrough test was completed in two stages. During the first stage (Day 1, from 0.0 to 4.5 hours), the gap in mass balance was 1.17% at the start of the breakthrough test and -1.63% in the end (Table 8.13). The H_2S concentration measured at the outlet was 0 ppm consistently. During the second stage (Day 2, from 4.5 to 8.4 hours), the mass balance was 0.18% and -0.27% for the start and the end of the test respectively (Table 8.13). After 6.5 hours, the biochar reached its maximum adsorption capacity. The corresponding H_2S concentration measured at the outlet was 0.35 ppm, and the amount of H_2S processed by the biochar column was 0.27 mg. The mass of biochar measured in prior to the breakthrough test was 0.2202 g. Thus, the adsorption capacity of the biochar with particle size ranging from 0.105 to 0.25 mm was 1.2297 mg/g.

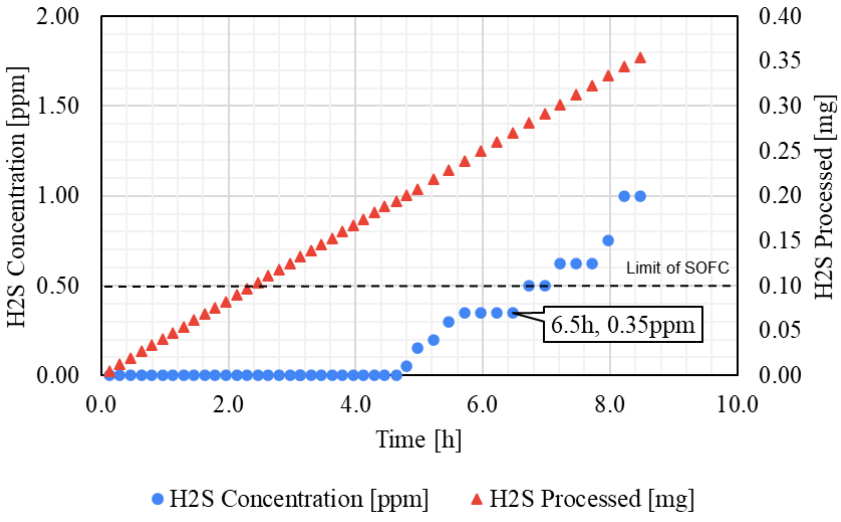

Figure 4.10 Breakthrough Test 2 with 0.105 - 0.25 mm biochar

4.3 Biogas Conditioning

4.3.1 H_2S Removal under pH 8

While the sludge in the AnMBR was controlled around 8, biogas was collected without being processed by the BC from Day 206 (Sep 02, 2022) to Day 223 (Sep 19, 2022), and then collected after the BC from Day 226 (Sep 22, 2022) to Day 244 (Oct 10, 2022). The composition of the biogas collected during each time period has been listed in Table 4.2. The H_2S removal efficiency of the BC in this case was 100.0%.

Table 4.2 Composition of the biogas collected under pH 8

Compound	Day 206 – Day 223 (Collected without the BC)	Day 226 – Day 244 (Collected after the BC)
CH_4	85.4% ± 0.2%	84.4% ± 0.1%
N_2	12.1% ± 1.1%	13.8% ± 0.8%
CO_2	2.5% ± 0.4%	1.8% ± 0.3%
NH_3	25 ppm (Range: 5 to 100 ppm)	0 ppm (Range: 0.25 to 3 ppm)
H_2S	20 ppm (Range: 10 to 200 ppm)	0 ppm (Range: 0.2 to 6 ppm)
CH_3SH	0.375 ppm (Range: 0.1 to 2.5 ppm)	0 ppm (Range: 0.1 to 2.5 ppm)

Based on the adsorption capacity of the biochar (1.2297 mg/g), the H_2S concentration in the biogas (20 ppm or 0.02786 mg/L), and the target volume of the biogas processed by the BC (25 L), 0.5664 g of biochar should be added to the adsorption column for removing H_2S from the biogas without the risk of breakthrough. The characteristics of biogas and biochar have been summarized in Table 8.14 for the second collection period (Day 226 – Day 244) while the biogas was collected after the BC. The specific H_2S adsorption capacity of the BC was above 1.3713 mg/g according to the measurement results.

4.3.2 H_2S Removal under pH 7 (Data Set 1)

While the sludge pH was 7, biogas was collected without the BC from Day 276 (Nov 11, 2022) to Day 286 (Nov 21, 2022), and after the BC from Day 289 (Nov 24, 2022) to Day 293 (Nov 28, 2022). The BC used during this period and onwards was a new column with an inside diameter (ID) of 0.60 cm. Then, biogas was collected after the BC again from Day 296 (Dec 01, 2022) to Day 301 (Dec 06, 2022), and the amount of biochar was increased by 10%, in which case the BC reached its maximum capacity restricted by the column size. The biogas composition of each collection period has been shown in Table 4.3. The H_2S removal efficiency of the BC during each collection period was 99.8% and 99.8% – 100.0% respectively.

Table 4.3 Composition of the biogas collected under pH 7 (data set 1)

Compound	Day 276 – Day 286 (Collected without the BC)	Day 289 – Day 293 (Collected after the BC)	Day 296 – Day 301 (Collected after the BC)
CH_4	71.3% ± 0.2%	76.0% ± 0.3%	77.7% ± 0.1%
N_2	3.9% ± 0.5%	2.7% ± 1.7%	1.7% ± 3.3%
CO_2	24.7% ± 0.4%	21.3% ± 0.9%	20.6% ± 0.2%
NH_3	0.7 ppm (Range: 0.25 to 3 ppm)	0 ppm (Range: 0.25 to 3 ppm)	0 ppm (Range: 0.25 to 3 ppm)
H_2S	120 ppm (Range: 10 to 200 ppm)	0.2 ppm (Range: 0.2 to 6 ppm)	Between 0 and 0.2 ppm (Range: 0.2 to 6 ppm)
CH_3SH	0.375 ppm (Range: 0.1 to 2.5ppm)	0 ppm (Range: 0.1 to 2.5ppm)	0 ppm (Range: 0.1 to 2.5ppm)

In comparison to the biochar mass in the BC from Day 289 to Day 293 (Table 8.15), the biochar mass in the BC from Day 296 to Day 301 (Table 8.16) was increased by 10%, while the biogas characteristics were relatively consistent. In both cases, the amount of biochar loaded to the BC was able to process the target biogas volume and remove H_2S without breakthrough. The specific H_2S adsorption capacity of the BC was above 1.2514 mg/g from Day 289 to Day 293 and above 1.2288 mg/g from Day 296 to Day 301.

4.3.3 H_2S Removal under pH 7 (Data Set 2)

To increase the reliability of the experimental results, the measurements of the biogas composition continued after the first data set was obtained. For the second data set (Table 4.4), biogas was collected without the BC from Day 304 (Dec 09, 2022) to Day 309 (Dec 14, 2022), and after the BC from Day 311 (Dec 16, 2022) to Day 315 (Dec 20, 2022). Even though the H_2S removal efficiency of the BC reached 99.6%, the H_2S concentration in the biogas after being processed by the BC was 0.6 ppm, which exceeded the limit set for SOFC (0.5 ppm).

Table 4.4 Composition of the biogas collected under pH 7 (data set 2)

Compound	Day 304 – Day 309 (Collected without the BC)	Day 311 – Day 315 (Collected after the BC)
CH_4	75.3% ± 0.3%	77.6% ± 0.4%
N_2	2.1% ± 3.2%	1.2% ± 5.4%
CO_2	22.6% ± 0.9%	21.2% ± 1.0%
NH_3	Between 0 and 0.25 ppm (Range: 0.25 to 3 ppm)	0 ppm (Range: 0.25 to 3 ppm)
H_2S	150 ppm (Range: 10 to 200 ppm)	0.6 ppm (Range: 0.2 to 6 ppm)
CH_3SH	0.375 ppm (Range: 0.1 to 2.5ppm)	0 ppm (Range: 0.1 to 2.5ppm)

When the BC was fully loaded with biochar (1.4955 mg) and glass beads, and the initial H_2S concentration was 150 ppm (0.2089 mg/L), the BC could only process 8.80 L biogas based on its adsorption capacity (1.2297 mg/g). In this adsorption test (Table 8.17), the actual biogas volume processed by the BC was 9.14 L instead of 8.80 L. The

specific H_2S adsorption capacity of the BC was less than 1.2764 mg/g, since the H_2S concentration measured at the end of the adsorption test was above 0.5 ppm.

4.3.4 H_2S Removal under pH 7 (Data Set 3)

For the third data set (Table 4.5), biogas was collected without the BC from Day 323 (Dec 28, 2022) to Day 324 (Dec 29, 2022), and after the BC from Day 324 (Dec 29, 2022) to Day 328 (Jan 02, 2023). The initial H_2S concentration was 110 ppm, and the biogas used for measurement was collected one day before the BC was attached to the AnMBR. After the biogas was processed by the BC, the H_2S concentration was reduced to 2.3 ppm, and the corresponding H_2S removal efficiency was 97.9%.

Table 4.5 Composition of the biogas collected under pH 7 (data set 3)

Compound	Day 323 – Day 324 (Collected without the BC)	Day 324 – Day 328 (Collected after the BC)
CH_4	75.2% ± 0.1%	77.6% ± 0.1%
N_2	2.3% ± 0.0%	0.9% ± 1.7%
CO_2	22.5% ± 0.1%	21.5% ± 0.4%
NH_3	0 ppm (Range: 0.25 to 3 ppm)	0 ppm (Range: 0.25 to 3 ppm)
H_2S	110 ppm (Range: 10 to 200 ppm)	2.3 ppm (Range: 0.2 to 6 ppm)
CH_3SH	0.25 ppm (Range: 0.1 to 2.5ppm)	0 ppm (Range: 0.1 to 2.5ppm)

From Day 324 to Day 328 (Table 8.18), when the BC was fully loaded with biochar and glass beads, and the target volume of biogas to be processed by the BC was 12 L. Although, in case the H_2S concentration during adsorption was higher than the initial value (110 ppm), 9.39 L biogas was collected after the BC instead. However, at the end of the collection period, the H_2S concentration (2.3 ppm) exceeded the SOFC tolerance (0.5 ppm). Therefore, the H_2S concentration might have increased during adsorption, or the specific adsorption capacity of biochar was less than 0.9621 mg/g assuming that the H_2S concentration remained constant while the biogas was processed by the BC.

4.3.5 Summary of H_2S Concentration under pH 7

As shown in Table 4.6, the change in H_2S concentration (collected without the BC) under pH 7 has been monitored periodically from Day 276 (Nov 11, 2022) to Day 365 (Feb 08, 2023), during which the H_2S concentration ranged between 110 ppm and over 2400 ppm (probably 2600 ppm according to the color indication of the measuring tube).

The relative standard deviation (RSTD) and the number of strokes (N) for different Dräger tubes have been listed in Table 8.19, which were summarized based on the datasheets provided by the supplier. Although, in practice, the RSTD of Dräger tubes could be insignificant since the color indication of the tubes were the same for triplicate measurements. Therefore, the concentrations of NH_3, H_2S, and CH_3SH were obtained by single measurements.

Table 4.6 H_2S concentration under pH 7

Period	H2S Concentration [ppm]	Measuring Range [ppm]
Nov 11 – Nov 21, 2022	120	10 – 200
Dec 09 – Dec 14, 2022	150	10 – 200
Dec 20 – Dec 23, 2022	200	100 – 2000
Dec 23 – Dec 28, 2022	190	10 – 200
Dec 28 – Dec 29, 2023	110	10 – 200
Jan 02 – Jan 03, 2023	180	10 – 200
Jan 03 – Jan 04, 2023	220	10 – 200
Jan 04 – Jan 05, 2023	>250	10 – 200
Jan 05 – Jan 06, 2023	>250	10 – 200
Jan 06 – Jan 10, 2023	2600	100 – 2000
Jan 10 – Jan 11, 2023	1350	100 – 2000
Jan 11 – Jan 12, 2023	950	100 – 2000
Jan 13 – Jan 17, 2023	600	100 – 2000
Jan 17 – Jan 18, 2023	210	10 – 200
Jan 18 – Jan 19, 2023	130	10 – 200
Jan 19 – Jan 20, 2023	210	10 – 200
Jan 20 – Jan 23, 2023	360	100 – 2000
Feb 03 – Feb 06, 2023	800	100 – 2000
Feb 06 – Feb 08, 2023	800	100 – 2000

4.3.6 CO_2 Addition under pH 8

From Day 83 (May 02, 2022) to Day 106 (May 25, 2022), the AnMBR biogas was collected without being processed by the BC, while the sludge pH was controlled around 8. The biogas composition was measured on Day 447 before CO_2 addition (Table 8.20), and on Day 457 after CO_2 addition (Table 8.21). 9.22 L CO_2 was added to 15.99 L biogas. As a result, the ratio between CH_4 and CO_2 was reduced to 1.04.

O_2 and H_2O could be excluded from the biogas composition so that the results would be comparable to Figure 4.5 where the effect of air entering the biogas bag and the effect of water vapor were neglected. To exclude O_2 from the biogas composition measured by GC, N_2 percentage associated with air was deducted from the total N_2 percentage, and the fractions of other compounds were normalized so that the total percentage of all the gas compounds would be 100%. H_2O was automatically excluded since water vapor was not measured by GC. However, after O_2 and H_2O were excluded, the N_2 concentration in the biogas would be 4.8%, but the average N_2 concentration under pH 8 was 16.8% according to Figure 4.5. Therefore, the effect of air entering the biogas bag should not be neglected.

O_2 and H_2O were included in the following table (Table 4.7), where both effects (air and water vapor) were considered. To include O_2, the O_2 fractions measured by GC remained as part of the biogas. To incorporate water vapor, partial pressure of water vapor and the absolute pressure of biogas were determined first. During the collection period, the gauge pressure of the biogas produced by the AnMBR was around 4 mbar (400 Pa) according to the data logged by the PC, so that the absolute pressure in this

case was 101725 Pa. The partial pressure of the water vapor was 6010 Pa (Equation 8.16). Therefore, the water vapor content in biogas was expected to be 5.9% before CO_2 addition (Equation 8.17). After 15.99 L biogas containing 5.9% water vapor was mixed with 9.22 L CO_2 with no water vapor under the same atmospheric pressure, the water vapor content in the mixed gas would be 3.7%. Once the water vapor fractions were determined, the fractions of other compounds were normalized to achieve 100% of gas in total.

Table 4.7 Composition of SOFC biogas (O_2 and H_2O included), pH 8

Compound	Composition before CO_2 addition (measured on Day 447)	Composition after CO_2 addition (measured on Day 457)
CH_4	48.2% ± 0.2%	31.2% ± 3.4%
N_2	35.9% ± 0.1%	27.8% ± 7.0%
CO_2	1.0% ± 7.9%	30.0% ± 4.7%
O_2	9.0% ± 0.1%	7.2% ± 7.1%
H_2O	5.9% ± 0.0%	3.7% ± 0.0%
NH_3	0 ppm (Range: 0.25 to 3 ppm)	0 ppm (Range: 0.25 to 3 ppm)
H_2S	0.2 ppm (Range: 0.2 to 6 ppm)	Between 0 and 0.2 ppm (Range: 0.2 to 6 ppm)
CH_3SH	0 ppm (Range: 0.1 to 2.5ppm)	0 ppm (Range: 0.1 to 2.5ppm)

4.3.7 CO_2 Addition under pH 7

As mentioned in *section 4.3.3 H2S Removal under pH 7 (Data Set 2)*, from Day 311 (Dec 16, 2022) to Day 315 (Dec 20, 2022), the AnMBR biogas was collected after the BC under pH 7. 2.16 L CO_2 was added to 2.67 L biogas to achieve the CH_4/CO_2 ratio of 1.11. The biogas composition before CO_2 addition was first measured on Day 315 as shown in Table 4.4 where O_2 and H_2O were excluded. Then, it was measured again on Day 491 (Table 8.22). If O_2 and H_2O were excluded from the biogas composition measured on Day 491, the N_2 concentration would be negative (-25.7%). Therefore, O_2 and H_2O were considered when the biogas composition was normalized. The biogas composition after CO_2 addition was measured on Day 491 as well (Table 8.23). H_2O was added as part of the biogas in Table 4.8 based on the GC measurement results.

Table 4.8 Composition of SOFC biogas (O_2 and H_2O included), pH 7

Compound	Composition before CO_2 addition (measured on Day 491)	Composition after CO_2 addition (measured on Day 491)
CH_4	62.8% ± 3.0%	36.6% ± 1.4%
N_2	20.4% ± 7.7%	19.7% ± 3.5%
CO_2	1.8% ± 0.3%	32.8% ±1.1%
O_2	9.0% ± 3.6%	7.6% ± 2.0%
H_2O	5.9% ± 0.0%	3.3% ± 0.0%
NH_3	0 ppm [1] (Range: 0.25 to 3 ppm)	0 ppm [1] (Range: 0.25 to 3 ppm)
H_2S	0.3 ppm (Range: 0.2 to 6 ppm)	0.1 ppm (Range: 0.2 to 6 ppm)
CH_3SH	0 ppm [1] (Range: 0.1 to 2.5ppm)	0 ppm [1] (Range: 0.1 to 2.5ppm)

[1] These values were assumed based on the NH_3 and H_2S concentrations measured on Day 315.

4.4 Performance of SOFC

4.4.1 Fueling with the Biogas Conditioned under pH 8 (1st SOFC Experiment)

In the first SOFC experiment, the biogas conditioned under pH 8 was supplied to the SOFC, and the methane in the conditioned biogas was utilized through internal dry reforming. The furnace temperature during heating was measured via the thermocouple wire that went through the air diffuser, and recorded by the thermometer (Figure 8.19). The furnace temperature increased linearly by 182 °C/h during the SOFC experiment. In the end, the furnace temperature was stable at 910 °C ± 0.11%. The SOFC performance under the forming gas mode and the biogas mode has been summarized in Table 4.9.

Table 4.9 SOFC performance with different fuels, 1st SOFC experiment

Parameter	Forming gas	Biogas
Composition [–]	5% H_2, 95% N_2	30.0% CO_2, 7.2% O_2, 27.8% N_2, 31.2% CH_4, 3.7% H_2O
Flowrate [mL/min]	250	35
Max power output, max P [W]	0.5675 ± 0.75%	1.1456 ± 0.51%
Resistance under max P [Ω]	0.799 ± 0.17%	0.2632 ± 0.15%
Voltage under max P [V]	0.6735 ± 0.39%	0.5491 ± 0.28%
Current under max P [A]	0.8426 ± 0.39%	2.0864 ± 0.25%
Power density under max P [mW/cm^2]	368.6453 ± 0.75%	744.1807 ± 0.51%
Current density under max P [mA/cm^2]	547.3827 ± 0.39%	1355.38 ± 0.25%
Fuel utilization efficiency under max P [–]	50%	36%

From 15:29:06 to 15:29:28 while the resistance was controlled at 0.799 Ω ± 0.17%, the maximum power output of SOFC using forming gas as the fuel was observed: 0.5675 W ± 0.75%, in which case the power density was 368.6453 mW/cm^2 ± 0.75%. The current according to the electronic load was 0.8426 A ± 0.39%. The theoretical current, assuming 100% utilization efficiency, was 1.6705 A. When the measured current was compared with the theoretical current (Equation 8.22), the forming gas utilization efficiency could be determined: 50%.

From 16:05:15 to 16:05:29, the SOFC was operated under the biogas mode. As mentioned in *section 3.6 Operational Procedure of SOFC*, the conditioned biogas was supplied to the anode at 35 mL/min. This flowrate was much higher than the biogas production rate of the AnMBR, because (1) CO_2 was added to the AnMBR biogas after H_2S removal, and (2) the electronic load might not be able to detect the current if the flowrate of the fuel gas was too low. The maximum power output captured by the electronic load was 1.1456 W ± 0.51% while the resistance was controlled at 0.2632 Ω ± 0.15%, and the power density was 744.1807 mW/cm^2 ± 0.51%. The measured current and the theoretical current were 2.0864 A ± 0.25% and 5.8373 A respectively. Therefore, the biogas utilization efficiency was 36% (Equation 8.23).

The overall SOFC performance using forming gas as the fuel has been shown in Figure 8.20. The resistance was increased overtime from 0.4 Ω to 1.1 Ω in increments of 0.1 Ω. The maximum power output was observed when the resistance was around 0.8 Ω. The polarization curve for the forming gas test was constructed was constructed (Figure 8.21). The results summarized in Table 4.9 were consistent with the polarization curve.

The performance of biogas-fueled SOFC has been shown in Figure 4.11. The maximum power output was observed when the resistance was 0.2632 Ω, which was the initial and the lowest possible setting of the electronic load. Then, the resistance was increased overtime from 0.3 Ω to 1.2 Ω in increments of 0.1 Ω. Consequently, current and power decreased while voltage increased and plateaued at approximately 0.8 V. The polarization curve for the biogas test was constructed to demonstrate the responses of cell voltage and power density as current density changes (Figure 4.12).

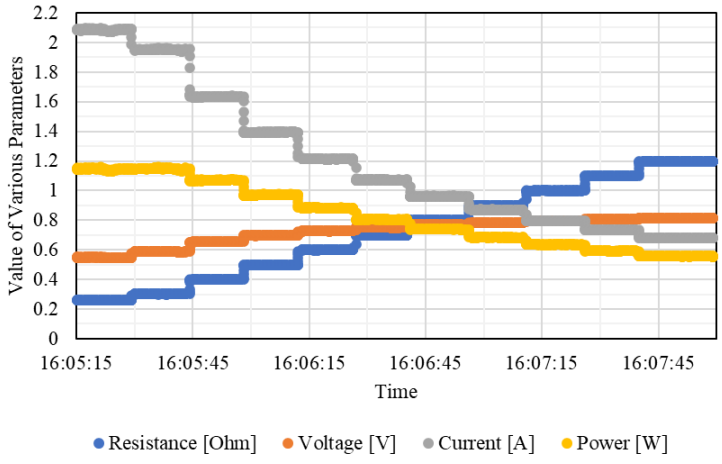

Figure 4.11 SOFC performance with biogas, 1st SOFC experiment

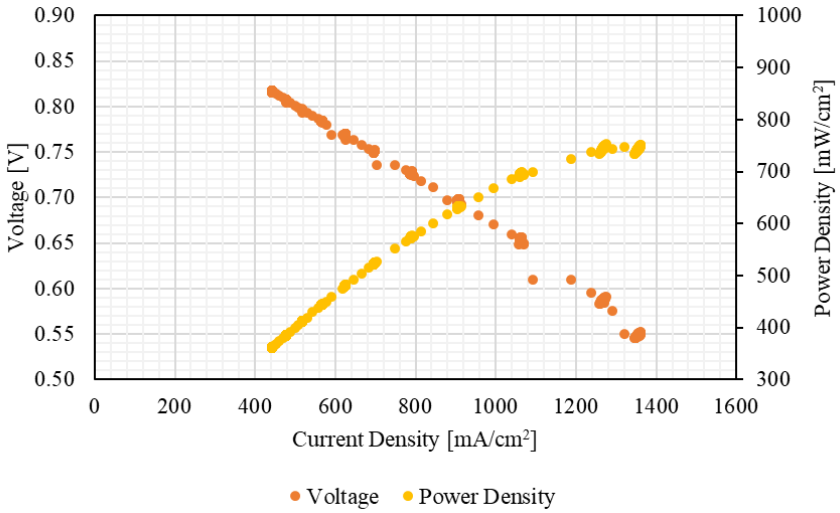

Figure 4.12 Polarization curve for the biogas test, 1st SOFC experiment

Under the biogas mode, the exhaust gas from the anode side was measured by a flowmeter and then collected in a gas bag. The flowrate of the exhaust gas was 45.7 mL/min, which was 31% higher than the flowrate of the biogas injected into the SOFC (35 mL/min). This phenomenon could be attributed to (1) the products of the methane reforming and fuel oxidation, and (2) air leakage from the cathode side to the anode side during the SOFC experiment. The composition of the exhaust was measured by GC. The GC measurement results were normalized with O_2 and unknown gases included, to represent the authentic composition of the exhaust gas (Table 4.10). The CH_4 fraction in the exhaust was multiplied by the exhaust flowrate to determine the flowrate of CH_4 leaving the system (1.74 mL/min). Similarly, the flowrate of CH_4 entering the system could be determined as well (10.92 mL/min). The fuel utilization efficiency should be 84% when the CH_4 flowrates were compared. This value was much higher than the fuel utilization efficiency calculated previously based on Equation 8.23 (36%). This phenomenon might be attributed to the incomplete conversion of CH_4, where part of the CH_4 in the fuel was converted to the intermediate compounds such as CO and H_2, and then left the system immediately without been oxidized.

Table 4.10 Composition of SOFC exhaust gas, 1st SOFC experiment

Compound	Exhaust Composition
CH_4	3.8% ± 4.6%
N_2	54.4% ± 2.5%
CO_2	10.6% ± 7.2%
O_2	6.0% ± 3.2%
Unknown	25.2% ± 7.6%

4.4.2 Fueling with the Biogas Conditioned under pH 7 (2nd SOFC Experiment)

The second SOFC experiment was conducted following the same operational procedure, except the biogas conditioned under pH 7 was used as the fuel when the SOFC was operated under the biogas mode. As shown in Figure 8.22, the heating rate was 186 °C/h

and the dwell temperature of the furnace was 910 °C ± 0.11%. The performance of the SOFC has been summarized in the following table.

Table 4.11 SOFC performance with different fuels, 2nd SOFC experiment

Parameter	Forming gas	Biogas
Composition [–]	5% H_2, 95% N_2	32.8% CO_2, 7.6% O_2, 19.7% N_2, 36.6% CH_4, 3.3% H_2O
Flowrate [mL/min]	250	35
Max power output, max P [W]	0.5519 ± 0.27%	1.2388 ± 0.06%
Resistance under max P [Ω]	1.000 ± 0.14%	0.2810 ± 0.00%
Voltage under max P [V]	0.7429 ± 0.16%	0.5902 ± 0.02%
Current under max P [A]	0.7429 ± 0.14%	2.0991 ± 0.04%
Power density under max P [mW/cm^2]	358.5469 ± 0.27%	804.7269 ± 0.06%
Current density under max P [mA/cm^2]	482.6219 ± 0.14%	1363.5931 ± 0.04%
Fuel utilization efficiency under max P [–]	44%	31%

When the SOFC was operated under the forming gas mode, the resistance was adjusted from 0.3 Ω to 1.2 Ω incrementally (Figure 8.23). The maximum power output was observed (0.5519 W ± 0.27%) when the resistance was controlled around 1 Ω. The fuel utilization efficiency in this case was 44%. The polarization curve for the forming gas test has been shown in Figure 8.24.

Under the biogas mode, the resistance was adjusted from 0.281 Ω to 0.3 Ω, and from 0.3 Ω to 1.2 Ω incrementally (Figure 4.13). The initial resistance was 0.281 Ω, and the maximum power output was observed immediately (1.2388 W ± 0.06%). The corresponding fuel utilization efficiency was 31%. In the polarization curve for the biogas test (Figure 4.14), and the outliers were not considered for determining the peak power or the peak power density.

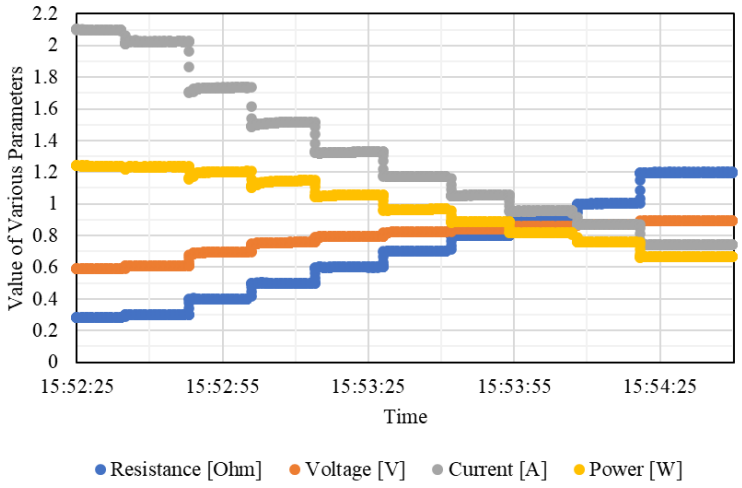

Figure 4.13 SOFC performance with biogas, 2nd SOFC experiment

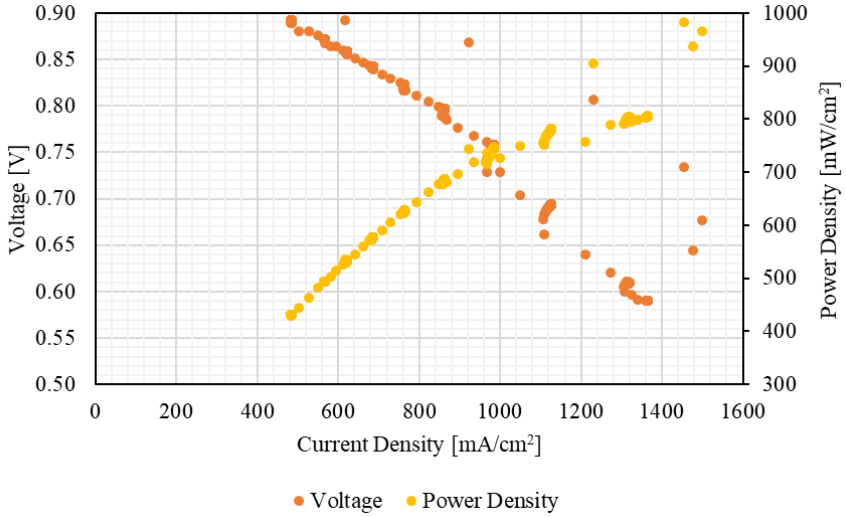

Figure 4.14 Polarization curve for the biogas test, 2nd SOFC experiment

The exhaust gas was collected under the biogas mode while the resistance was controlled around 0.281 Ω. The composition of the exhaust gas was measured by GC (Table 4.12). The exhaust gas flowrate was 47.20 mL/min. Therefore, based on the CH_4 fraction in the exhaust gas (1.3%), the flowrate of outgoing CH_4 was 0.61 mL/min. In comparison to the flowrate of incoming CH_4 (12.81 mL/min), 95% of CH_4 was utilized, which was inconsistent with the fuel utilization efficiency calculated according to Equation 8.23 (31%). As mentioned in the previous section, part of the methene reforming products (H_2 and CO) might exit the system without being oxidized. The unknown gases in the exhaust gas could be H_2O, H_2 and CO.

Table 4.12 Composition of SOFC exhaust gas, 2nd SOFC experiment

Compound	Exhaust Composition
CH_4	1.3% ± 4.1%
N_2	33.0% ± 0.9%
CO_2	17.1% ± 0.1%
O_2	6.0% ± 2.1%
Unknown	42.6% ± 0.9%

5. Discussion

5.1 Effect of AnMBR pH on Biogas Composition

Based on the results presented in *section 4.1.3 Biogas Composition* and *section 4.3 Biogas Conditioning*, the composition of the AnMBR biogas collected under different sludge pH conditions (pH 8 and pH 7) has been summarized in Table 5.1 (H_2O excluded) and Table 5.2 (H_2O included). RSTD of the results in both tables have been omitted. O_2 and the fraction of N_2 associated with air were excluded from the GC results because it was assumed that the air in the biogas samples were from the ambient environment during sampling. Water vapor was not measured by the GC. Therefore, the major compounds in the biogas were normalized without H_2O as shown in Table 5.1. Although, as mentioned in *section 4.3.6 CO2 Addition under pH 8*, the water vapor content in the AnMBR biogas (5.9%) could also be incorporated given the sludge temperature and the headspace pressure of the AnMBR. The fractions of other major compounds were adjusted accordingly in Table 5.2.

Table 5.1 Biogas composition under different sludge pH (H_2O excluded)

Compounds	Concentration (pH 8)	Concentration (pH 7)
CH_4	79.6%	72.8%
CO_2	3.6%	22.4%
N_2	16.8%	4.8%
NH_3	25 ppm	0 – 0.7 ppm
H_2S	20 ppm	110 – 2600 ppm
CH_3SH	0.375 ppm	0.25 – 0.375 ppm

Table 5.2 Biogas composition under different sludge pH (H_2O included)

Compounds	Concentration (pH 8)	Concentration (pH 7)
CH_4	74.9%	68.5%
CO_2	3.4%	21.1%
N_2	15.8%	4.5%
H_2O	5.9%	5.9%
NH_3	25 ppm	0 – 0.7 ppm
H_2S	20 ppm	110 – 2600 ppm
CH_3SH	0.375 ppm	0.25 – 0.375 ppm

As pH decreased from pH 8 to pH 7, all of the interested compounds changed according to the hypotheses in terms of their concentrations in biogas, except for CH_3SH. When the sludge pH was reduced to 7, the concentration of CH_3SH did not increase as predicted. The change in pH had less effect on CH_4 when compared with other compounds. Under pH 7, more CO_2 was released from the sludge, so that less CO_2 would be required to balance the ratio between CH_4 and CO_2 during CO_2 addition. However, removing H_2S from the AnMBR biogas was more challenging under pH 7 in comparison to pH 8. The H_2S concentration in biogas could increase by a magnitude of

10 or even 100 as pH decreased from 8 to 7. Therefore, the BC should be loaded with more biochar or replaced with new biochar more frequently to prevent breakthrough.

5.2 SOFC Operational Strategy

Biogas production, conditioning, and utilization was processed by AnMBR, BC, and SOFC respectively. Since the continuous operation has not been achieved yet, the quality of biogas might change overtime. As mentioned in *section 4.3.6 CO2 Addition under pH 8* and *section 4.3.7 CO2 Addition under pH 7*, the biogas stored in the gas bags might have been contaminated by air, so that the biogas composition measured before CO_2 addition was different from the original composition. Therefore, the results of SOFC performance are not sufficient to represent the SOFC performance in a continuous operation, where AnMBR, BC, and SOFC are connected. Although, to demonstrate the principle of SOFC operational strategy in a continuous operation, the results of the biogas conditioning under pH 8 and the results of the SOFC performance in the first SOFC experiment were analyzed.

Based on the average biogas production rates mentioned in *section 4.1.4 Biogas Production Rate*, and the average biogas compositions presented in Table 5.2, different biogas conditioning strategies have been proposed for operating the AnMBR-BC-SOFC system under pH 8 (Figure 5.1) and pH 7 (Figure 5.2). In both cases, the BC would be loaded with 1.4955 g biochar, which is the maximum amount of biochar that could be added to the BC for removing H_2S from the AnMBR biogas. The adsorption capacity of the biochar used in this experiment is 1.2297 mg/g, which has been verified in multiple adsorption tests (*section 4.3 Biogas Conditioning*). Therefore, the biochar could adsorb 1.8390 g H_2S before it needs to be replaced. The frequency of replacing the biochar in the BC depends on the initial H_2S concentration. The final H_2S concentration in the biogas after being processed by the BC should not exceed 0.5 ppm. After H_2S removal, the ratio between CH_4 and CO_2 would be balanced via either CO_2 addition (marked in blue) or exhaust recycling (marked in orange). After biogas conditioning is completed, the biogas would be ready for the SOFC operation. At the anode side, the conditioned biogas enters SOFC from the fuel entrance, and exits from the exhaust outlet. The volume of the exhaust gas discharged from the anode side is expected to be 31% more than the volume of the conditioned biogas (*section 4.4.*). At the cathode side, air is injected into SOFC at a constant flowrate of 288 L/d (or 200 min/min), and discharged through the furnace. The method for balancing the ratio between CH_4 and CO_2 would affect the amount of power that could be generated by SOFC in the end, since the flowrate and the composition of the conditioned biogas would change when different methods are applied. Based on the flowrate of the conditioned biogas and the CH_4 content in the conditioned biogas, the power generated by SOFC could be determined using Equation 8.18 where the theoretical current is further multiplied by the fuel utilization rate (36% according to Table 4.9), Equation 8.19 where the resistance is 0.2632 Ω, and Equation 8.20.

SOFC operational strategy under pH 8. While the sludge pH was controlled around 8, the average biogas production rate was 1.31 L/d. After 50.47 days, 66.01 L biogas containing 20 ppm (or 0.02786 mg/L) H_2S would be processed by the BC, in which

case the amount of H_2S adsorbed by the BC (1.8390 mg) would reach the maximum adsorption capacity of the biochar. Therefore, the biochar in the BC should be replaced at least every 50.47 days. Once H_2S is removed, 1.31 L/d of biogas (containing 74.9% CH_4, 3.4% CO_2, and other compounds as shown in Table 5.2) could be mixed with 0.93 L/d of CO_2 (containing 100% CO_2) in a gas bag, to achieve the 1:1 ratio between CH_4 and CO_2. Then, 2.24 L/d of conditioned biogas would enter SOFC with the predicted composition as shown in Table 5.3. Alternatively, 1.31 L/d of biogas could be mixed with 13.87 L/d of exhaust gas, whose composition is assumed to be the same as the composition presented in Table 4.10. In total, 15.18 L/d of fuel would be utilized in SOFC for energy conversion. The predicted composition of the fuel has been shown in Table 5.3. Finally, SOFC could generate 0.0092 W power if the BC treatment is used along with CO_2 addition for biogas conditioning, or 0.0220 W power if the BC treatment is used in combination with exhaust recycling instead.

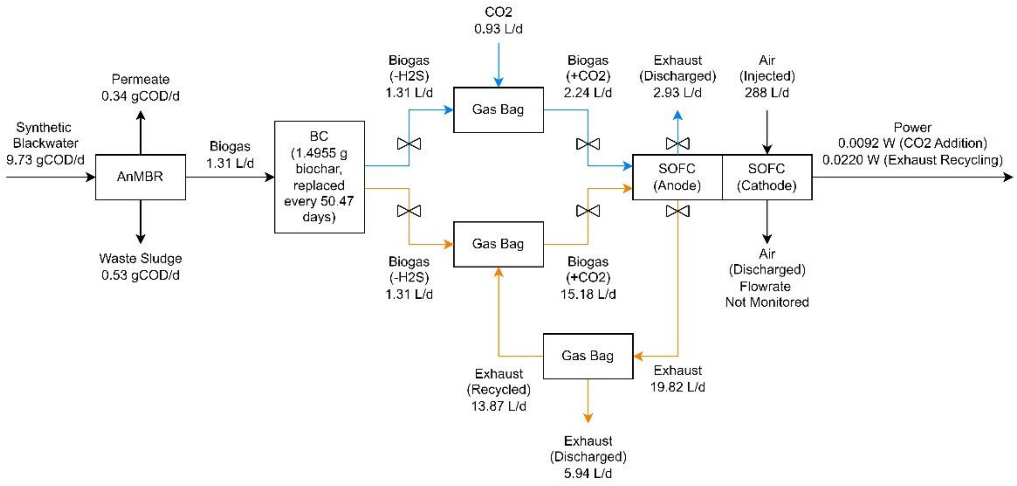

Figure 5.1 SOFC operational strategy (pH 8)

Table 5.3 Predicted composition of conditioned biogas, pH 8

Compounds	Concentration (BC treatment + CO_2 addition)	Concentration (BC treatment + exhaust recycling)
CH_4	43.7%	10.0%
CO_2	43.7%	10.0%
N_2	9.2%	51.0%
O_2	0.0%	5.5%
Unknown (incl. H_2O)	3.4%	23.6%
NH_3	0 ppm	0 ppm
H_2S	0 ppm	0 ppm
CH_3SH	0 ppm	0 ppm

SOFC operational strategy under pH 7. The average biogas production rate under pH 7 is 1.94 L/d. The H_2S concentration in the biogas ranges between 110 ppm (or 0.1532 mg/L) and 2600 ppm (3.6218 mg/L). The amount of biochar added to the BC

(1.4955 g biochar with adsorption capacity of 1.2297 mg/g) could adsorb 1.8390 g H_2S. Therefore, the BC could process 12.00 L biogas with 110 ppm H_2S, or 0.5078 L biogas with 2600 ppm H_2S, before the biochar is exhausted. Under the constant biogas flowrate of 1.94 L/d, the biochar should be replaced every 0.26 to 6.18 days, depending on the initial H_2S concentration. After H_2S removal, 0.92 L/d of CO_2 could be added to the biogas so that the conditioned biogas with the composition as predicted in Table 5.4 would enter SOFC at a flowrate of 2.86 L/d. Alternatively, 13.66 L/d of recycled exhaust gas could be added to the biogas instead. The composition of the conditioned biogas would change accordingly (Table 5.4), and the flowrate of the conditioned biogas would be 15.60 L/d. In the end, SOFC could generate 0.0170 W if adsorption and CO_2 addition were applied for biogas conditioning, or 0.0331 W if adsorption and exhaust recycling were applied instead for biogas conditioning.

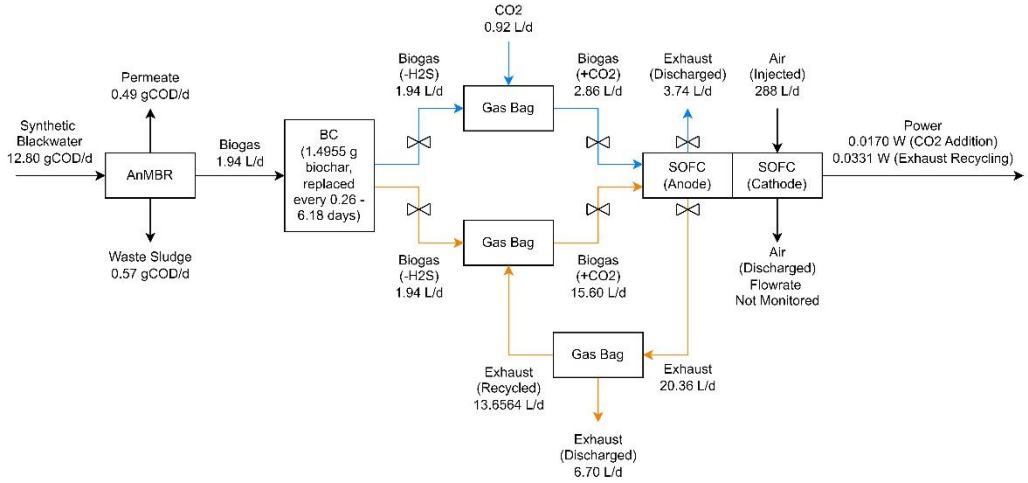

Figure 5.2 SOFC operational strategy (pH 7)

Table 5.4 Predicted composition of conditioned biogas, pH 7

Compounds	Concentration (BC treatment + CO_2 addition)	Concentration (BC treatment + exhaust recycling)
CH_4	46.5%	11.9%
CO_2	46.5%	11.9%
N_2	3.1%	48.2%
O_2	0.0%	5.2%
Unknown (incl. H_2O)	4.0%	22.8%
NH_3	0 ppm	0 ppm
H_2S	0 ppm	0 ppm
CH_3SH	0 ppm	0 ppm

For each scenario, the amount of CO_2 or exhaust gas required for further biogas conditioning was compared with the amount of available biogas after H_2S removal (Table 5.5). Less CO_2 or exhaust gas would be required to balance the ratio between CH_4 and CO_2 under pH 7, since the initial CO_2 concentration in the biogas would be higher when the pH is lower. The required exhaust gas as shown in the following table

was the initial amount of exhaust gas required for biogas conditioning. During the SOFC operation, the flowrate of the exhaust gas should be adjusted according to the changes in the exhaust composition.

Table 5.5 CO_2 or exhaust gas required for biogas conditioning

pH	Required CO_2 [L_{CO2}/L_{Biogas}]	Required Exhaust Gas [$L_{Exhaust}/L_{Biogas}$]
8	0.71	10.61
7	0.47	7.03

5.3 Potentials of the Scaled-up System

The average household in the Netherlands consists of 2.13 people as per 2022 (CBS, 2022b). According to Watergebruik Thuis (WGT) 2021 (Vewin, 2022), a report about water use at home in the Netherlands, the average water consumption for flushing toilet is 30.2 L/d per person. If an average person produces 2 L/d of waste, the total blackwater production per household in the Netherlands would be approximately 68.59 L/d, which is equivalent to 377.22 gCOD/d per household using 5.5 gCOD/L as the COD content of blackwater (Lettinga et al., 1993). When compared with the average organic loading rate (OLR) of the AnMBR system (Table 5.6), the OLR for treating blackwater generated by 1 household (377.22 gCOD/d) would be 38.78 and 29.47 times higher under pH 8 and pH 7 respectively. Therefore, given the average methane production rate measured in this experiment (Table 5.6), the methane production rate of the scaled-up system (for 1 household) could be estimated under each pH condition (Table 5.7).

Table 5.6 OLR (in gCOD/d) and CH4 production rate of the AnMBR system

pH	Organic Loading Rate [gCOD/d]	Methane Production Rate [L/d]
8	9.73 ± 34%	1.07 ± 24%
7	12.80 ± 18%	1.36 ± 11%

Table 5.7 OLR (in gCOD/d) and CH4 production rate of the scaled-up system (for 1 household)

pH	Organic Loading Rate [gCOD/d]	Methane Production Rate [L/d]
8	377.22	41.57
7	377.22	40.00

Based on the methane flowrate and the maximum power produced in the SOFC experiment, the power generated by the scaled-up system (for 1 household) could be estimated. The methane flowrate applied in the SOFC experiment was 15.72 L/d, which was determined with the biogas flowrate (35 mL/min or 50.40 L/d) and the methane content (31.2%). The maximum power produced by SOFC was 1.1456 W in the first SOFC experiment, which could be used as a reference to estimate the power generated by the scaled-up system, along with the methane production rates of the scaled-up system as shown in Table 5.7 (Equation 8.24). The power produced by the AnMBR

system and other scaled-up systems could be estimated using the same approach. Based on the estimated power, the daily electricity production could be estimated as well. The estimation results of the power and electricity produced at different scales have been summarized in Table 5.8 and Table 5.9 respectively.

Table 5.8 Estimated power produced by the AnMBR and other scaled-up systems

pH	5.5L AnMBR [W]	1 Household [W]	23 Households [W]	57 Households [W]
8	5.32E-03	8.01	4.24E+03	2.60E+04
7	8.54E-03	7.41	3.92E+03	2.41E+04

Table 5.9 Estimated electricity produced by the AnMBR and other scaled-up systems

pH	5.5L AnMBR [kWh/d]	1 Household [kWh/d]	23 Households [kWh/d]	57 Households [kWh/d]
8	1.28E-04	0.19	101.65	624.34
7	2.05E-04	0.18	94.12	578.07

For an average household in the Netherlands, the daily amount of electricity that could be potentially generated from the blackwater treatment (0.19 kWh/d under pH 8 and 0.18 kWh/d under pH 7) could be compared with the daily household electricity consumption using the multi-tier framework (MTF) as shown in Table 5.10 (Bhatia & Angelou, 2015). The average household electricity consumption in the Netherlands is 2810 kWh/y as per 2021 (CBS, 2022a), which is equivalent to 7699 Wh/d. Therefore, an average household in the Netherlands can be classified as a Tier 4 household. For an average household in the Netherlands, the electricity produced from the blackwater treatment can compensate approximately 2% of the total electricity consumption under either pH condition. For a Tier 4 household in general (Table 5.11), the electricity produced from the blackwater treatment is able to compensate 2 – 6% (under pH 8) or 2 – 5% (under pH 7) of the total electricity consumption.

Table 5.10 Multi-tier matrix for the electricity consumption of 1 household (Bhatia & Angelou, 2015)

Descritpion	Tier 1 [Wh/d]	Tier 2 [Wh/d]	Tier 3 [Wh/d]	Tier 4 [Wh/d]	Tier 5 [Wh/d]
Electricity Consumption of 1 Household	≥ 12	≥ 200	≥ 1000	≥ 3425	≥ 8219

Table 5.11 Comparing the electricity production with the electricity consumption within 1 household

Description	Compared with Tier 1	Compared with Tier 2	Compared with Tier 3	Compared with Tier 4	Compared with Tier 5
Electricity Production of 1 Household under pH 8	96 – 1601%	19 – 96%	6 – 19%	2 – 6%	0 – 2%
Electricity Production of 1 Household under pH 7	89 – 1483%	18 – 89%	5 – 18%	2 – 5%	0 – 2%

The electricity consumed by the treatment system itself should be considered for the energy balance. The power and electricity consumption of the treatment system at different scales have been summarized in Table 5.12 and Table 5.13 respectively. Only the most energy intensive equipment (AnMBR pumps including the acid dosing pump and SOFC furnace) are included for calculating the power and electricity consumption of the treatment system. The 5.5 L AnMBR tested in this experiment and an average household in the Netherlands would have a negative energy balance, meaning the electricity production would be lower than the electricity consumption. To compensate the electricity consumption of the treatment system itself under pH 8 or pH 7, 23 households are required for the blackwater treatment. To compensate the total electricity consumption of the treatment system and the household demand under either pH condition, 57 households are required for the blackwater treatment. Therefore, the treatment system should be scaled up, in order to compensate its own electricity consumption and to achieve a positive energy balance.

Table 5.12 Estimated power consumed by the AnMBR and other scaled-up systems

Power	5.5L AnMBR [W]	1 Household [W]	23 Households [W]	57 Households [W]
AnMBR Pumps	243	458	1510	2960
SOFC Furnace	2400	2400	2400	2400
Household Demand	–	321	7378	18284
Total	2643	3179	11288	23644

Table 5.13 Estimated electricity consumed by the AnMBR and other scaled-up systems

Electricity	5.5L AnMBR [kWh/d]	1 Household [kWh/d]	23 Households [kWh/d]	57 Households [kWh/d]
AnMBR Pumps	5.83	10.99	36.24	71.04
SOFC Furnace	57.60	57.60	57.60	57.60
Household Demand	–	7.70	177.07	438.82
Total	63.43	76.29	270.91	567.46

While energy is recovered from blackwater, suspended solids and COD would be removed as well. The by-products of the system, such as permeate and waste sludge, could be reused. For example, the permeate could be reused for irrigation, and the waste sludge could be reused as a raw material to make biochar. Besides black water, kitchen waste can also be fed to AnMBR as an additional source of nutrients, in which case, a higher energy production is expected when AnMBR and SOFC are connected.

5.4 Limitations of the Current System

The limitations of the current system should be considered before the main components (AnMBR, BC, and SOFC) of the system are connected for continuous operation in the future. The limitations have been summarized as follows.

Alternative solutions for the black water treatment. AnMBR could be replaced with other black water treatment technologies that are less energy intensive. For example, Chinese dome digester with roughing filter can be used for blackwater treatment and

biogas production. No external is necessary for this combination. However, in comparison to AnMBR, Chinese dome digesters would require more floor space, and the quality of the effluent discharged from roughing filters would be lower. The upflow anaerobic sludge bed (UASB) technology is a competitive alternative to AnMBR in terms of energy consumption. However, UASB reactors might have lower effluent quality when compared with AnMBR due to different solids separation mechanisms.

Biogas storage. The gas bags used in this experiment were not reliable for storing biogas, because the composition of the biogas stored in the gas bags would change overtime. The gas bags might be sufficient as a buffer for mixing biogas with CO_2 or exhaust gas, but further investigation is needed to support this hypothesis.

Effect of micro-aeration. Micro-aeration was incorporated into the AnMBR operation to promote hydrolysis and reduce H_2S concentration in biogas (Jeníček et al., 2017). Although, if excessive air is added to the AnMBR, the methanogenesis process might be inhibited and the residual oxygen might end up in the AnMBR biogas, and affect the methane reforming mechanisms during the SOFC operation. Therefore, further studies are required to determine the appropriate amount of the air adding to the AnMBR.

Empty permeate tube. Throughout the whole AnMBR operation, it was observed that the permeate tube was empty even through there was permeate being extracted from the membrane unit. The empty permeate tube might affect the backwashing efficiency, and accelerate membrane fouling. A possible explanation for this phenomenon is that the dissolved CH_4 and CO_2 are released from liquid phase to gas phase due to the change in gauge pressure (from positive to negative). The mass balance of CH_4 and the mass balance of CO_2 could be checked to test this hypothesis. The CH_4 that escaped from the permeate tube might be one of the causes for the gaps found in COD balance figures (Figure 8.11 and Figure 8.12).

Order of operation. H_2S removal and CO_2 addition could be switched so that CO_2 would be added to the biogas bag first before H_2S is removed. In this way, the biogas compounds would be diluted with additional CO_2, and the initial H_2S concentration would be lower for the BC. Therefore, less biochar would be required for H_2S removal, and the operational cost of the system would be lower. Although, it might be safer to remove H_2S first before adding CO_2, to ensure that the final H_2S concentration in the conditioned biogas would not exceed the limit of SOFC.

Preparation of the BC. The BC should be prepared with caution. To achieve the target height of the biochar layer, the BC should be tapped gently. The BC is sensitive to movement. Therefore, after the BC is loaded, the BC needs to be closed gently, so the biochar height would stay the same. The top and bottom connections of the BC should be sealed with PTFE tape, laboratory film, and vacuum grease to prevent leakage.

Alternative adsorbents. In this experiment, cow manure biochar was used in the BC for H_2S removal. The specific adsorption capacity of the cow manure biochar (0.105 – 0.25 mm), in relation to the SOFC tolerance (0.5 ppm), was 1.2297 mg/g. According to a literature article (Su et al., 2021), the H_2S removal capacity of cow manure biochar could reach up to 29.81 mg/g. Even though the source material is the same in this case, the H_2S removal capacity measured in this experiment is much lower. The H_2S removal

capacity could be influenced by many factors, such as pyrolysis temperature (Shang et al., 2016). The cow manure biochar used in this experiment was produced without temperature control. Alternatively, other adsorbents with higher adsorption capacity could be used for H_2S removal. The anaerobic sludge discharged from the AnMBR could also be made into biochar, in which case the by-product of the AnMBR would not be wasted.

Cell cracking. The cell might crack during the SOFC operation. To prevent the cell from cracking, the following protocols are recommended: (1) after the nickel foam (0.55 mm) and the mica sealing (0.7 mm, deformable) are glued to the nickel diffuser, a roller can be used to make the surface flat so that there would not be any gap between the cell and the nickel foam; (2) after the assembly is closed and secured at the four corners, the springs should be tightened one by one, half circle by half circle; (3) oxygen should be supplied to both sides of the cell at the beginning of the experiment while the furnace temperature is increasing; (4) the furnace should not be shut down immediately at the end of the experiment (a cooling rate of 300 °C/h is recommended by the SOFC supplier).

Sealing between the electrodes. If the mica sealing fails, air might leak from the cathode side to the anode side while the SOFC is operated under the biogas mode. As mentioned previously, after the nickel foam and the mica sealing are secured on the nickel diffuser, a roller can be used to make the surface flat. However, the roller should avoid the edge of the mica ring, or else the mica ring might be too thin for sealing. Furthermore, to ensure proper sealing when the furnace temperature reached the target temperature, the springs should be tightened again because the alumino-silicate felts would shrink as the furnace temperature increases. The initial and final length of each spring was 29.5 mm and 27.5 mm respectively in both SOFC experiments.

Pathways of methane reforming. The current assuming 100% fuel utilization efficiency was calculated based on the number of electrons transferred during the dry reforming (where CH_4 and CO_2 are converted to H_2 and CO) and fuel oxidation. However, O_2 and H_2O in the conditioned biogas could also act as methane reforming agents. The pathways of methane reforming could be studied in the future, to provide a more accurate estimation about the electron transfer mechanisms.

6. Conclusions and Recommendations

The anaerobic membrane bioreactor (AnMBR), biochar column (BC), and solid oxide fuel cell (SOFC) were integrated in this experiment for blackwater treatment and energy production. Synthetic blackwater was prepared as the feed water for the AnMBR. Depending on the sludge pH, the biogas produced by the AnMBR may have different compositions, which may also change the SOFC operational strategy. The aim of this research project is to investigate the effect of the AnMBR pH on the biogas composition, and to determine the SOFC operational strategy under pH 8 and pH 7.

The AnMBR performance was assessed under different pH conditions (pH 8 and pH 7). The COD removal efficiency (permeate COD versus feed water COD) was above 90% throughout the experiment. On average, 96% of the COD in the feed water was removed. The average methane production efficiency (methane COD versus feed water COD) was 26.0% under pH 8 and 29.5% under pH 7, and the average methane production rate was 1.07 L/d under pH 8 and 1.36 L/d under pH 7. When pH was reduced from 8 to 7, the CH_4 concentration in the biogas (including water vapor) decreased from 74.9% to 68.5%, while the CO_2 and H_2S concentration increased from 3.4% to 21.1% and from 20 ppm to 110 – 2600 ppm respectively.

The AnMBR biogas was processed by the BC for H_2S removal and then mixed with additional CO_2 to balance the ratio between CH_4 and CO_2. To avoid sulfur poisoning during the SOFC operation, H_2S was removed from the biogas by the cow manure biochar in the BC. The target H_2S concentration in the biogas after the BC treatment was less than 0.5 ppm. The adsorption capacity of the cow manure biochar with particle size ranging between 0.105 and 0.25 mm was 1.2297 mg/g, which has been verified using the biogas produced under pH 8 and pH 7. H_2S removal was more challenging under pH 7 because the initial H_2S concentration in the biogas was higher. Therefore, the H_2S concentration was monitored for a longer period under pH 7. After H_2S removal, CO_2 was added to the biogas so that the ratio between CH_4 and CO_2 was approximately 1:1. This ratio was designed to reduce the risk of carbon deposition during the SOFC operation.

Finally, in the first SOFC experiment, the biogas conditioned under pH 8 was utilized by the SOFC for energy conversion. The SOFC was operated under 910 °C for the biogas mode, where 35 mL/min of biogas containing 31.2% CH_4 and 30.0% CO_2 was pumped to the anode and 200 mL/min of air was released from the compressed air cylinder to the cathode. Voltage and current were measured by the electronic load, which was operated under the constant resistance (CR) mode. The maximum output of the SOFC was 1.1456 W, which was determined by comparing the power produced by the SOFC under different resistance settings. The resistance was 0.2632 Ω when the maximum power output was observed. The same operational procedure was followed in the second SOFC experiment, except the fuel gas was the biogas conditioned under pH 7. Since the biogas stored in the gas bags was contaminated with air overtime, only the experimental results of the first SOFC experiment were analyzed for SOFC operational strategies and the potentials of the scaled-up system.

SOFC operational strategies were proposed according to (1) the characteristics of the biogas produced by the AnMBR under different pH conditions, (2) the adsorption capacity of the cow manure biochar, and (3) the SOFC tolerance for sulfur poisoning and carbon deposition. Moreover, the power that could be produced by the SOFC in the end using the conditioned biogas as the fuel was estimated. Under pH 8, the BC should be replaced every 50.47 days to prevent H_2S breakthrough. After H_2S is removed from the AnMBR biogas, 0.71 L of CO_2 or 10.61 L of exhaust gas would be required per liter of available biogas, so that the CO_2 concentration would match the CH_4 concentration in the biogas. The power output of the SOFC would be 0.0092 W (CO_2 addition) or 0.0220 W (exhaust recycling) depending on the biogas conditioning strategy. Under pH 7, 0.47 L of CO_2 or 7.03 L of exhaust gas would be required for balancing the ratio between CH_4 and CO_2. The power out of the SOFC using the biogas conditioned under pH 7 would be 0.0170 W (CO_2 addition) or 0.0331 W (exhaust recycling).

Advantages and disadvantages of operating the AnMBR-BC-SOFC system under different pH conditions should be considered before the system is scaled up. Even though less CO_2 or exhaust gas would be required for biogas conditioning under pH 7, the operational cost is expected to be higher under pH 7 in comparison to pH 8, because (1) the biochar in the BC needs to be replaced more frequently, and (2) continuous acid addition would be necessary to maintain the sludge pH around 7.

The potentials of the scaled-up systems have been assessed. A positive energy balance would be achieved under either pH condition if 57 households contribute their blackwater for energy recovery. The energy balance was determined based on the electricity production of the system, and the total electricity consumption of the system and the households. The combined AnMBR-BC-SOFC system is a complete solution for blackwater treatment and energy production, while all the by-products could be reused commercially.

Further investigation is needed to overcome the limitations of the current system. Other blackwater treatment technologies that are less energy intensive could be considered as a replacement of AnMBR. The biogas quality would change if stored in a gas bag over a long period of time. The influence of micro-aeration on the AnMBR performance and the biogas composition was not studied in this project. The empty permeate tube should be avoided. H_2S removal and CO_2 addition could be switched. The BC should be prepared with caution. Adsorbents with higher H_2S removal capacity could be used instead of the cow manure biochar. The cell could crack and the sealing between the electrodes could fail if the SOFC is not operated properly. Further studies on the methane reforming pathways would provide better estimation about the electron transfer mechanisms.

7. References

Alhashimi, H. A., & Aktas, C. B. (2017). Life cycle environmental and economic performance of biochar compared with activated carbon: A meta-analysis. *Resources, Conservation and Recycling, 118*, 13-26. https://doi.org/https://doi.org/10.1016/j.resconrec.2016.11.016

Appelo, C. A. J., & Postma, D. (2005). Geochemistry, Groundwater and Pollution (C.A.J. Appelo, & D. Postma, Eds.) (2nd ed.). *CRC Press*. https://doi.org/https://doi.org/10.1201/9781439833544

Aslam, A., Khan, S. J., & Shahzad, H. M. A. (2022, 2022/01/01/). Anaerobic membrane bioreactors (AnMBRs) for municipal wastewater treatment- potential benefits, constraints, and future perspectives: An updated review. *Science of The Total Environment, 802*, 149612. https://doi.org/https://doi.org/10.1016/j.scitotenv.2021.149612

Bari, S. (1996, 1996/09/01/). Effect of carbon dioxide on the performance of biogas/diesel duel-fuel engine. *Renewable Energy, 9*(1), 1007-1010. https://doi.org/https://doi.org/10.1016/0960-1481(96)88450-3

Basu, P. (2018). Chapter 5 - Pyrolysis. In P. Basu (Ed.), *Biomass Gasification, Pyrolysis and Torrefaction (Third Edition)* (pp. 155-187). Academic Press. https://doi.org/https://doi.org/10.1016/B978-0-12-812992-0.00005-4

Bhatia, M., & Angelou, N. (2015). *Beyond Connections: Energy Access Redefined. ESMAP Technical Report 008/15*. World Bank. http://hdl.handle.net/10986/24368

CBS. (2022a). *Energy consumption private dwellings; type of dwelling and regions*. CBS. https://www.cbs.nl/en-gb/figures/detail/81528ENG

CBS. (2022b). *Households today*. CBS. https://www.cbs.nl/en-gb/visualisations/dashboard-population/households/households-today

Dwivedi, S. (2020, 2020/09/07/). Solid oxide fuel cell: Materials for anode, cathode and electrolyte. *International Journal of Hydrogen Energy, 45*(44), 23988-24013. https://doi.org/https://doi.org/10.1016/j.ijhydene.2019.11.234

Gęca, M., Wiśniewska, M., & Nowicki, P. (2022, 2022/07/01/). Biochars and activated carbons as adsorbents of inorganic and organic compounds from multicomponent systems – A review. *Advances in Colloid and Interface Science, 305*, 102687. https://doi.org/https://doi.org/10.1016/j.cis.2022.102687

Goodman, P. (2002, 2002/03/01). Current and future uses of gold in electronics. *Gold Bulletin*, *35*(1), 21-26. https://doi.org/10.1007/BF03214833

Haga, K., Adachi, S., Shiratori, Y., Itoh, K., & Sasaki, K. (2008, 2008/09/30/). Poisoning of SOFC anodes by various fuel impurities. *Solid State Ionics*, *179*(27), 1427-1431. https://doi.org/https://doi.org/10.1016/j.ssi.2008.02.062

Hai, F. I., Riley, T., Shawkat, S., Magram, S. F., & Yamamoto, K. (2014). Removal of Pathogens by Membrane Bioreactors: A Review of the Mechanisms, Influencing Factors and Reduction in Chemical Disinfectant Dosing. *Water*, *6*(12), 3603-3630.

Henze, M., van Loosdrecht, M. C. M., Ekama, G. A., & Brdjanovic, D. (2008). *Biological Wastewater Treatment: Principles, Modelling and Design*. IWA Publishing. https://doi.org/10.2166/9781780401867

Hunt, J., Ferrari, A., Lita, A., Crosswhite, M., Ashley, B., & Stiegman, A. E. (2013, 2013/12/27). Microwave-Specific Enhancement of the Carbon–Carbon Dioxide (Boudouard) Reaction. *The Journal of Physical Chemistry C*, *117*(51), 26871-26880. https://doi.org/10.1021/jp4076965

Irvine, J. T., Dobson Jw Fau - Politova, T., Politova T Fau - Martin, S. G., Martin Sg Fau - Shenouda, A., & Shenouda, A. Co-doping of scandia-zirconia electrolytes for SOFCs. (1359-6640 (Print)).

Jeníček, P., Horejš, J., Pokorná-Krayzelová, L., Bindzar, J., & Bartáček, J. (2017, 2017/08/01/). Simple biogas desulfurization by microaeration – Full scale experience. *Anaerobe*, *46*, 41-45. https://doi.org/https://doi.org/10.1016/j.anaerobe.2017.01.002

Joshi, A. V., Steppan, J. J., Taylor, D. M., & Elangovan, S. (2004, 2004/07/01). Solid Electrolyte Materials, Devices, and Applications. *Journal of Electroceramics*, *13*(1), 619-625. https://doi.org/10.1007/s10832-004-5168-x

Karbanee, N., van Hille, R. P., & Lewis, A. E. (2008, 2008/03/01). Controlled Nickel Sulfide Precipitation Using Gaseous Hydrogen Sulfide. *Industrial & Engineering Chemistry Research*, *47*(5), 1596-1602. https://doi.org/10.1021/ie0711224

Kenney, B., & Karan, K. (2005). Comparison of LSM and LSCF cathodes of solid oxide fuel cells by AC-impedance spectroscopy Paper no IGEC-1-100. First international green energy conference (IGEC-2005) Proceedings, Canada.

Laosiripojana, N., Wiyaratn, W., Kiatkittipong, W., Arpornwichanop, A., Soottitantawat, A., & Assabumrungrat, S. (2009). Reviews on Solid Oxide Fuel Cell Technology. *Engineering Journal*, *13*, 65-84. https://doi.org/https://doi.org/10.4186/ej.2009.13.1.65

Larminie, J., & Dicks, A. (2003). Introduction. In *Fuel Cell Systems Explained* (pp. 1-24). https://doi.org/https://doi.org/10.1002/9781118878330.ch1

Lettinga, G., de Man, A., van der Last, A. R. M., Wiegant, W., van Knippenberg, K., Frijns, J., & van Buuren, J. C. L. (1993). Anaerobic Treatment of Domestic Sewage and Wastewater. *Water Science and Technology*, *27*(9), 67-73. https://doi.org/10.2166/wst.1993.0179

Lewis, A. E. (2010, 2010/09/01/). Review of metal sulphide precipitation. *Hydrometallurgy*, *104*(2), 222-234. https://doi.org/https://doi.org/10.1016/j.hydromet.2010.06.010

Leyva-Ramos, R., Aguilar-Armenta, G., Gonzalez-Gutierrez, L. V., Guerrero-Coronado, R. M., & Mendoza-Barron, J. (2004, 2004/06/01). Ammonia exchange on clinoptilolite from mineral deposits located in Mexico [https://doi.org/10.1002/jctb.1035]. *Journal of Chemical Technology & Biotechnology*, *79*(6), 651-657. https://doi.org/https://doi.org/10.1002/jctb.1035

Maaz, M., Yasin, M., Aslam, M., Kumar, G., Atabani, A. E., Idrees, M., Anjum, F., Jamil, F., Ahmad, R., Khan, A. L., Lesage, G., Heran, M., & Kim, J. (2019, 2019/07/01/). Anaerobic membrane bioreactors for wastewater treatment: Novel configurations, fouling control and energy considerations. *Bioresource Technology*, *283*, 358-372. https://doi.org/https://doi.org/10.1016/j.biortech.2019.03.061

Maxim, L. D., & Utell, M. J. (2014). Aluminosilicate Fibers. In P. Wexler (Ed.), *Encyclopedia of Toxicology (Third Edition)* (pp. 156-160). Academic Press. https://doi.org/https://doi.org/10.1016/B978-0-12-386454-3.01161-1

Mehta, N. S., Sahu, P. K., Tripathi, P., Pyare, R., & Majhi, M. R. (2018, 2018/07/01/). Influence of alumina and silica addition on the physico-mechanical and dielectric behavior of ceramic porcelain insulator at high sintering temperature. *Boletín de la Sociedad Española de Cerámica y Vidrio*, *57*(4), 151-159. https://doi.org/https://doi.org/10.1016/j.bsecv.2017.11.002

Mogensen, D., Grunwaldt, J. D., Hendriksen, P. V., Nielsen, J. U., & Dam-Johansen, K. (2014, 2014/06/24). Methane Steam Reforming over an Ni-YSZ Solid Oxide Fuel Cell Anode in Stack Configuration. *Journal of Chemistry*, *2014*, 710391. https://doi.org/10.1155/2014/710391

Ozgun, H., Ersahin, M. E., Zhou, Z., Tao, Y., Spanjers, H., & van Lier, J. B. (2019, 2019/06/01/). Comparative evaluation of the sludge characteristics along the height of upflow anaerobic sludge blanket coupled ultrafiltration systems. *Biomass and Bioenergy*, *125*, 114-122. https://doi.org/https://doi.org/10.1016/j.biombioe.2019.04.001

Pell, A. N. (1997, 1997/10/01/). Manure and Microbes: Public and Animal Health Problem? *Journal of Dairy Science*, *80*(10), 2673-2681. https://doi.org/https://doi.org/10.3168/jds.S0022-0302(97)76227-1

Qin, J., Qian, S., Chen, Q., Chen, L., Yan, L., & Shen, G. (2019, 2019/06/05/). Cow manure-derived biochar: Its catalytic properties and influential factors. *Journal of Hazardous Materials*, *371*, 381-388. https://doi.org/https://doi.org/10.1016/j.jhazmat.2019.03.024

Saadabadi, S. A., Illathukandy, B., & Aravind, P. V. (2021, 2021/08/01). Direct internal methane reforming in biogas fuelled solid oxide fuel cell; the influence of operating parameters [https://doi.org/10.1002/ese3.887]. *Energy Science & Engineering*, *9*(8), 1232-1248. https://doi.org/https://doi.org/10.1002/ese3.887

Saadabadi, S. A., Thallam Thattai, A., Fan, L., Lindeboom, R. E. F., Spanjers, H., & Aravind, P. V. (2019). Solid Oxide Fuel Cells fuelled with biogas: Potential and constraints. *Renewable Energy*, *134*, 194-214. https://doi.org/https://doi.org/10.1016/j.renene.2018.11.028

Saebea, D., Authayanun, S., & Patcharavorachot, Y. (2020, 2020/02/01/). Performance analysis of direct steam reforming of methane in SOFC with SDC-based electrolyte. *Energy Reports*, *6*, 391-396. https://doi.org/https://doi.org/10.1016/j.egyr.2019.08.078

Saleh, J. M., Roberts, M. W., & Kemball, C. (1962). The interaction of methyl mercaptan with nickel and tungsten films [10.1039/TF9625801642]. *Transactions of the Faraday Society*, *58*(0), 1642-1648. https://doi.org/10.1039/TF9625801642

Santarelli, M. (2015, 2015/11/01/). DEMOSOFC project to install first European plant to produce clean energy from waste water. *Fuel Cells Bulletin*, *2015*(11), 14-15. https://doi.org/https://doi.org/10.1016/S1464-2859(15)30363-1

Shang, G., Liu, L., Chen, P., Shen, G., & Li, Q. (2016, 2016/05/03). Kinetics and the mass transfer mechanism of hydrogen sulfide removal by biochar derived from rice hull. *Journal of the Air & Waste Management Association*, *66*(5), 439-445. https://doi.org/10.1080/10962247.2015.1122670

Sitthikhankaew, R., Predapitakkun, S., Kiattikomol, R., Pumhiran, S., Assabumrungrat, S., & Laosiripojana, N. (2011, 2011/01/01/). Comparative Study of Hydrogen Sulfide Adsorption by using Alkaline Impregnated Activated Carbons for Hot Fuel Gas Purification. *Energy Procedia*, *9*, 15-24. https://doi.org/https://doi.org/10.1016/j.egypro.2011.09.003

Smith, A. L., Stadler, L. B., Cao, L., Love, N. G., Raskin, L., & Skerlos, S. J. (2014, 2014/05/20). Navigating Wastewater Energy Recovery Strategies: A Life Cycle Comparison of Anaerobic Membrane Bioreactor and Conventional Treatment Systems with Anaerobic Digestion. *Environmental Science & Technology*, *48*(10), 5972-5981. https://doi.org/10.1021/es5006169

Speight, J. G. (2019). Chapter 13 - Upgrading by Gasification. In J. G. Speight (Ed.), *Heavy Oil Recovery and Upgrading* (pp. 559-614). Gulf Professional Publishing. https://doi.org/https://doi.org/10.1016/B978-0-12-813025-4.00013-1

Staniforth, J., & Ormerod, R. M. (2003, 2003/09/01). Running solid oxide fuel cells on biogas. *Ionics*, *9*(5), 336-341. https://doi.org/10.1007/BF02376583

Su, L., Chen, M., Zhuo, G., Ji, R., Wang, S., Zhang, L., Zhang, M., & Li, H. (2021). Comparison of Biochar Materials Derived from Coconut Husks and Various Types of Livestock Manure, and Their Potential for Use in Removal of H2S from Biogas. *Sustainability*, *13*(11).

Sun, W., Nešić, S., Young, D., & Woollam, R. C. (2008, 2008/03/01). Equilibrium Expressions Related to the Solubility of the Sour Corrosion Product Mackinawite. *Industrial & Engineering Chemistry Research*, *47*(5), 1738-1742. https://doi.org/10.1021/ie070750i

van Linden, N., Spanjers, H., & van Lier, J. B. (2022). Fuelling a solid oxide fuel cell with ammonia recovered from water by vacuum membrane stripping. *Chemical Engineering Journal*, *428*, 131081. https://doi.org/https://doi.org/10.1016/j.cej.2021.131081

Vewin. (2022). *Vewin publishes research on Water Use at Home*. Vewin. https://www.vewin.nl/nieuws/paginas/Vewin_publiceert_onderzoek_Watergebruik_Thuis_1290.aspx?source=%2Fnieuws%2FPaginas%2Fdefault.aspx#:~:text=Het%20CBS%20heeft%20in%20opdracht,liter%20per%20persoon%20per%20dag.

Yentekakis, I. V., Papadam, T., & Goula, G. (2008, 2008/09/30/). Electricity production from wastewater treatment via a novel biogas-SOFC aided process. *Solid State Ionics*, *179*(27), 1521-1525. https://doi.org/https://doi.org/10.1016/j.ssi.2007.12.049

Yoon, S. P., Han, J., Nam, S. W., Lim, T.-H., & Hong, S.-A. (2004, 2004/09/10/). Improvement of anode performance by surface modification for solid oxide fuel cell running on hydrocarbon fuel. *Journal of Power Sources*, *136*(1), 30-36. https://doi.org/https://doi.org/10.1016/j.jpowsour.2004.05.002

Zhan, Z., Lin, Y., Pillai, M., Kim, I., & Barnett, S. A. (2006, 2006/10/20/). High-rate electrochemical partial oxidation of methane in solid oxide fuel cells. *Journal of Power Sources*, *161*(1), 460-465. https://doi.org/https://doi.org/10.1016/j.jpowsour.2006.04.139

Zhang, J., Lenser, C., Menzler, N. H., & Guillon, O. (2020, 2020/01/01/). Comparison of solid oxide fuel cell (SOFC) electrolyte materials for operation at 500 °C. *Solid State Ionics*, *344*, 115138. https://doi.org/https://doi.org/10.1016/j.ssi.2019.115138

Zhao, L., Cao, X., Mašek, O., & Zimmerman, A. (2013, 2013/07/15/). Heterogeneity of biochar properties as a function of feedstock sources and production temperatures. *Journal of Hazardous Materials*, *256-257*, 1-9. https://doi.org/https://doi.org/10.1016/j.jhazmat.2013.04.015

8. Appendix

8.1 Appendix A: Supplementary Tables

Table 8.1 Procedure for membrane cleaning (Day 237)

Step	Scheme	Recirculation Solution	Backwashing Solution	Duration [min]
1	A	NaOH (pH around 12)	None	40
2	A	Demi water	None	40
3	A	HCl (pH around 3)	None	40
4	B	Demi water	Demi water	40
5	A	Demi water	None	20

Table 8.2 Procedure for membrane cleaning (Day 286 and Day 322)

Step	Scheme	Recirculation Solution	Backwashing Solution	Duration [min]
1	A	Demi water	None	20
2	B	NaOH (pH around 12)	NaOH (pH around 12)	80
3	B	Demi water	Demi water	40
4	B	HCl (pH around 3)	HCl (pH around 3)	80
5	B	Demi water	Demi water	40

Table 8.3 Procedure for membrane cleaning (Day 342)

Step	Scheme	Recirculation Solution	Backwashing Solution	Duration [min]
1	A	Demi water	None	10
2	B	NaOH (pH around 12)	NaOH (pH around 12)	40
3	B	Demi water	Demi water	40
4	B	HCl (pH around 3)	HCl (pH around 3)	40
5	B	Demi water	Demi water	40

Table 8.4 Preparing 1L of substrate for the SMA test (pH 8 and pH 7)

Components	Value
Sodium acetate trihydrate [g]	4.253
Micronutrients solution [mL]	10.640
Demineralized water [mL]	989.360

Table 8.5 Design parameters for the SMA test

Parameters	Value (pH 8)	Value (pH 7)
Sludge VSS [g/L]	1.7633 [1]	1.2983 [2]
Sludge Volume [L]	0.2500	0.2500
Substrate COD [g/L]	2.0000	2.0000
Substrate Volume [L]	0.1102	0.0811

[1] This value was estimated based on the VSS measurements of previously collected sludge under pH 8.
[2] This value was estimated based on the VSS measurements of previously collected sludge under pH 7.

Table 8.6 Preparing samples for the SMA test A (pH 8)

Sample Number	Sludge [mL]	Substrate [mL]	Demi Water [mL]	Total [mL]
A1 (Neg)	250	0	150	400
A2 (Neg)	250	0	150	400
A3 (Neg)	250	0	150	400
A4 (Sub)	250	110.208	39.792	400
A5 (Sub)	250	110.208	39.792	400
A6 (Sub)	250	110.208	39.792	400

Table 8.7 Preparing samples for the SMA test B (pH 7)

Sample Number	Sludge [mL]	Substrate [mL]	Demi Water [mL]	Total [mL]
B1 (Neg)	250	0	150	400
B2 (Neg)	250	0	150	400
B3 (Neg)	250	0	150	400
B4 (Sub)	250	81.146	68.854	400
B5 (Sub)	250	81.146	68.854	400
B6 (Sub)	250	81.146	68.854	400

Table 8.8 Preparing 1L of buffer for the SMA test and the BMP test

NaOH solution (3M)	1	L
Thymolphthalein (0.4%)	5	mL

Table 8.9 Preparing samples for the BMP test (pH 8)

Sample Number	Sludge [mL]	Cellulose [mL]	Substrate [mL]	Demi Water [mL]	Total [mL]
Neg1	300	0	0	100	400
Neg2	300	0	0	100	400
Neg3	300	0	0	100	400
Pos1	300	52.10	0	47.90	400
Pos2	300	52.10	0	47.90	400
Pos3	300	52.10	0	47.90	400
Sub1	300	0	62.76	37.24	400
Sub2	300	0	62.76	37.24	400
Sub3	300	0	62.76	37.24	400

Table 8.10 TMP and permeability before and after cleaning

Day	TMP [mbar]	Permeability [LMH/bar]	Comment
Day 195	37.5	146.8	Initial value
Day 237	185.0	29.5	Before cleaning
Day 238	82.5	65.3	After cleaning
Day 286	300.0	18.3	Before cleaning
Day 287	170.0	33.2	After cleaning
Day 322	305.0	17.7	Before cleaning
Day 323	194.5	30.0	After cleaning

Table 8.11 Efficiency of TMP reduction and permeability recovery

Day	TMP Reduction Efficiency	Permeability Recovery Efficiency	Comment
Day 237	69%	44%	1st cleaning
Day 286	60%	51%	2nd cleaning
Day 322	82%	90%	3rd cleaning

Table 8.12 Mass balance check for Breakthrough Test 1

Stage	Flow	Flowrate [mL/min]	Avg. Flowrate [mL/min]	Gap
Start	Inflow	25.57	25.65	–
		25.73		
	Outflow	25.70	25.71	0.22%
		25.71		
End	Inflow	25.98	25.95	–
		25.93		
	Outflow	25.85	25.75	-0.77%
		25.65		

Table 8.13 Mass balance check for Breakthrough Test 2

Day	Stage	Flow	Flowrate [mL/min]	Avg. Flowrate [mL/min]	Gap
Day 1	Start	Inflow	25.13	25.25	–
			25.36		
		Outflow	25.58	25.54	1.17%
			25.51		
		Outflow	24.23	24.84	-1.63%
			24.37		
			25.90		
Day 2	Start	Inflow	25.26	25.15	–
			25.05		
		Outflow	25.20	25.20	0.18%
			25.20		
	End	Inflow	25.00	24.92	–
			24.84		
		Outflow	24.75	24.86	-0.27%
			24.96		

Table 8.14 Characteristics of biogas and biochar from Day 226 to Day 244

Parameter	Target Value	Measured Value
Average biogas flowrate [L/d]	1.39	1.39
H_2S concentration [ppm]	–	20
Volume of biogas process by the BC [L]	25.00	27.90
H_2S adsorbed by the BC [mg]	0.6965	0.7773
Biochar mass [g]	0.5664	0.5668
Biochar height [cm]	5.41	5.41
Bichar volume [cm3]	1.43	1.43
GHSV [1/h]	41	41
Adsorption capacity of the biochar [mg/g]	1.2297	> 1.3713

Table 8.15 Characteristics of biogas and biochar from Day 289 *to Day* 293

Parameter	Target Value	Measured Value
Average biogas flowrate [L/d]	2.00	2.32
H_2S concentration [ppm]	–	120
Volume of biogas process by the BC [L]	10.00	10.16
H_2S adsorbed by the BC [mg]	1.6716	1.6990
Biochar mass [g]	1.3593	1.3577
Biochar height [cm]	12.14	11.84
Biochar volume [cm3]	1.39	1.61
GHSV [1/h]	24	29
Adsorption capacity of the biochar [mg/g]	1.2297	> 1.2514

Table 8.16 Characteristics of biogas and biochar from Day 296 *to Day* 301

Parameter	Target Value	Measured Value
Average biogas flowrate [L/d]	2.00	2.24
H_2S concentration [ppm]	–	120
Volume of biogas process by the BC [L]	10.00	10.99
H_2S adsorbed by the BC [mg]	1.6716	1.8371
Biochar mass [g]	1.4953	1.4950
Biochar height [cm]	13.35	13.36
Bichar volume [cm3]	3.78	3.78
GHSV [1/h]	22	25
Adsorption capacity of the biochar [mg/g]	1.2297	> 1.2288

Table 8.17 Characteristics of biogas and biochar from Day 311 to Day 315

Parameter	Target Value	Measured Value
Average biogas flowrate [L/d]	2.00	2.29
H_2S concentration [ppm]	–	150
Volume of biogas process by the BC [L]	8.80	9.14
H_2S adsorbed by the BC [mg]	1.8390	1.9102
Biochar mass [g]	1.4955	1.4965
Biochar height [cm]	13.36	13.36
Bichar volume [cm3]	3.78	3.78
GHSV [1/h]	22	24
Adsorption capacity of the biochar [mg/g]	1.2297	< 1.2764

Table 8.18 Characteristics of biogas and biochar from Day 324 to Day 328

Parameter	Target Value	Measured Value
Average biogas flowrate [L/d]	2.00	2.31
H_2S concentration [ppm]	–	110
Volume of biogas process by the BC [L]	12.00	9.39
H_2S adsorbed by the BC [mg]	1.8390	1.4385
Biochar mass [g]	1.4955	1.4952
Biochar height [cm]	13.36	13.36
Biochar volume [cm3]	3.78	3.78
GHSV [1/h]	22	25
Adsorption capacity of the biochar [mg/g]	1.2297	< 0.9621

Table 8.19 RSTD and N for different Dräger tubes

Compound	Range	RSTD	N
NH_3	5 – 100 ppm	± 10 – 15 %	1
NH_3	0.25 – 3 ppm	± 10 – 15 %	10
H_2S	0.2 – 6 ppm	± 15 – 20 %	1
H_2S	10 – 200 ppm	± 5 – 10 %	1
H_2S	100 – 2000 ppm	± 5 – 10 %	1
CH_3SH	0.1 – 2.5 ppm	± 10 – 15 %	10

Table 8.20 Biogas composition (before CO_2 addition) according to GC, pH 8

Sample	CO_2 [%]	O_2 [%]	N_2 [%]	CH_4 [%]	Total [%]
Sample 1	1.1%	9.6%	38.2%	51.1%	100.0%
Sample 2	1.0%	9.6%	38.1%	51.3%	100.0%
Sample 3	1.0%	9.6%	38.2%	51.2%	100.0%
Average	1.1%	9.6%	38.2%	51.2%	100.0%
RSTD	7.9%	0.1%	0.1%	0.2%	0.0%

Table 8.21 Biogas composition (after CO_2 addition) according to GC, pH 8

Sample	CO_2 [%]	O_2 [%]	N_2 [%]	CH_4 [%]	Total [%]
Sample 1	30.4%	7.8%	30.1%	31.7%	100.0%
Sample 2	32.9%	6.9%	26.5%	33.7%	100.0%
Sample 3	30.3%	7.8%	30.0%	31.9%	100.0%
Average	31.2%	7.5%	28.9%	32.4%	100.0%
RSTD	4.7%	7.1%	7.0%	3.4%	0.0%

Table 8.22 Biogas composition (before CO_2 addition) according to GC, pH 7

Sample	CO_2 [%]	O_2 [%]	N_2 [%]	CH_4 [%]	Total [%]
Sample 1	1.9%	9.5%	21.0%	67.6%	100.0%
Sample 2	1.9%	9.4%	20.5%	68.2%	100.0%
Sample 3	1.9%	10.0%	23.6%	64.4%	100.0%
Average	1.9%	9.6%	21.7%	66.7%	100.0%
RSTD	0.3%	3.6%	7.7%	3.0%	0.0%

Table 8.23 Biogas composition (after CO_2 addition) according to GC, pH 7

Sample	CO_2 [%]	O_2 [%]	N_2 [%]	CH_4 [%]	Total [%]
Sample 1	33.5%	8.1%	21.2%	37.3%	100.0%
Sample 2	34.2%	7.8%	20.0%	38.0%	100.0%
Sample 3	34.1%	7.8%	19.9%	38.2%	100.0%
Average	33.9%	7.9%	20.3%	37.8%	100.0%
RSTD	1.1%	2.0%	3.5%	1.4%	0.0%

8.2 Appendix B: Supplementary Figures

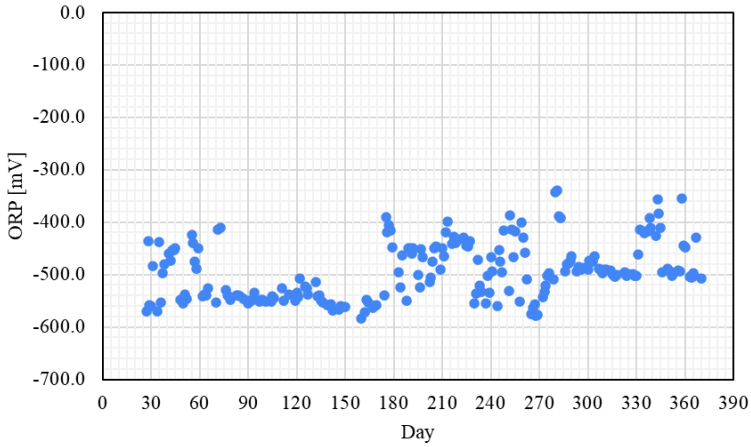

Figure 8.1 Sludge ORP

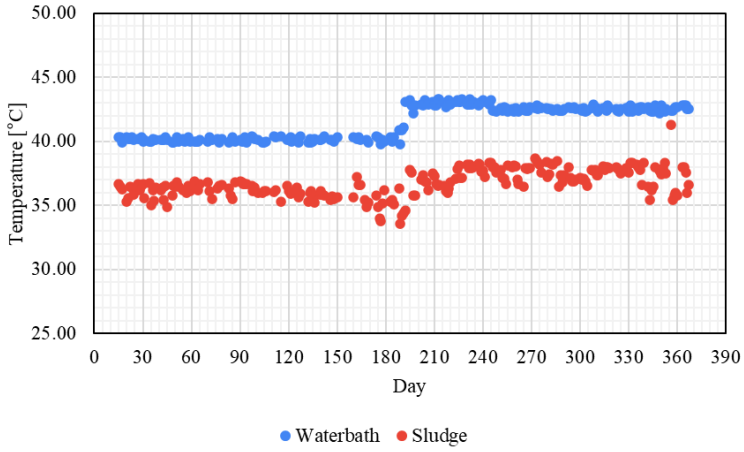

Figure 8.2 Sludge and waterbath temperature

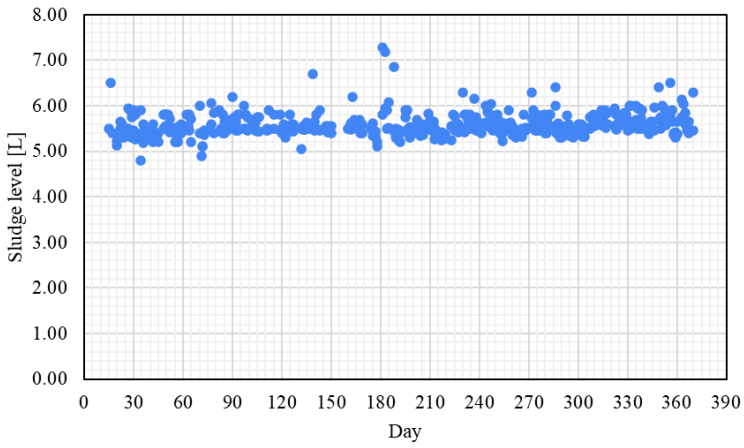

Figure 8.3 Sludge level

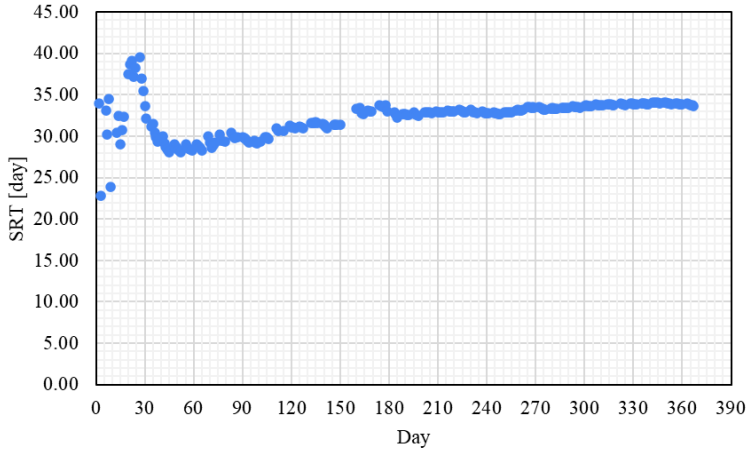

Figure 8.4 Sludge SRT

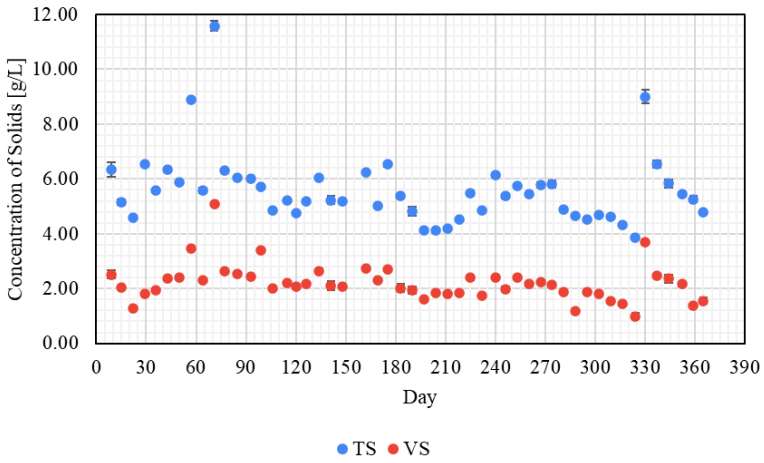

Figure 8.5 TS and VS of the sludge

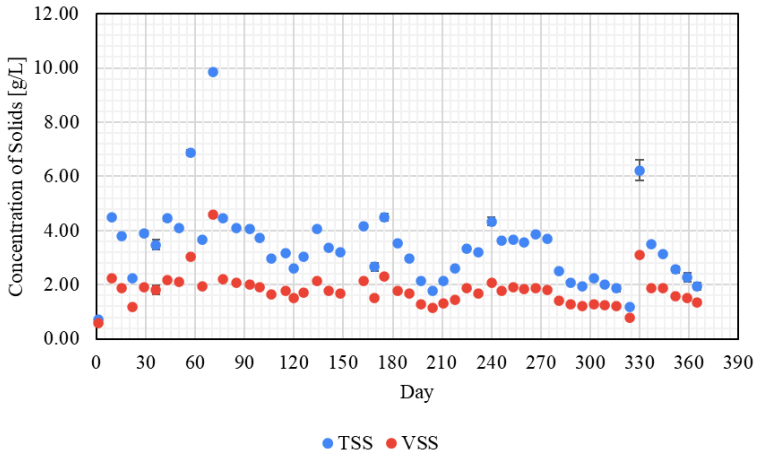

Figure 8.6 TSS and VSS of the sludge

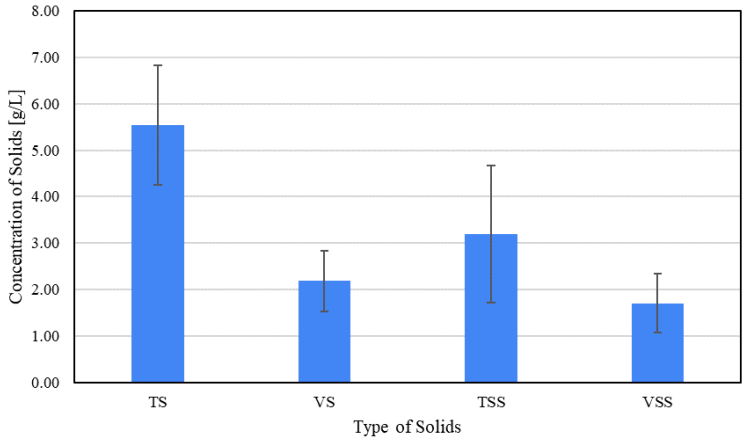

Figure 8.7 Summary for Solids Concentrations

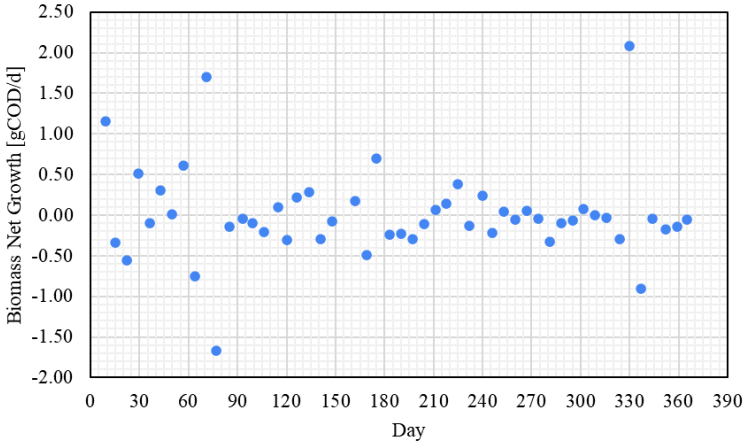

Figure 8.8 Biomass net growth

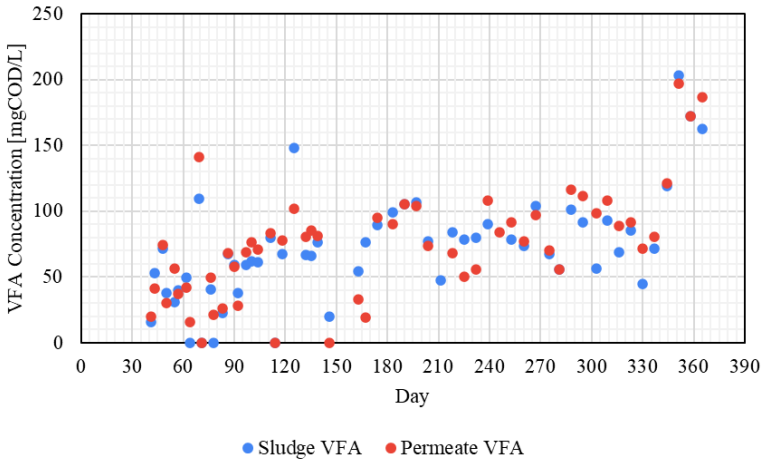

Figure 8.9 VFA in sludge and permeate

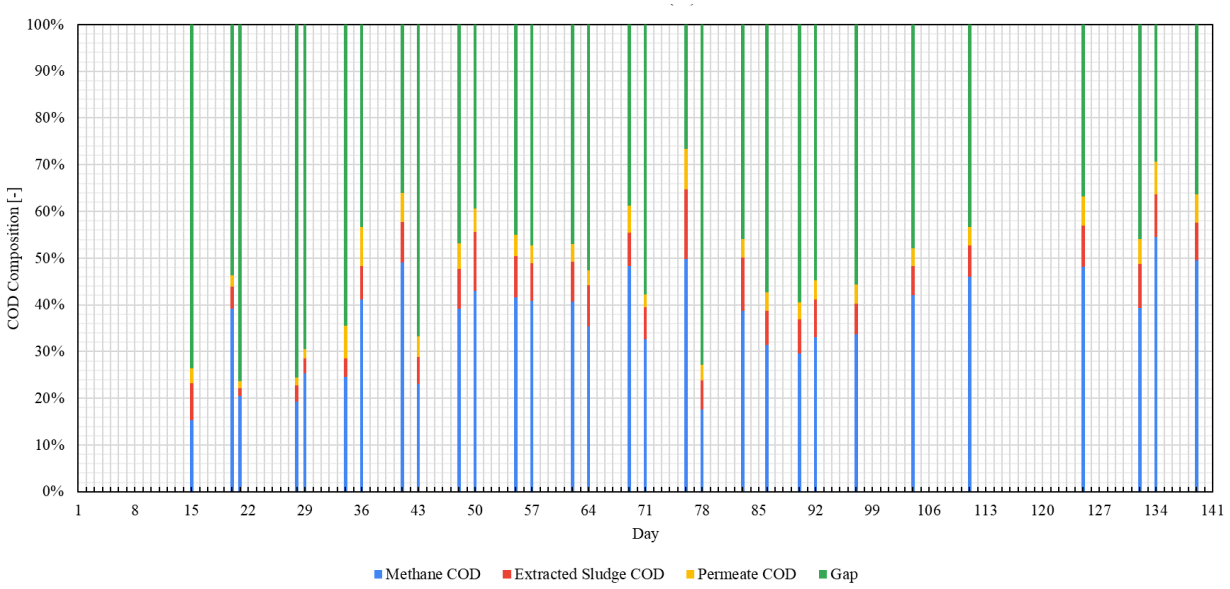

Figure 8.10 COD balance (A) calculated by the old method under pH 8

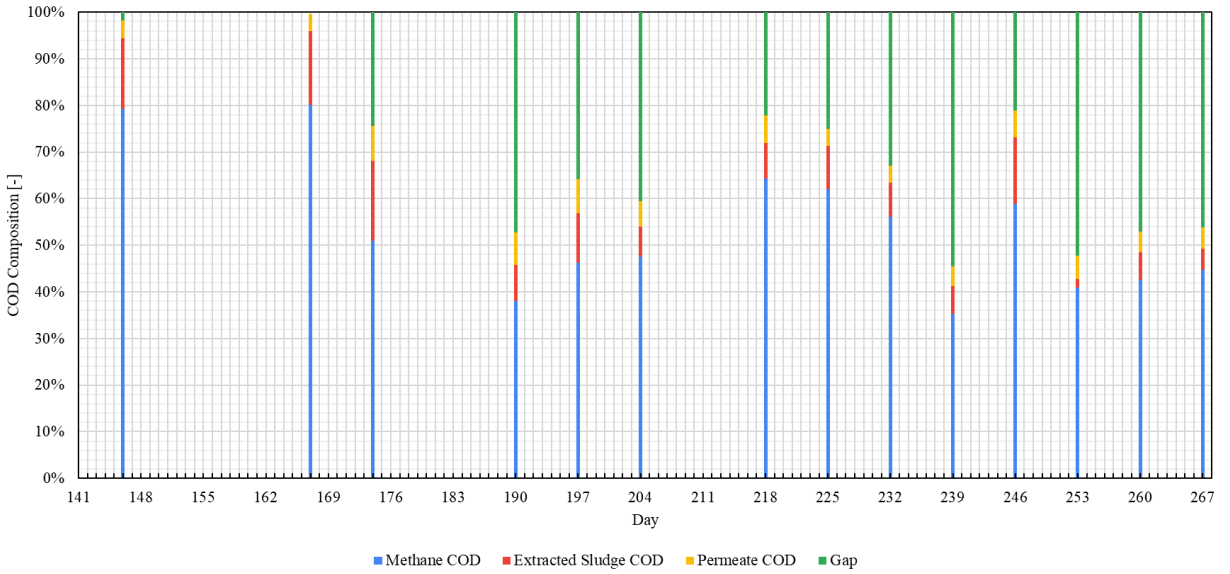

Figure 8.11 COD balance (B) calculated by the new method under pH 8

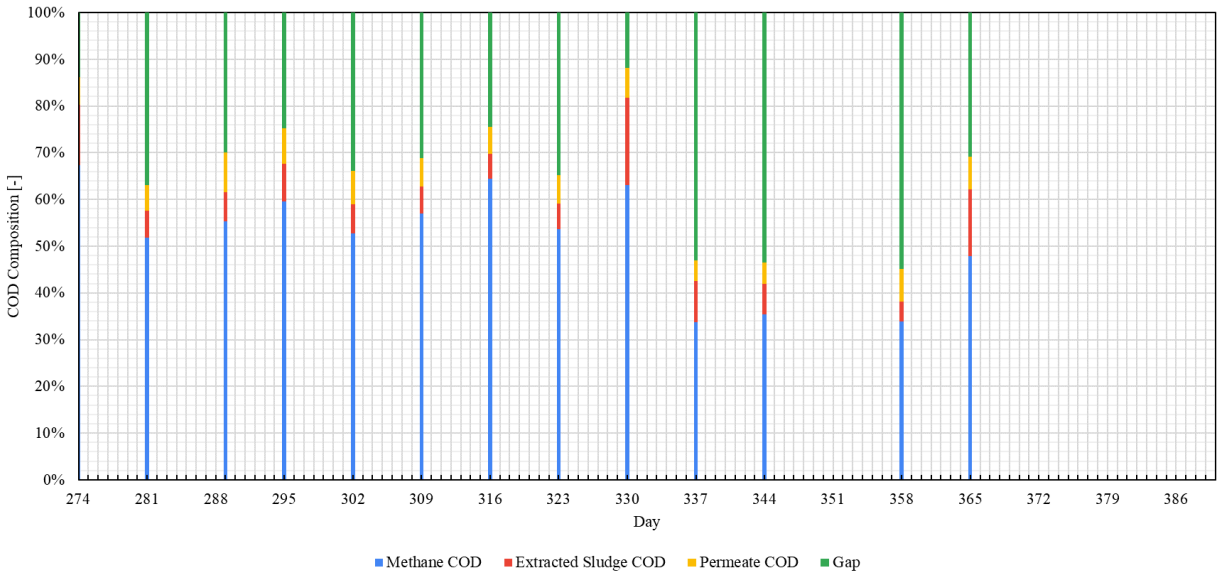

Figure 8.12 COD balance (C) calculated by the new method under pH 7

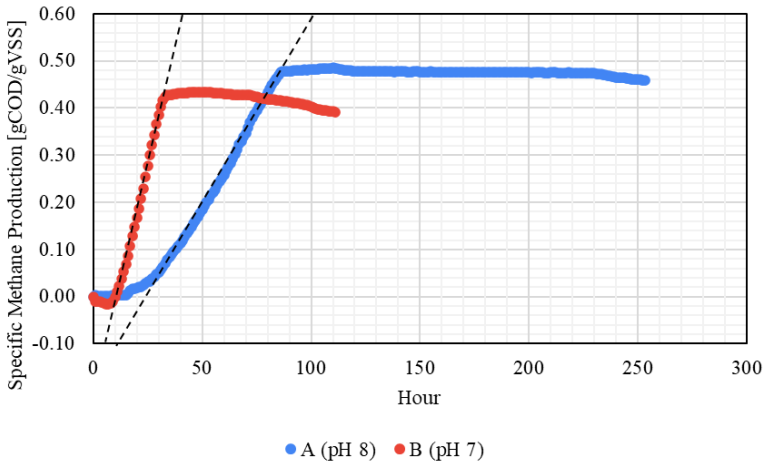

Figure 8.13 SMA results of Test A and Test B

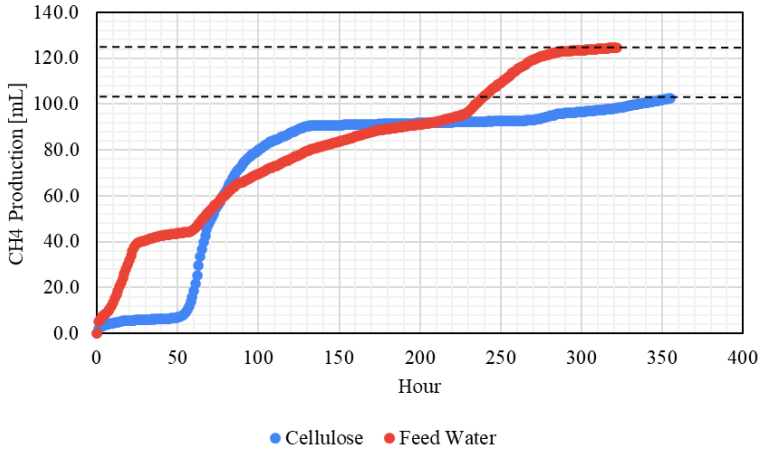

Figure 8.14 Methane production in BMP Test

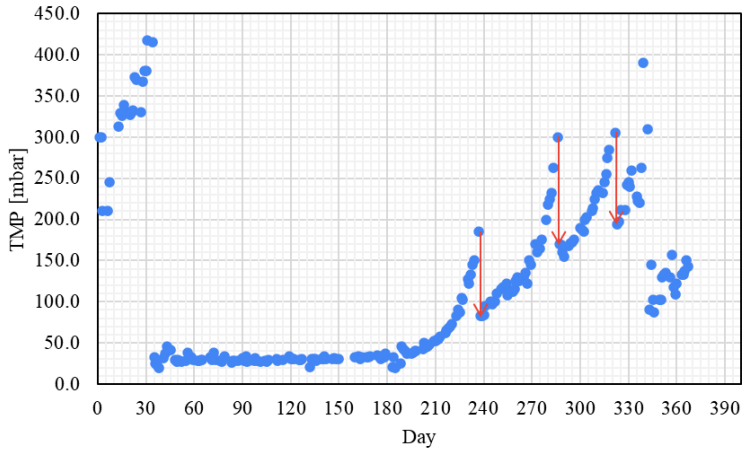

Figure 8.15 TMP

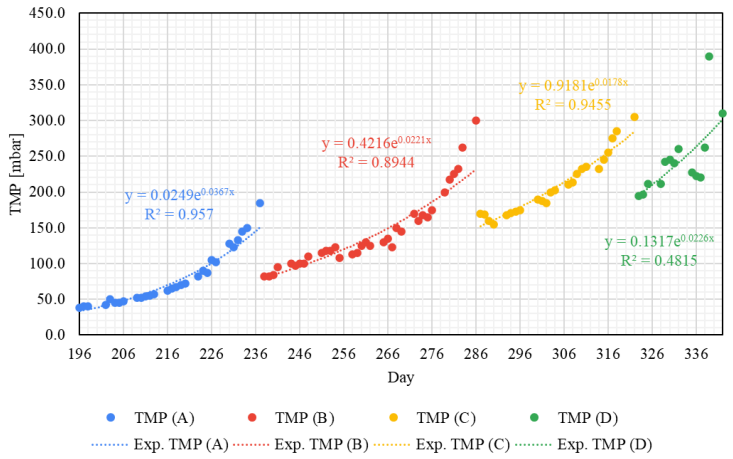

Figure 8.16 TMP from Day 196 to Day 342

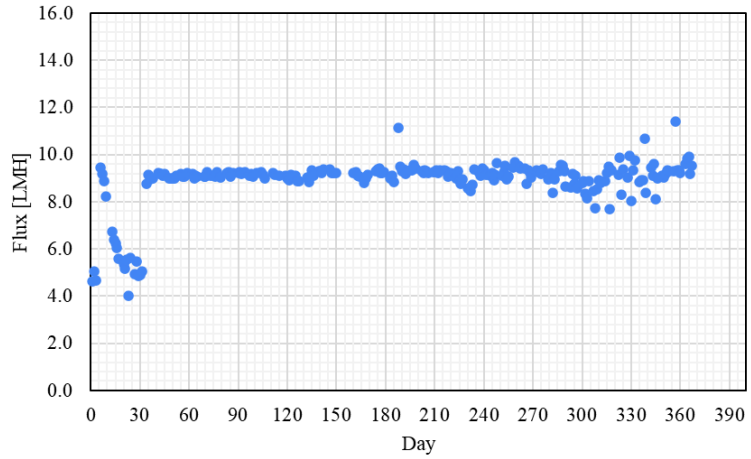

Figure 8.17 Flux

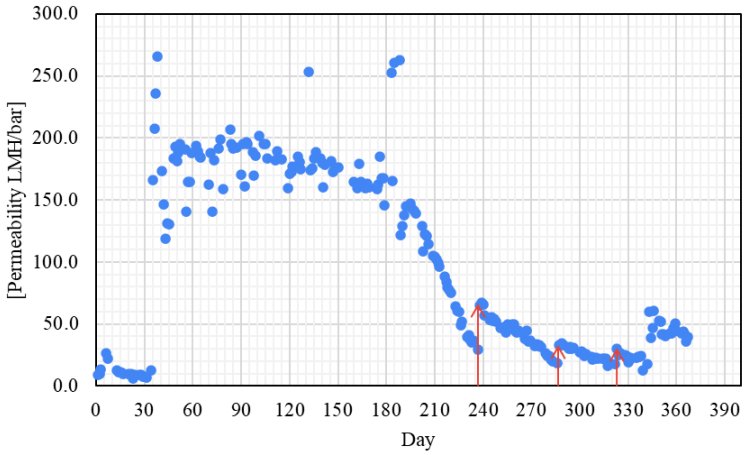

Figure 8.18 Permeability

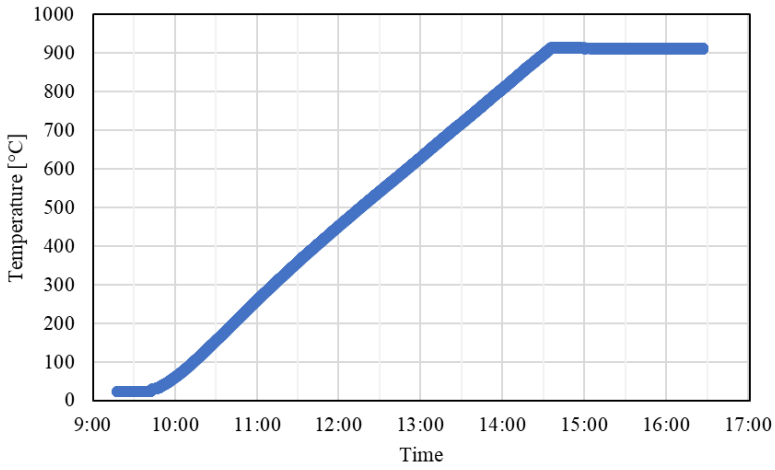

Figure 8.19 Furnace temperature during heating, 1st SOFC experiment

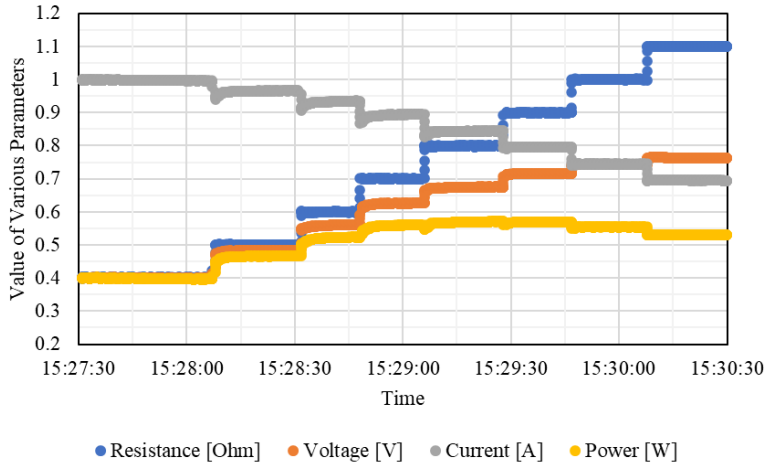

Figure 8.20 SOFC performance with forming gas, 1st SOFC experiment

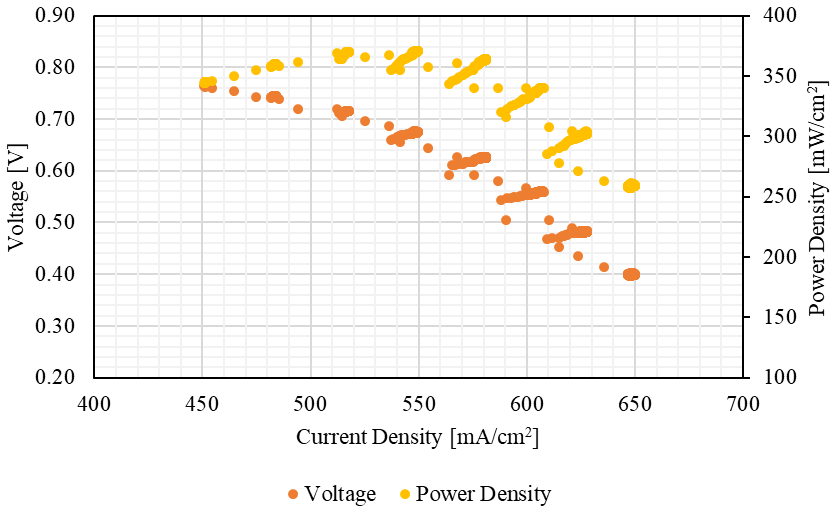

Figure 8.21 Polarization curve for the forming gas test, 1st SOFC experiment

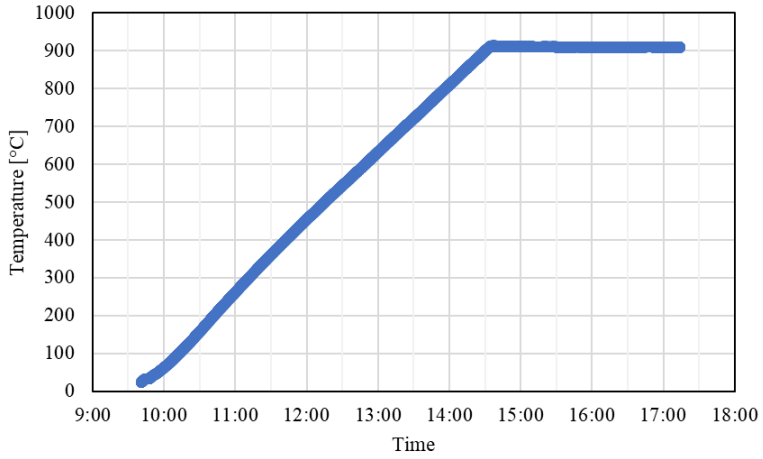

Figure 8.22 Furnace temperature during heating, 2nd SOFC experiment

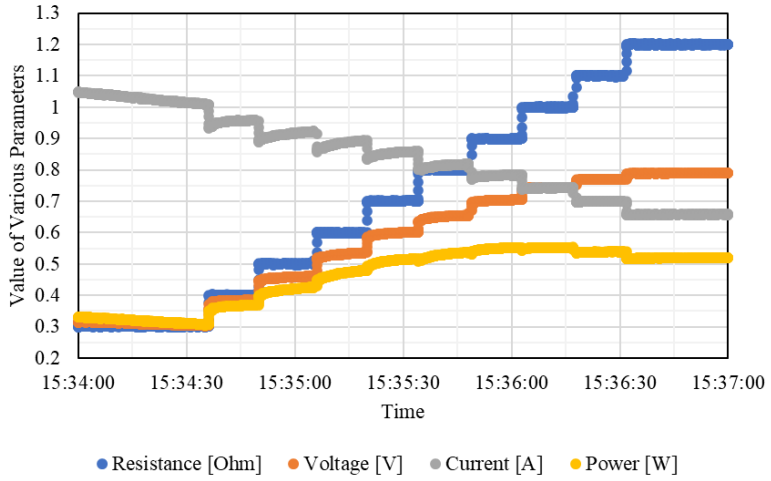

Figure 8.23 SOFC performance with forming gas, 2nd SOFC experiment

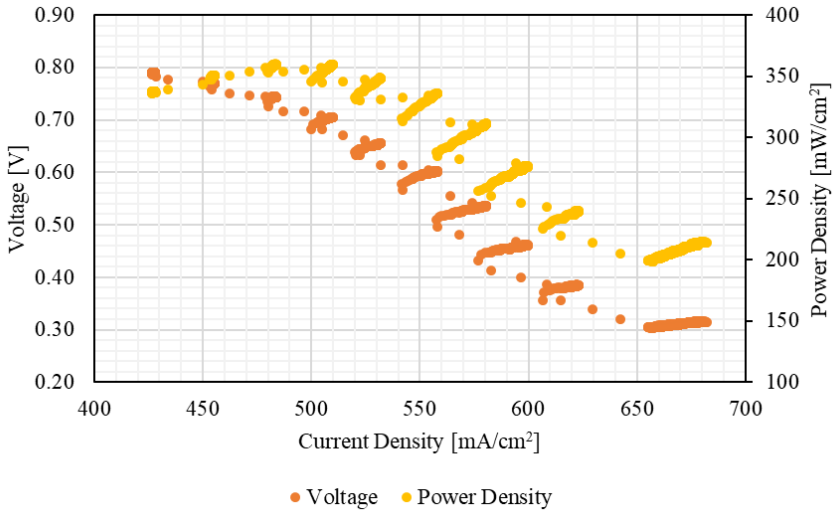

Figure 8.24 Polarization curve for the forming gas test, 2nd SOFC experiment

8.3 Appendix C: Supplementary Equations

Equation 8.1 Total alkalinity

$$TA = \frac{100 V_{HCl} C_{HCl}}{2 V_s}$$

$where$:
$TA = total\ alkalinity\ [gCaCO_3/L]$
$V_{HCl} = volume\ of\ the\ HCl\ solution\ [mL]$
$C_{HCl} = molar\ concentration\ of\ the\ HCl\ solution\ [mol/L]$
$V_s = volume\ of\ the\ sludge\ sample\ [mL]$

Equation 8.2 COD removal efficiency

$$\eta_{COD} = \frac{COD_{in} - COD_{out}}{COD_{in}} \times 100\% = \frac{Q_f C_f - Q_p C_p}{Q_f C_f} \times 100\%$$

$where$:
$\eta_{COD} = COD\ removal\ efficiency\ [-]$
$COD_{in} = influent\ COD\ [gCOD/d]$
$COD_{out} = effluent\ COD\ [gCOD/d]$
$Q_f = flowrate\ of\ the\ feed\ water\ [L/d]$
$C_f = COD\ concentration\ of\ the\ feed\ water\ [gCOD/L]$
$Q_p = flowrate\ of\ the\ permeate\ [L/d]$
$C_p = COD\ concentration\ of\ the\ permeate\ [gCOD/L]$

Equation 8.3 Biogas production rate

$$r_{biogas} = \frac{\Delta V_g - \Delta V_s}{\Delta t}$$

$where$:
$r_{biogas} = biogas\ production\ rate\ [L/d]$
$\Delta V_g = volume\ of\ biogas\ produced\ [L]$
$\Delta V_s = change\ in\ sludge\ volume\ [L]$
$\Delta t = duration\ [d]$

Equation 8.4 Methane production rate

$$r_{CH4} = \frac{V_{CH4}}{V_{biogas}} r_{biogas}$$

$where$:
$r_{CH4} = methane\ production\ rate\ [L/d]$
$V_{CH4}/V_{biogas} = fraction\ of\ methane\ in\ biogas\ [\%]$
$r_{biogas} = biogas\ production\ rate\ [L/d]$

Equation 8.5 COD of produced methane

$$COD_{CH4} = \frac{64 Pr_{CH4}}{1000 RT}$$

$where$:
$COD_{CH4} = COD\ of\ produced\ methane\ [gCOD/d]$
$P = atmospheric\ pressure\ [101325\ Pa]$
$r_{CH4} = methane\ production\ rate\ [L/d]$
$R = ideal\ gas\ constant\ [8.3145\ J \cdot mol^{-1} \cdot K^{-1}]$
$T = temperature\ [298.15\ K]$

Equation 8.6 Methane production efficiency

$$\eta_{CH4} = \frac{COD_{CH4}}{COD_{in}} \times 100\%$$

$where$:
$\eta_{CH4} = methane\ production\ efficiency\ [-]$
$COD_{CH4} = COD\ of\ produced\ methane\ [g/d]$
$COD_{in} = influent\ COD\ [g/d]$

Equation 8.7 Specific methanogenic activity (SMA)

$$COD_{CH4} = \frac{64 P(\bar{V}_{sub} - \bar{V}_{neg})}{10^6 RT}$$

$where$:
$COD_{CH4} = COD\ of\ produced\ methane\ [gCOD]$
$P = atmospheric\ pressure\ [101325\ Pa]$
$\bar{V}_{sub} = average\ methane\ production\ (sub)\ [mL]$
$\bar{V}_{neg} = average\ methane\ production\ (neg)\ [mL]$
$R = ideal\ gas\ constant\ [8.3145\ J \cdot mol^{-1} \cdot K^{-1}]$
$T = temperature\ [298.15\ K]$

$$P_s = \frac{COD_{CH4}}{VSS_{sludge}}$$

$where$:
$P_s = specific\ methane\ production\ [gCOD/gVSS]$
$COD_{CH4} = COD\ of\ produced\ methane\ [gCOD]$
$VSS_{sludge} = VSS\ of\ sludge\ per\ test\ bottle\ [gVSS]$

$$SMA = \frac{24 \Delta P_s}{\Delta t}$$

$where$:
$SMA = specific\ methanogenic\ activity\ [gCOD \cdot gVSS^{-1} \cdot d^{-1}]$
$\Delta P_s/\Delta t = most\ representative\ slope\ [gCOD \cdot gVSS^{-1} \cdot h^{-1}]$

Equation 8.8 Biochemical methane potential (BMP)

$$BMP = \frac{\lim (\bar{V}_{pos/sub} - \bar{V}_{neg})}{COD_{pos/sub}}$$

$where$:
$BMP = biochemical\ methane\ potential\ [mL/gCOD]$
$\bar{V}_{pos/sub} = average\ methane\ production\ (pos\ or\ sub)\ [mL]$
$\bar{V}_{neg} = average\ methane\ production\ (neg)\ [mL]$
$COD_{pos/sub} = COD\ of\ cellulose\ (pos)\ or\ feed\ water\ (sub)\ [gCOD]$

Equation 8.9 Transmembrane pressure (TMP)

$$TMP = \frac{P_f + P_c}{2} - P_p$$

$where$:
$TMP = transmembrane\ pressure\ [mbar]$
$P_f = feed\ pressure\ [mbar]$
$P_c = concentrate\ pressure\ [mbar]$
$P_p = permeate\ pressure\ [mbar]$

Equation 8.10 Flux

$$J = \frac{Q_p}{24A_m}$$

$where$:
$J = flux\ [LMH]$
$Q_p = flowrate\ of\ the\ permeate\ [L/d]$
$A_m = membrane\ area\ [m^2]$

Equation 8.11 Permeability

$$K = \frac{1000J}{TMP} e^{-0.031(T-20)}$$

$where$:
$K = permeability\ [LMH/bar]$
$J = flux\ [LMH]$
$TMP = transmembrane\ pressure\ [mbar]$
$T = sludge\ temperature\ [°C]$

Equation 8.12 Gas hourly space velocity (GHSV)

$$GHSV = \frac{60 Q_{in}}{V_{biochar}}$$

$where$:
$GHSV = gas\ hourly\ space\ velocity [h^{-1}]$
$Q_{in} = biogas\ inflow\ [mL/min]$
$V_{biochar} = biochar\ volume\ [cm^3]$

Equation 8.13 Converting H_2S in ppm to H_2S in mg/L

$$\mathbf{1\ ppm\ H_2S} = \frac{1\ \mu L\ H_2S}{1\ L\ biogas}$$

$$= \left(\frac{101325\ Pa\ \times\ 10^{-9}\ m^3\ H_2S}{8.3145\ \frac{J}{mol \cdot K}\ \times\ 298.15\ K}\right) \times \left(34.08 \times 10^3 \frac{mg}{mol}\right) \times \frac{1}{1\ L\ biogas}$$

$$= 1.393\ \times 10^{-3}\ \frac{mg\ H_2S}{L\ biogas}$$

$$\mathbf{20\ ppm\ H_2S} = 20 \times \left(1.393\ \times 10^{-3}\ \frac{mg\ H_2S}{L\ biogas}\right) = 0.02786\ \frac{mg\ H_2S}{L\ biogas}$$

Equation 8.14 H_2S processed by the BC

$$M_{H_2S} = \frac{60}{1000} Q_{in} t c_{H_2S}$$

$where$:
$M_{H_2S} = H_2S\ processed\ by\ the\ BC\ [mg]$
$Q_{in} = biogas\ inflow\ [mL/min]$
$t = processing\ time\ [h]$
$c_{H_2S} = H_2S\ concentration\ [mg/L]$

Equation 8.15 Specific adsorption capacity of biochar

$$q_s = \frac{M_{H_2S}}{M_{biochar}} = \frac{c_{H_2S} V_{biogas}}{M_{biochar}}$$

$where$:
$q_s = specific\ adsorption\ capacity\ [mg/g]$
$M_{H_2S} = H_2S\ processed\ by\ the\ BC\ before\ breakthrough\ [mg]$
$M_{biochar} = biochar\ added\ to\ the\ BC\ [g]$
$c_{H_2S} = H_2S\ concentration\ [mg/L]$
$V_{biogas} = volume\ of\ biogas\ processed\ by\ the\ BC\ [L]$

Equation 8.16 Estimating partial pressure of water vapor (saturation pressure) using the Clausius–Clapeyron Equation

$$e_s = e_{s0} \cdot exp\left(\frac{l_v}{R_v T_0}\right) \cdot exp\left(\frac{-l_v}{R_v T}\right)$$

$where$:
$e_s = saturation\ pressure\ at\ T\ [hPa]$
$e_{s0} = saturation\ pressure\ at\ T_0\ [6.11\ hPa]$
$T_0 = reference\ temperature\ T_0\ [273\ K]$
$l_v = enthalpy\ of\ vaporization\ [2.4131 \times 10^6\ Jkg^{-1}\ at\ 37°C]$
$R_v = gas\ constant\ for\ water\ vapor\ [461.5\ Jkg^{-1}K^{-1}]$
$T = temperature\ inside\ of\ the\ bioreactor\ [310\ K\ at\ 37°C]$

Equation 8.17 Water vapor content in biogas

$$F_{H_2O} = \frac{100 e_s}{P_{abs}} \times 100\% = \frac{100 e_s}{P_g + P_{atm}} \times 100\%$$

$where$:
$F_{H_2O} = fraction\ of\ water\ vapor\ in\ biogas\ [-]$
$e_s = saturation\ pressure\ of\ water\ vapor\ [hPa]$
$P_{abs} = absolute\ pressure\ [Pa]$
$P_g = gauge\ pressure\ [Pa]$
$P_{atm} = \ atmospheric\ pressure\ [Pa]$

Equation 8.18 Estimating current based on the mass flow of CH4

$$I = \frac{8 P r_{CH4}}{RT} \cdot F$$

$where$:
$I = \ current\ [A]$
$P = atmospheric\ pressure\ [101325\ Pa]$
$r_{CH4} = flowrate\ of\ utilized\ methane\ [m^3/s]$
$R = ideal\ gas\ constant\ [8.3145\ J \cdot mol^{-1} \cdot K^{-1}]$
$T = temperature\ [293.15\ K]$
$F = Faraday\ constant\ [96485\ C/mol]$

Equation 8.19 Ohm's law

$$V = IR$$

$where$:
$V = voltage\ [V]$
$I = current\ [A]$
$R = resistance\ [\Omega]$

Equation 8.20 Electric power output

$$P = VI$$

$where$:
$P = electric\ power\ [W]$
$V = voltage\ [V]$
$I = current\ [A]$

Equation 8.21 Surface power density

$$P_s = \frac{P}{A_{cathode}}$$

$where$:
$P_s = surface\ power\ density\ [W/cm^2]$
$P = electric\ power\ [W]$
$A_{cathode} = surface\ area\ of\ the\ cathode\ [cm^2]$

Equation 8.22 Forming gas utilization efficiency

$$\eta_{forming\ gas} = \frac{I_{meas}}{I_{theor}} \times 100\% = I_{meas}(\frac{2Pr_{H2}}{RT} \cdot F)^{-1} \times 100\%$$

$where$:
$\eta_{forming\ gas} = forming\ gas\ utilization\ efficiency\ [-]$
$I_{meas} = measured\ current\ [A]$
$I_{theor} = theoretical\ current\ [A]$
$P = atmospheric\ pressure\ [101325\ Pa]$
$r_{H2} = flowrate\ of\ available\ hydrogen\ [m^3/s]$
$R = ideal\ gas\ constant\ [8.3145\ J \cdot mol^{-1} \cdot K^{-1}]$
$T = temperature\ [293.15\ K]$
$F = Faraday\ constant\ [96485\ C/mol]$

Equation 8.23 Biogas utilization efficiency

$$\eta_{biogas} = \frac{I_{meas}}{I_{theor}} \times 100\% = I_{meas}(\frac{8Pr_{CH4}}{RT} \cdot F)^{-1} \times 100\%$$

$where$:
$\eta_{biogas} = biogas\ utilization\ efficiency\ [-]$
$I_{meas} = measured\ current\ [A]$
$I_{theor} = theoretical\ current\ [A]$
$P = atmospheric\ pressure\ [101325\ Pa]$
$r_{CH4} = flowrate\ of\ available\ methane\ [m^3/s]$
$R = ideal\ gas\ constant\ [8.3145\ J \cdot mol^{-1} \cdot K^{-1}]$
$T = temperature\ [293.15\ K]$
$F = Faraday\ constant\ [96485\ C/mol]$

Equation 8.24 Relation between power, current, and methane flowrate under the constant resistance (CR) mode

$$\frac{P_2}{P_1} = \frac{(I_2)^2}{(I_1)^2} = \frac{(r_{CH4,2})^2}{(r_{CH4,1})^2}$$

$where$:
$P_1\ and\ P_2 = power\ [W]$
$I_1\ and\ I_2 = current\ [A]$
$r_{CH4,1}\ and\ r_{CH4,2} = flowrate\ of\ utilized\ methane\ [L/d]$

8.4 Appendix D: Photos of the Equipment

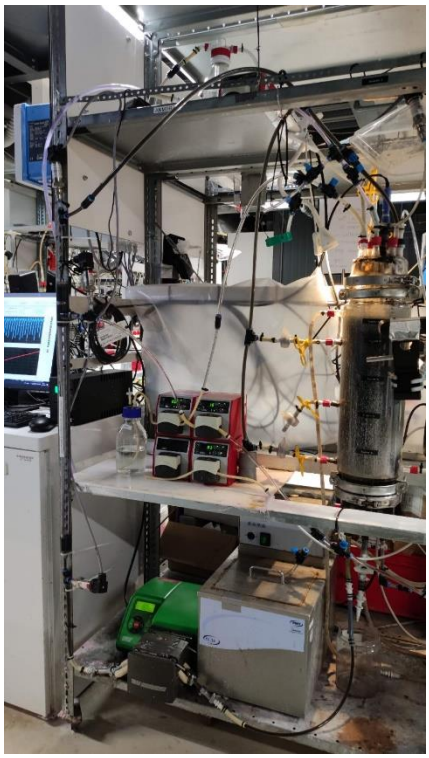

Photo 8.1 AnMBR

Photo 8.2 BC

Photo 8.3 SOFC (partial)

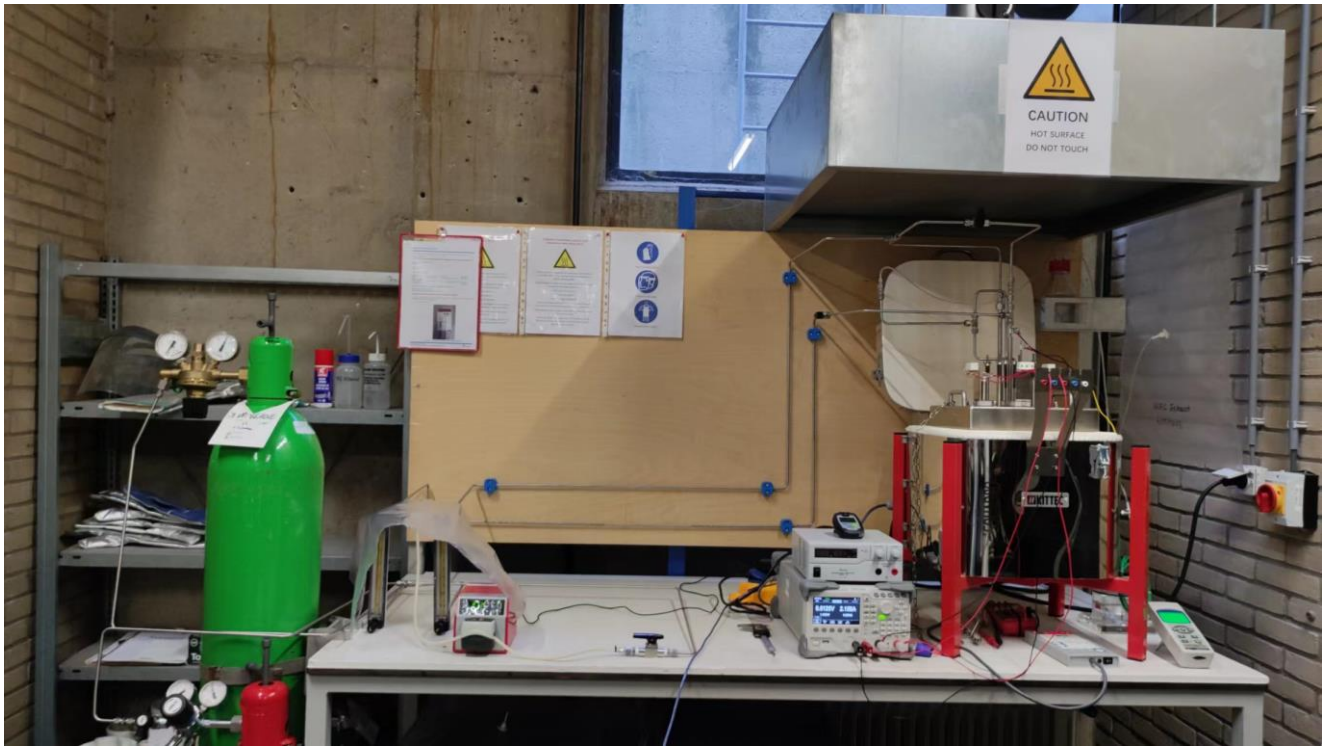

Photo 8.4 SOFC

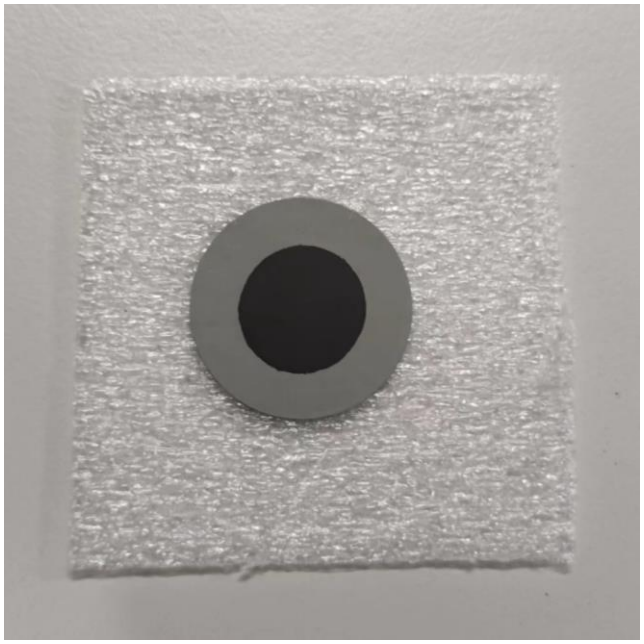

Photo 8.5 Cathode (black) and electrolyte (grey)

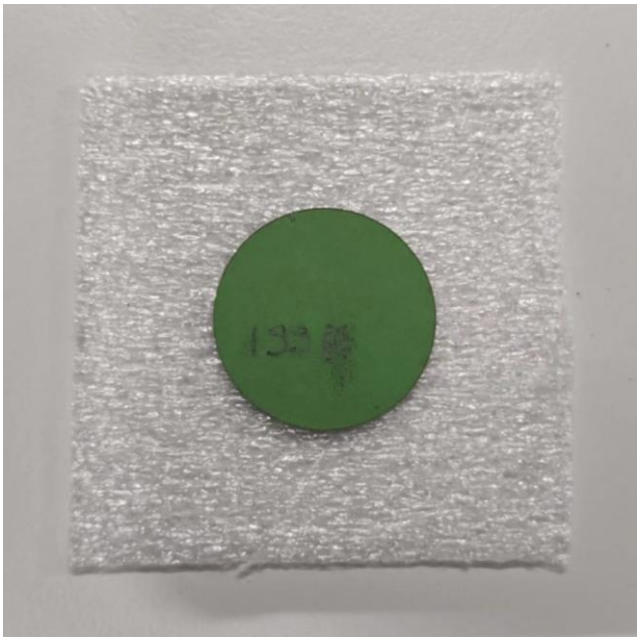

Photo 8.6 Anode (green)